Wisconsin Highway Research Program

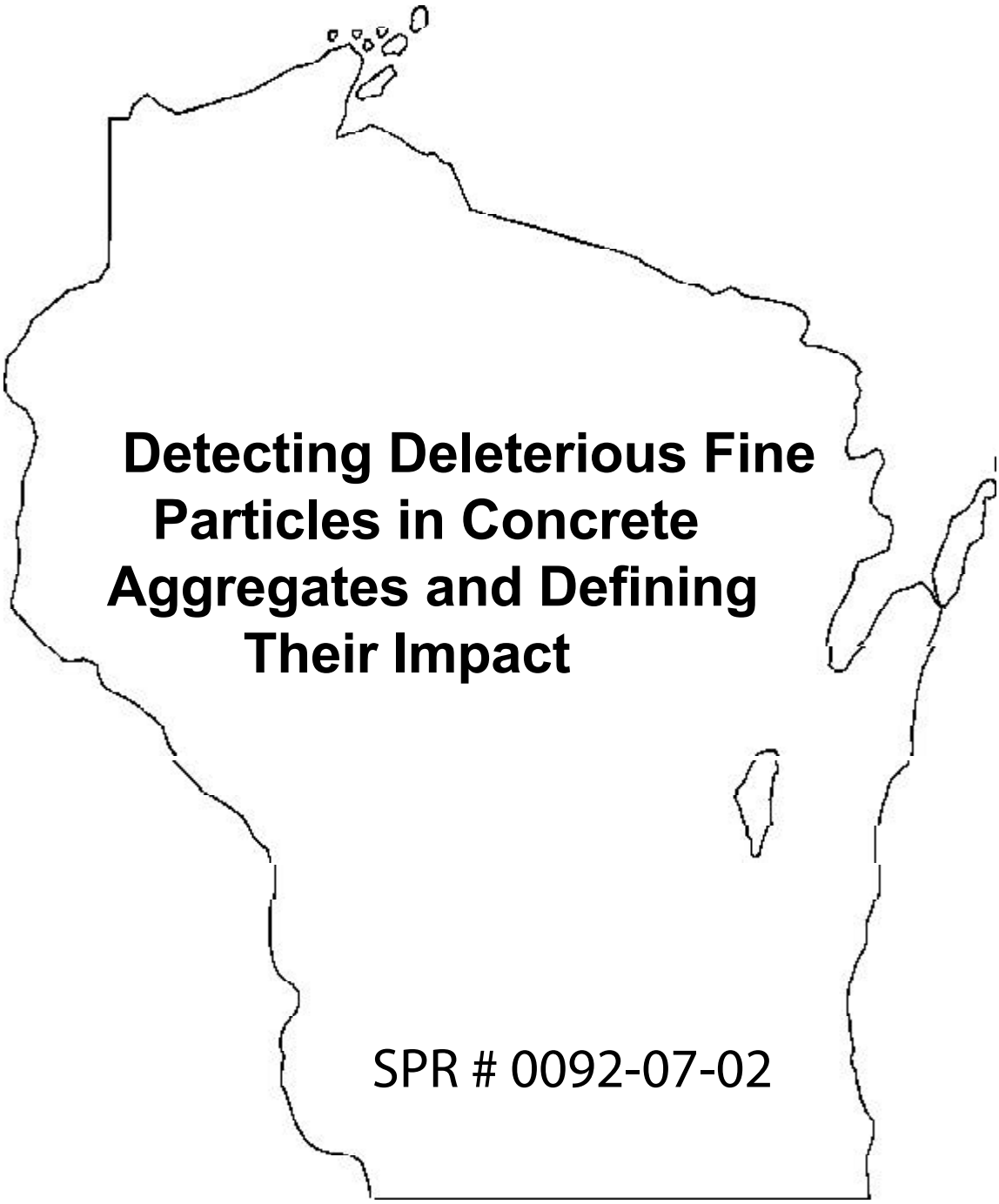

Detecting Deleterious Fine Particles in Concrete Aggregates and Defining Their Impact

SPR # 0092-07-02

Steven Cramer, Ph.D, Marc Anderson, Ph.D.
Isabel Tejedor, Ph.D, Jose Munoz, Ph.D.
Jacob Effinger, and Ramsey Kropp

University of Wisconsin - Madison
Department of Civil and Environmental Engineering

October 2010

WHRP 10-13

WISCONSIN HIGHWAY RESEARCH PROGRAM #0092-07-02

Detecting Deleterious Fine Particles in Concrete Aggregates and Defining Their Impact

Final Report

Steven M. Cramer
Marc Anderson
Isabel Tejedor
Jose Munoz
Jacob Effinger
Ramsey Kropp

University of Wisconsin – Madison
Department of Civil and Environmental Engineering

Submitted to:
THE WISCONSIN DEPARMENT OF TRANSPORTATION

October 2010

Acknowledgements

The authors gratefully acknowledge the support of the Wisconsin Highway Research Program for the financial support of this project. Accomplishment of the research was achieved through the valued contributions of a team of experts. This research team wants to mention the extensive help and collaboration of the staff of the Wisconsin Department of Transportation (James Parry, P.E., and Thomas E. Sand), the Wisconsin Concrete Pavement Association (Kevin W. McMullen, P.E.). The donations of materials by material suppliers and aggregate producers were greatly appreciated and without the cooperation of these companies, this research would not have been possible. Finally, the assistance of William Lang and Carole Kraak of the Structure and Materials Testing Laboratory at the University of Wisconsin-Madison is appreciated.

Disclaimer

This research was funded through the Wisconsin Highway Research Program by the Wisconsin Department of Transportation and the Federal Highway Administration under Project 0092-07-02. The contents of this report reflect the views of the authors who are responsible for the facts and accuracy of the data presented herein. The contents do not necessarily reflect the official views of the Wisconsin Department of Transportation or the Federal Highway Administration at the time of publication.

Technical Report Documentation Page

1. Report No. WHRP 10-13	2. Government Accession No	3. Recipient's Catalog No
4. Title and Subtitle Detecting Deleterious Fine Particles in Concrete Aggregates and Defining Their Impact		5. Report Date October 2010 6. Performing Organization Code Wisconsin Highway Research Program
7. Authors Steven Cramer, Marc Anderson, M. Isabel Tejedor, Jose F Muñoz, Jacob Effinger, and Ramsey Kropp		8. Performing Organization Report No.
9. Performing Organization Name and Address Department of Civil and Environmental Engineering University of Wisconsin-Madison 1415 Engineering Drive Madison, WI 53706		10. Work Unit No. (TRAIS) 11. Contract or Grant No. WisDOT SPR# 0092-07-02
12. Sponsoring Agency Name and Address Wisconsin Department of Transportation Division of Business Services Research Coordination Section 4802 Sheboygan Ave. Rm 104 Madison, WI 53707		13. Type of Report and Period Covered Final Report, 2008-2010 14. Sponsoring Agency Code

15. Supplementary Notes

16. Abstract

This study examined the types of microfines in aggregates found in northern Wisconsin and their influence on concrete prepared according to WisDOT specifications. Aggregates were collected from 28 sources and 69 percent were found to contain clay particles known to be deleterious in concrete. Seven aggregates sources were selected from the 28 for detailed evaluation including concrete performance. The microfines from the aggregates were evaluated by x-ray diffraction and thermal gravimetric analysis. Concrete performance testing included strength, shrinkage, porosity and rapid chloride ion penetrability for concrete subject to standard wet curing and dry curing. A rapid field test for microfine identification was attempted but found to be unsuitable for field conditions but potentially useful for laboratory identification of microfines with further development. The results of this research suggest the current P200 threshold for naturally occurring microfines associated with coarse and fine aggregates in the WisDOT Standard Specification results in acceptable concrete performance when conditions are optimal and meet typical ASTM laboratory test requirements. When microfines are present in aggregates, if air entrainment, uncontrolled water additions, certain intentional or unintentional chemical additions, and curing are not carefully monitored and controlled, then microfines in Wisconsin concrete aggregates can and do cause deleterious impacts.

17. Key Words Fines, microfines, clays, P200, coarse aggregate, fine aggregate, curing, slump, compressive strength, tensile strength	18. Distribution Statement No restriction. This document is available to the public through the National Technical Information Service 5285 Port Royal Road Springfield VA 22161

19. Security Classif.(of this report) Unclassified	19. Security Classif. (of this page) Unclassified	20. No. of Pages	21. Price

Form DOT F 1700.7 (8-72) Reproduction of completed page authorized

Executive Summary

The aggregates used for concrete production contain microfine materials (particle size <75µm) that can impact the workability, strength, and durability of concrete. ASTM C33 is incorporated into the WisDOT Standard Specification to regulate the maximum amount of microfines allowed. This test limits the amount of material passing a US #200 sieve to 1.5 percent of coarse aggregate weight and 3 percent of fine aggregate weight (P200 test) when clays are present. Field experiences in Wisconsin raise the question whether these limits are adequate, although solid evidence to answer the question has not been produced. Previous laboratory studies of naturally occurring microfines were unable to explain the poor performance of pavements. The potential harm from the microfine fraction of an aggregate is related to the mineralogy of the aggregate source and the quantity of microfines present. Microfines because of their high surface area have the potential to adsorb, and in some cases absorb water. In addition, some microfines are highly reactive materials that may alter the cement hydration. The microfine testing method currently employed by the state is unable to differentiate between different microfine mineralogies and its adequacy for determining the suitability of an aggregate source has been questioned.

Aggregate samples were obtained from 28 locations in Wisconsin and the microfine fractions were analyzed for their mineralogy and clay content with 69 percent of the samples showing the presence of clay particles. Seven aggregate samples were selected and concrete specimens from washed and unwashed aggregates were prepared. The aggregates samples included sources dominated by dolomitic material and sources dominated by igneous material. Identical concrete samples were cured under ideal and non-ideal conditions to attempt to determine the cause of the discrepancy between laboratory and field observations. The effect of microfines on early physical properties, mechanical properties, chemical properties, and the microstructure of the samples were measured. In addition, the cement paste samples were analyzed to determine changes in hydration.

Dolomitic microfines had little effect on the workability of or the effectiveness of air-entraining agent (AEA). Igneous microfines, especially those with clay minerals, decreased the slump value and the effectiveness of AEA. When cured under moist conditions, both microfine mineralogies typically introduced beneficial properties, and when negative effects were measured they were small in magnitude. Dry cured concrete samples had decreased compressive strength, decreased tensile strength, increased porosity, and increased susceptibility to chloride penetration. Concretes prepared with igneous aggregates, especially those containing clay minerals in the microfine fraction, were most susceptible to

low humidity curing and showed important differences compared to washed control concretes.

A novel method, based on changes in conductivity, for identifying the mineralogical nature of microfines was investigated. This method measures the cation exchange capacity (CEC) of a sample. CEC is a widely used metric for estimation of the negative impact of microfine material. This method was found to provide results similar to sophisticated laboratory methods but required significantly less instrumentation. The method, however, initially lacked sensitivity and required significantly more aggregate processing than would be acceptable for field use. The results of this study suggest that only with additional development does this method have potential for laboratory determination of CEC.

The results of this research suggest the current threshold in content for naturally occurring microfines associated with coarse and fine aggregates in the WisDOT Standard Specification results in acceptable concrete performance when conditions are optimal and meet typical ASTM laboratory test requirements. This research outcome is consistent with that of the earlier study on the role of microfines in WHRP study #0092-00-07. When microfines are present in aggregates, if air entrainment, uncontrolled water additions, certain intentional or unintentional chemical additions, and curing are not carefully monitored and controlled, then microfines in Wisconsin concrete aggregates can and do cause deleterious impacts.

ASTM-type concrete conditions are rarely met in the field and clearly one or more of the factors that can prompt deleterious influence of microfines can and often do occur in the field production of concrete. Given the mismatch between laboratory and field curing and the increasing introduction of chemical complexity into concrete mix design, research that addresses concrete performance under controlled conditions that simulate factors in field production and placement is strongly needed. The ability to enhance the state's investment in highway pavements and to prevent premature distress that has been experienced over the past decade requires a knowledge base built on this type of research. Only with this type of research can the full significance of concrete microfines be established and strategies developed to control or avoid their introduction in situations where their impact is deleterious.

Table of Contents

1: Problem Statement

The aggregates used for concrete production usually contain microfine materials (particle size <75µm) that can impact the workability, strength, and durability of the final concrete product. Field experiences in Wisconsin suggest that the current threshold of microfine content, established by the Wisconsin Standard Specification (WisDOT 2010), may not prevent these effects. Laboratory studies have demonstrated that natural microfine materials do effect the performance of concrete, but that the extent of these effects has been insufficient to explain observations of early cracking in the field. The nature of the microfine fraction of an aggregate is a function of the mineralogy of the aggregate source. It is believed that the effect of microfines on concrete properties is related to the nature and quantity of the aggregate source, and therefore new aggregate sources should be analyzed for both quantity (P200 test) and mineralogy. The microfine testing method currently employed by the state is unable to differentiate between different microfine mineralogies.

The mismatch between laboratory and field results is likely due to differences in the nature of the microfines as well as a difference in the curing conditions of the concrete batches. Laboratory specimens were cured under the most favorable humidity and temperature conditions and allowed sufficient hydration time to develop a strong microstructure. Field based projects typically allow between one hour and eight hours to elapse from the time that material is poured until the curing compounds are applied to its surface, leaving the concrete largely unprotected during early curing. Through a better understanding of the effect that different microfines have on concrete, one should be able to have a more informed opinion concerning the proper choice of aggregate and therefore an improved concrete durability.

2: Objectives and Scope of Study

ASTM C33 and similarly the Wisconsin Department of Transportation (WisDOT) Standard Specification dictate the allowable microfine content of aggregates used in concrete production. In the absence of clay minerals, a maximum of 1.5 percent of the coarse aggregate weight and 3 percent of the fine aggregate weight is considered a safe level that will not affect concrete performance. Field experiences in Wisconsin have shown that this current threshold may not assure the satisfactory performance of the resultant concrete. In particular, it has been reported that the microfines of certain coarse aggregates, even those meeting ASTM C33 limits, may be responsible for the low strength and early cracking problems detected in concrete pavements (Munoz et al. 2010).

Previous WisDOT sponsored laboratory studies to survey the microfines associated with aggregate sources in the state (Gullerud and Cramer 2002; Muñoz et al. 2007), found most of the analyzed coarse aggregate microfines in Wisconsin to be inert with respect to the mechanical properties and the durability of concrete. Only in very few cases was a deleterious impact of microfines detected and the extent of the impact was insufficient to justify the problems observed in the field.

The objective of this study was to determine the impact of the microfine fraction on strength and durability in concrete materials, in particular in those aggregates that are in compliance with WisDOT Standard Specifications. In addition, the effect of curing conditions on these properties in the presence of microfines and an alternative method for measuring the harmfulness of microfines was explored.

The research plan consisted of four tasks:

1: Quantify the impact of total (from combined coarse and fine aggregates) clay content on concrete strength development, shrinkage and porosity. Advance a fundamental knowledge of the role of clays in concrete performance so that mitigation strategies can be formed in future research.
2: Quantify clay content from several Wisconsin sources of aggregates to determine the relative contribution of clay fines from coarse aggregates and from fine aggregates.
3: Determine the cause of the disparity seen between the impact of microfines on durability in laboratory and field settings
4: Develop a rapid test to detect clay particles in aggregate sources that is both indicative of their quantity, physical and chemical nature.

The aggregates investigated in this study were initially screened from pit-run materials, later large quantities of aggregates processed to meet the WisDOT Standard Specifications for microfine content were received from aggregate suppliers, for evaluation in concrete specimens. The aggregates and the associated microfines used were selected as representative of materials from northern Wisconsin used for concrete paving projects.

3: Background

The mechanical properties of concrete are the result of cement hydration and the properties of the interface between bulk cement paste and aggregate. Microfine materials can effect concrete by changing the amount of water required to reach the specified workability, decreasing the water to cement ratio in the cement paste and also by limiting

the amount of water available for the hydration reaction. Additionally, microfine material that is tightly bonded to aggregate surface, physically affects the interface transition zone (ITZ) and the strength and durability of final concrete product. The inclusion of microfines in aggregate can be similar to replacing a fraction of cement by a corresponding portion of a supplemental cementitious material (SCM) with a similar surface area or a reactive material that may or may not be favorable. Kanan et al. suggested that microfines, although adsorbing a significant amount of interstitial water would not contribute to the early mechanical properties of the whole material (Kanna et al. 1998).

Additives having pozzolanic properties, such as metakaolin, silica fume, slag, and fly ash have been mixed during the last 50 years with Portland cement to create high performance concrete (HPC). Numerous publications have shown that the sensitivity of traditional concrete to dry curing conditions is amplified by the addition of SCMs (Atis and Bilim 2007; Bentz 2007; Guneyisi and Mermerdas 2007; Lee 2008; Malhotra and Mehta 1996; Menendez et al. 2007; Ozer and Ozkul 2004; Ramezanianpour and Malholtra 1995; Safiuddin et al. 2007). It is expected that some microfines share this sensitizing effect with other SCMs, but do not improve the strength of the final concrete because of their lack of pozzolanic activity. The level of maturity of the cement paste will be less in these mixes than in plain cement and the concrete more vulnerable to damage due to poor curing (Kanna et al. 1998; Yurtdas et al. 2006). Microfines will adsorb interstitial water and prevent the hydration of the cement particles.

The water absorption capability of a clay mineral is the main characteristic appearing to have the greatest effect on concrete performance. To fully understand these mechanisms a brief review of clay mineral structure is presented here.

Clay minerals are phyllosilicates of small particle size (< 2 μm) (14). They are formed by combining two basic *sheet* structures: one is a continuous two-dimensional *tetrahedral sheet* of composition T_2O_5 (T=Si or Si^{4+}/Al^{3+}) with individual tetrahedra linked by sharing three corners of each, and with the fourth corner pointing in any direction. The second is an *octahedral sheet* built of YO_6 octahedrons sharing edges (Y=Al^{3+} or M^{g2+} or Fe^{3+}). The different combinations of octahedral and tetrahedral sheets that form the unit *layer* of clay, in turn, generate different types of clays: when the unit layer is comprised of one tetrahedral sheet superimposed on one octahedral sheet the clay is classified as a *1:1 layer silicate*; if the unit layer of the clay consists of two outer tetrahedral sheets and an inner octahedral sheet the clay is classified as *2:1 layer silicate*.

Negative charge development on silicate clays is mainly due to isomorphous substitution in either sheet. When the intra-layer charge balance of the 2:1 type silicates is incomplete, the net charge deficit is balanced by alkaline which are earth cations situated

between the layers. These cations can be replaced easily by a different cation if the clay is immersed in a solution of an appropriate salt. The most common exchange cations are calcium, sodium and magnesium.

In the case of smectites and vermiculites, the interlayer region contains water molecules. The amount of inter-lamellar water is a function of the exchangeable cation and the relative humidity of the ambient atmosphere, for instance, the water absorption will increase following this sequence $K^+ < Na^+ < Ca^{2+} < Mg^{2+}$ (Dontsova et al. 2004). The inter-layer water increases the separation of layers so that the repeat unit of the structure normal to the sheets is larger than that in the dehydrated minerals (≈1 nm), Ffor example, a fully hydrated vermiculate, containing two layers of inter-lamellar water and its basal spacing can increase up to 1.5 nm through hydration, and smectites, basal spacing could increase from 0.95 - 1.00 nm in the dehydrated state up to 1.25 - 1.9 nm in the hydrated form. The swelling behavior changes for certain clays in aqueous solution depending upon the nature of the cation located in the interlayer region, for example, while vermiculites, as well as K^+ and NH_4^+ smectites do not normally expand beyond 1.5 nm, most Na^+ and Li^+ smectites in water or dilute solutions swell macroscopically into a gel-like state in which the average layer separation is greater than 4.0 nm and increases in proportion to $1/\sqrt{c}$, where c is the electrolyte concentration in the liquid phase (16). This is known as macroscopic or double layer swelling and is associated with the formation of a diffuse electrical double layer on each surface of the structural layer of the silicate, and the clay particles are said to be *destacked* or *exfoliated*. The water molecules absorb in between layers increasing the basal spacing to a limit where the unit layers separate from each other. This process is known as *macroscopic swelling*. In contrast, those clays only able to swell between 1.0 and 2.2 nm are known to have *crystalline swelling*. It is expected that these two behaviors in water solutions may have different but possibly profound impact on concrete properties.

Concrete used for paving projects in Wisconsin must meet the WisDOT Standard Specifications but this requirement may not assure satisfactory concrete performance. It is postulated that microfine materials may affect strength and durability even below these limits. Furthermore, the effect of microfines on the properties of concrete is not only related to the quantity of microfines present, but as to the mineralogical character of these microfines, and the curing conditions of the concrete.

A review of the pertinent literature was conducted on research published through 2006. A bibliography of these articles can be found in Section 9.

4: Methods, Materials, and Testing

4.1: Selection and Characterization of Natural Coatings

The coarse and fine aggregates of interest were those with microfines containing some fraction of clay. Igneous aggregates from sources located in Northern Wisconsin were more likely to contain clay minerals, especially clays with a strong tendency to stick to the surface of coarse aggregates (Gullerud and Cramer 2002; Muñoz et al. 2007). Therefore, the Wisconsin Department of Transportation selected and sampled a total of 28 potential aggregate sources in the Northern part of the state that met three basic criteria:

1. A mix of coarse and fine aggregate absent large size fractions retained on the 1-1/2 inch sieve.
2. Coarse aggregates (3/4 inch top size) coated with varying amounts of microfines.
3. Fine aggregates containing microfines (approaching or exceeding 3 percent mass).

Further details concerning the collected samples are in the Appendix in Section 10 (Figure 10.1.1 and Table 10.1.1).

The initial samples consisted of unwashed pit run material. From the 28 samples collected, a representative sample of aggregates was chosen via three levels of analysis (Table 1). The first analytical level provided information related to the occurrence and nature of clay minerals in the microfines. Second level of testing, three different standard tests, ASTM C117 (P200), Caltrans Test No. 227 (California Cleanness Test, CCT), and AASHTO TP 57 (Methylene Blue Value, MBV), were used to predict the potential impact of the microfines on the performance of concrete (Hosking and Pike 1985; Quiroga et al. 2006; Tourenq and Tran 1997). At the third level of analysis, microfines from sources identified in the earlier levels were subjected to further analysis to determine the mineralogy of the microfines, this was accomplished using additional X-ray and thermo-gravimetric methods. Based on the information collected in this analysis, seven aggregate sources were selected as having a mineralogical composition representative of the Northern part of the state of Wisconsin.

Concrete specimens were prepared with Type I cement. The chemical composition of the cement is presented below (Table 2). This analysis was provided by the manufacturer and was acquired according to ASTM C114.

Table 1: Analytic Methods and Desired Results

Level	Test	Information	Selection Criterions
1	X-ray Diffraction	Presence of peaks at low angles characteristic of clay with moderate to high water	Samples with potential presence of clay microfines with moderate-high water absorption capacities
	Cation Exchange Capacity (CEC)	Nature and quantity of exchangeable cations in the microfines	
2	ASTM C117 (P200)	Preliminary quantification of the impact of microfines in concrete.	Microfines with a potential impact on concrete properties
	ASHTO TP57 (MBV)		
	California Test 227 (CCT)		
3	X-Ray Diffraction	Determination of the mineralogy of the microfines	
	Thermogravimetric Analysis		

Table 2: Manufacturer's Analysis of Cement Used for Research (in percent)

SiO_2	Al_2O_3	Fe_2O_3	MgO	CaO	SO_3	K_2O	Na_2O	Loss on Ignition	C_3S	C_3A	C_2S	C_4AF	Alkalis Eq.
20.5	4.64	2.68	2.39	63.31	2.52	0.43	0.23	2.71	60	7.8	12.3	8.2	0.51

4.2: Mix Design

A total of nine concrete mixes were ultimately prepared using the aggregate sources selected from a larger set. Aggregates for concrete specimen manufacturing were received from the same pits as identified in the earlier screening but were washed aggregates, split into fine and coarse fractions. Standard sieve analysis of the fine and coarse fractions of these aggregates were conducted and the results are shown in the Section 10 (Figures. 10.2.1 – 10.2.4). Some deviations from the aggregates and WisDOT No. 1 Stone and fine aggregate standards were noted.

The concrete mix designs were based on the WisDOT Grade A specifications and are itemized in Table 3. Seven of the mixes were produced using the original aggregate sources without any modification, and two rewashed batches of aggregates were prepared. The coarse aggregate fractions had two major mineralogies; four of the sources were composed of dolomitic limestone and the balance was igneous. Based on the mineralogy

of the coarse aggregates, the mixes were divided into two groups and one rewashed batch was prepared for each group. The tests completed were slump (ASTM C143), unit weight (ASTM C138), fresh air content (ASTM C231), compressive (ASTM C39, tensile (ASTM C496) strength, drying shrinkage (C490), capillary water absorption (RILEM TC 166), and rapid chloride-ion penetrability test (ASTM C 1202). All concrete specimens were cured under wet curing (WC) (100% RH) or dry curing (DC) (30 – 60% RH) conditions. These tests are summarized in Table 4.

Table 3: Concrete Mix Designs

Mix ID	Aggregate Type	Microfine Content (coarse % and fine %)	Cement Content (lb/yd^3)	Coarse/Fine/ Cement Ratios	Water/Cement Ratio	Target Air, Percent
CS2 – control	Igneous	~0/~0	564	3.5/2/1	0.45	6.0 ±1.0
S2	Igneous	1.16/4.86	564	3.5/2/1	0.45	6.0 ±1.0
S9	Dolomitic Limestone	0.55/1.60	564	3.5/2/1	0.45	6.0 ±1.0
S10	Dolomitic Limestone	0.53/0.66	564	3.5/2/1	0.45	6.0 ±1.0
S14	Dolomitic Limestone	0.70/5.30	564	3.5/2/1	0.45	6.0 ±1.0
S18	Igneous	1.38/0.66	564	3.5/2/1	0.45	6.0 ±1.0
S19	Igneous	0.86/1.47	564	3.5/2/1	0.45	6.0 ±1.0
CS28 - control	Dolomitic Limestone	~0/~0	564	3.5/2/1	0.45	6.0 ±1.0
S28	Dolomitic Limestone	0.32/1.04	564	3.5/2/1	0.45	6.0 ±1.0

Table 4: Tests Conducted on Plastic and Hardened Concrete Specimens

Test Standard	Common Name	Brief Overview of Method
ASTM C143	Slump test	An inverted cone of concrete is prepared. The cone is removed and the distance the concrete slumps is measured.
ASTM C138	Unit Weight	A sample of concrete is consolidated in a container of known volume and weighed.
ASTM C231	Air Content	A sample of concrete is consolidated in an air tight chamber with known volume. A small amount of pressurized air is added and the final pressure of the system is used to calculate the void volume.
ASTM C39	Compressive Strength	A well consolidated cylinder of concrete is prepared and cured. The sample is tested to failure under compression while measuring the stress/strain response.
ASTM C496	Tensile Strength	A well consolidated cylinder of concrete is prepared and cured. The sample is tested to failure under tension while measuring the stress/strain response.
ASTM C490	Drying Shrinkage	A well consolidated prism of concrete is prepared and changes in length are monitored as the sample cures.
ASTM C1202	Rapid Chloride Ion Penetrability	Opposing ends of sample of cured concrete are placed in electrically isolated reservoirs of chloride solution. A voltage bias is applied across the sample and the passing of charge is monitored to determine the susceptibility of the sample to chloride penetration.
RILEM TC 116	Capillary Water Adsorption	Two-inch mortar cubes are prepared and coated on four sides with epoxy leaving only the top and the bottom of each cube exposed. They are then oven dried at 80°C (176°F) until a stable weight is achieved. The amount of water absorbed is determined by measuring the new weight of the cubes after 10 min, 30 min, 1 hour, 2 hours, 12 hours, and 24 hours.

4.3: Microanalysis

4.3.1: Microanalysis of the Cement Paste

The microstructure and chemistry of the concrete and cement paste samples containing the above microfines were studied using X-ray diffraction, thermogravimetric (TG), Differential Thermal Analysis (DTA), N_2 absorption isotherms, scanning electron microscope (SEM), and energy dispersive X-ray spectroscopy (EDS). For these studies, a total of 12 cement paste specimens were prepared. For 11 batches, cement was mixed with one of the previously described microfines, the 12^{th} specimen served as the control and contained no microfines. Each cement paste specimen contained 20 g of cement powder with a water-cement ratio of 0.45, and a microfine concentration of 3 percent of the

weight of cement. The microfines were first mixed with the cement powder, then water was added and the mixture stirred for two minutes. The samples were maintained under high relative humidity until testing. The evolution of the samples was followed over a period of 14 days by X-ray diffraction. Paste diffractograms were recorded at 1 day, 7 days, and 14 days from pouring.

The hydration reaction kinetics were estimated by tracking both the disappearance of cement components, such as tricalcium silicate (C3S) and dicalcium silicate (C2S), and the appearance of hydration products, such as calcium hydroxide and ettringite. CaF_2 was added as an internal standard (2.5 percent in weight concentration) to obtain semi-quantitative information from the diffractograms. Peaks in the diffractograms were identified by comparison with the Powder Diffraction Files (PDF). Specimens were prepared using the selected microfines and additional pastes were prepared with three standardized clay minerals known to have pozzolanic activity (He et al. 1995; Malhotra and Mehta 1996): kaolin, sodium montmorillonite, and calcium montmorillonite.

The degree of hydration after 14 days was measured by thermogravimetric (TG) analysis and differential thermogravimetric analysis (DTA). Capillary porosity, pore volume and pore size distribution of the hardened cement pastes were measured using N_2 adsorption isotherms at 77°K. Surface areas were calculated using the Kelvin equation.

4.3.2: Microanalysis of the Concrete

The microstructure of the concrete samples was studied by a combination of scanning electron microscope (SEM) and energy dispersive X-ray spectroscopy (EDS). The combination of techniques allowed detection of different mineral morphologies and chemical composition in the cement paste. Backscattering electron (BSE) images of the samples at two different magnifications were taken using a LEO DSM 1530 Field Emission Scanning Electron Microscope at 15 keV.

Micrographs (2500x) were obtained and combined with EDS analysis to identify the principal mineralogical phases, to measure the microfine distribution and to determine the porosity of the ITZ. For the purpose of this study, a bulk area was defined as any cement paste site situated a minimum of 100 μm from a coarse aggregate. EDS analysis was performed using the Thermo-Scientific NSS software in the X-ray line-scan mode, the elemental composition was determined over a vector of 40 μm length, 40 points per vector, see Figure 1. The distribution of the microfines in the ITZ was estimated from the number of microfine particles intersected by each of the line scans. The porosity in the ITZ was determined with the same methodology as that described for the porosity profiles below.

Micrographs (1500x) were taken at increasing depths starting from the external surface of each sample. These images were combined to create a cross-section of the sample to determine the fraction of the system with a pore size between 5 and 50 μm (Lange et al. 1994).

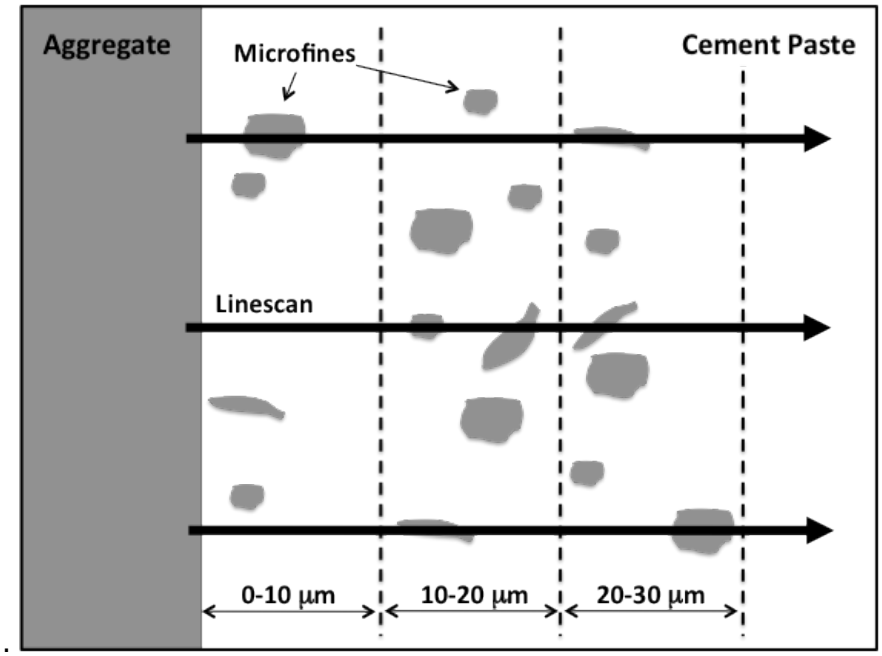

Figure 1: Schematic Representation of EDS Analysis

4.4: Conductivity Based Test for Cation Exchange Capacity (CEC)

A methodology based on electrical conductivity changes due to ion exchange reactions was investigated. Clays present in microfines contain cations that can be exchanged with an electrolyte solution. Upon exchange, the conductivity of the electrolyte solution should vary as each cation has its own unique specific conductivity. This change in conductivity can be used to determine the amount of cation exchanged and therefore the cation exchange capacity of the clay. Multiple combinations of exchanging cations, concentrations of electrolyte, and clay concentrations were tested using conductivity probes. Conductivity meters are simple, inexpensive, and robust instruments, and thus suitable to be used in the field. All clay suspensions requiring separation were centrifuged at 8500 g for 30 minutes.

This method was tested for solutions of Ca-Na nitrates, Ca-K nitrates, Ca-Mg nitrates, K-Mg nitrates, and Ca-Na-K nitrates. Nitrate was selected as the anion because of its low equivalent conductance and lack of complex ion formation or formation of insoluble

salts. The above-mentioned cations were selected because they are the most common exchangeable cations in clays or possess markedly different specific conductivities which serve to improve the sensitivity of the method, other cation combinations are possible if the clay is first fully exchanged prior to analysis. The clays tested, were samples obtained from the Clay Mineral Repository.

5: Results

5.1: Selection of the Aggregates by Microfine Content

The microfines fell into three major groups with respect to the presence of peaks at a d-spacing between 6 and 44 Å in their X-ray diffractogram, indicative of clay minerals (Table 5). The diffractograms of the first group showed sharp peaks in this region. Those of the second group display a broad band between 9 and 18 Å. The third group of microfines does not show peaks in this d-spacing region. The diffractograms of 19 of 28 specimens of microfines showed the presence of clay minerals. The diffractograms of the rest of the microfines, nine in total, did not have peaks indicative of clays. Peaks at 7.11, 14.52, and 9.91 Å are linked to kaolin type silicates, Na/Mg vermiculites and/or smectites, and K vermiculites respectively. Most of the microfines contain both 1:1 and 2:1 type clays. These ratios describe the microstructure of the clay by specifying the ratio of tetrahedral to octahedral layers as described earlier.

Table 5: Preliminary Characterization Results from Level 1 of the Selection Process

ID	XRD Peaks d-spacing (Å) at low angles	CEC (meq/100 g)	Classification
S1	14	43.21	I*
S2	No peaks	33.31	III♣
S3	Broad peak between 18 - 9	58.97	II◊
S4	No peaks	39.04	III
S5	13.6 and 7	53.54	I
S6	Peak at 6.5	53.57	I
S7	Broad peak between 18 - 9	55.69	II
S8	Bread peak between 18 – 9	58.65	II
S9	Peaks at 25.6, 14.2, 10, and 7	46.19	I
S10	Broad peak between 18 – 9	53.15	II
S11	Broad peak between 18 - 9	59.77	II
S12	12	56.64	I
S13	Peaks 16, 14.7, and 11	63.58	I
S14	13.7	53.8	I
S15	Broad peak between 18 - 9	52.52	II
S16	No peaks	56.41	III
S17	No peaks	61.61	III
S18	15.8	68.26	I
S19	No peaks	65.6	III
S20	Broad peak between 18 - 9	58.48	II
S21	10.1, 8.6, and 7.1	53.6	I
S22	14.4 and 7.3	50.39	I
S23	No peaks	56.41	III
S24	No peaks	51.53	III
S25	7.3	54.3	I
S26	No peaks	51.91	III
S27	No peaks	66.52	III
S28	Broad peak between 18 – 9	52.51	II

* I: presence of clays
◊ II: sign of presence of clays
♣ III: absence of clays

The microfines displayed similar values for cation exchange capacity (CEC) regardless of mineralogy. Only four samples, S1, S2, S4, and S9, had CEC values under 50 mEq/100 g. The CEC value for most natural clays measures between 1.7 and 74 mEq/100 g (Jaynes and Bigham 1986). The similar CEC values of the different microfine samples suggest that, the microfines contain a mix of different types of clay minerals. Samples with no indication of clay minerals but with CEC values greater than 51 mEq/100 g could be due to the presence of clay minerals having low crystallinity that are not visible with X-ray analysis.

The results of the X-ray analysis were used as the principal selective factor for the first round of selection. A total of nine aggregates were selected for further testing (Table 6). The selected aggregates consisted of: four for which the diffractogram showed sharp peaks of clay minerals (S1, S9, S14, and S18), three with microfines diffractograms showing a broad band at high d-spacing values (S10, S15, and S28), and two with no clay mineral appearing in the diffractogram of their microfines. The difference between these two consisted in having a low (S2) and a high (S19) CEC.

The California Cleanness Test (CCT) values and the Methylene Blue Values (MBV) were obtained to determine the potential impact of the microfines on concrete performance. The results are summarized in Table 6. The microfine quantities in the fine aggregate sources S1, S2, and S14 were above the WisDOT P200 limits. The CCT values for aggregates except S18 were above 75, the recommended threshold value established by the California Department of Transportation. The Methylene Blue Values varied from 0.7 to 32.5 mg/g. Microfines with a MBV higher than 3 mg/g can provoke high water demand in concrete mixes (Quiroga et al. 2006). All microfines except S1 are likely to cause disruptions in the entrained air content and slump of concrete. Microfines were classified to be innocuous, have an impact at levels higher than WisDOT limits, or have an effect even under WisDOT limits.

Table 6: Results of Classification of the Selected Microfines

	Coarse Aggregate		Fine Aggregate		Evaluation			
ID	**P200 (%)**	**CCT**	**P200 (%)**	**MBV (mg/g)**	**M/C Ratio**	**CCT**	**MBV**	**Classification**
S1	2.41	89	3.68	2.3	0.162	High	Low	Innocuous
S2	1.16	97	4.86	7.5	0.146	High	Moderate	Impact @ P200 > C33 Limits
S9	0.55	81	1.6	22	0.054	Medium	High	Impact @ P200 > C33 Limits
S10	0.53	91	0.66	13.2	0.032	High	Moderate	Impact @ P200 > C33 Limits
S14	0.7	91	5.3	5.4	0.141	High	Low	Innocuous
S15	0.45	91	1.93	9.5	0.058	High	Moderate	Impact @ P200 > C33 Limits
S18	1.38	69	0.66	32.4	0.060	Low	High	Impact @ P200 < C33 Limits
S19	0.86	81	1.47	26.2	0.061	Medium	High	Impact @ P200 < C33 Limits
S28	0.32	94	1.04	6.7	0.034	High	Low	Innocuous

Seven aggregates out of the previous nine were chosen for use in concrete mixes eliminating S1 and S15. These aggregates contain microfines of the three main groups created from the analysis at Level 2: S14 and S28 labeled as innocuous; S2, S9, and S10

as potentially causing negative effects at quantities above the WisDOT P200 threshold; and S18 and S19 as potentially causing negative effects even at quantities under the WisDOT P200 threshold.

5.2: Mineralogical Characterization of Microfines from Selected Aggregates

5.2.1: X-ray Analysis

The results of the X-ray analysis were summarized in Table 7. An example diffractogram is provided in Figure 2. Microfine specimens were mixes of different minerals with quartz as a major component except for S9 and S28 samples. The microfines were further divided into two groups according to the nature of the non-quartz minerals present. Group A consists of microfines from S9, S10, S14, and S28 that contain significant quantities of dolomite and/or calcite. These microfines were principally associated with dolomitic limestone aggregates. Group B microfines from S2, S18, and S19 consist mainly of igneous rocks. These microfines are low in magnesium, calcium carbonate content and contain clay minerals, principally 1:1 and 2:1 phyllosilicates.

Table 7: Mineralogical Properties of Selected Microfines

Group	Sample	X-ray	TG/DTA (% of loss)
A	S9	Quartz, Dolomite, & 2:1 phyllosilicate (vermiculite)	Dolomite (23.65)
	S10	Quartz, Dolomite	Dolomite (18.70)
	S14	Quartz, Dolomite, & Calcite	Dolomite & Proto-dolomite (16.61)
	S28	Quartz, Dolomite, & Tectosilicate (anorthite)	Dolomite (33.36)
B	S2	Quartz, Tectosilicate (microcline), & 1:1 (Illite and kaolinite) and 2:1 phyllosilicate (vermiculite)	Fe/Al hydroxide dehydroxylation (0.37) 1:1 & 2:1 Clay Mineral dehydroxylation (1.54)
	S18	Quartz, Tectosilicate (anorthite), & 2:1 phyllosilicate (vermiculite)	Fe/Al hydroxide dehydroxilation (0.40) 1:1 & 2:1 Clay Mineral dehydroxilation (1.82)
	S19	Quartz and Tectosilicate (albite)	Fe/Al hydroxide dehydroxilation (0.40) 1:1 & 2:1 Clay Mineral dehydroxilation (1.51)

5.2.1.1: Group A: Microfines from Dolomitic Limestone Aggregates.

The majority of the microfine portion of Group A aggregates consists of quartz. Peaks in the diffractograms other than quartz were associated with dolomite in S10 and a mix of carbonates, dolomite, and calcite in S14. In the diffractograms of microfines from S9 and S28, the most intense peak does not belong to quartz, but is associated with the 104 reflection of dolomite. The diffractogram of the microfines from the S10 and S14 sources contains a small peak associated with 2:1 phyllosilicates (d = 14.43 Å).

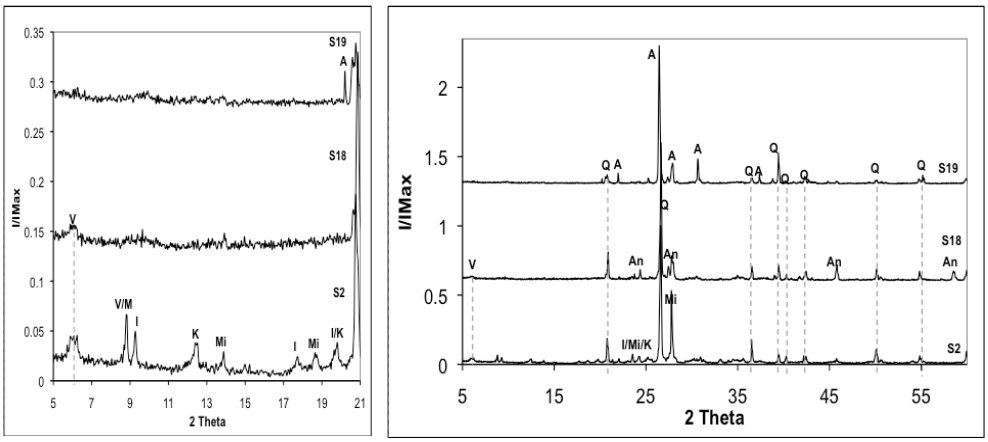

Figure 2: X-ray Diffractograms of the Group B of Microfine Samples. A: albite, An: anorthite, I: illite, K: kaolinite, M: muscovite, Mi: microcline, Q: quartz, and V: vermiculite

5.2.1.2: Group B: Microfines from Igneous Aggregates.

Quartz was also the dominant mineral in the Group B microfines. The samples contained aluminosilicates, principally tectosilicates from the feldspar group. S2 contained microcline ($KAlSi_3O_3$) along with 1:1 phyllosilicates such as illite and kaolin. Group B microfines also contained 2:1 phyllosilicates such as vermiculite. S18 only had peaks corresponding to anorthite ($CaAl_2Si_2O_8$) and vermiculite. S19 did not contain any phyllosilicates (clays), and the only feldspar that was found was albite ($NaAlSi_3O_3$).

5.2.2: <u>Thermal Analysis</u>

Thermogravimetric analysis (TGA) was used to determine the mineral composition of the microfine samples. This method uses mass or temperature changes as the microfines are heated to determine mineral content.

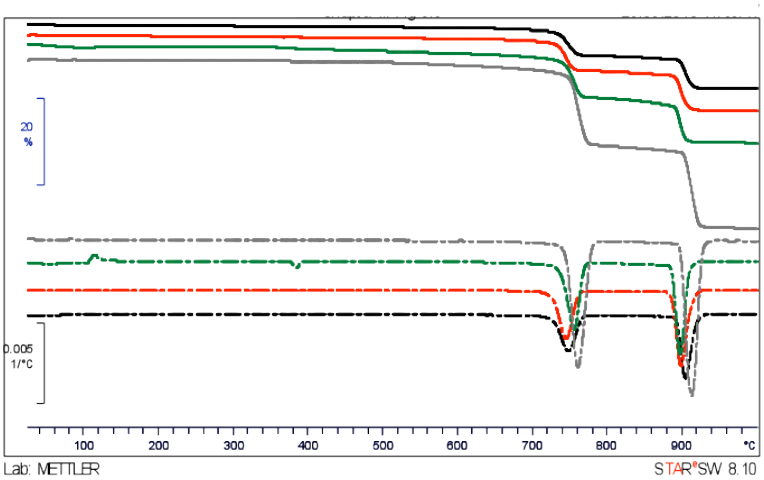

Figure 3: TG (Top) and DTG (Bottom) Curves for Group A Microfines: S28 (Grey), S9 (Green), S10 (Black), and S14 (Red)

5.2.2.1: Group A: Microfines from Dolomitic Limestone Aggregates.

Representative TG and DTG curves of these microfines heated under a CO_2 atmosphere are shown in Figure 3. The quantitative information extracted from these curves is presented in Table 8. TG curves for all of the microfines show losses characteristic of the decomposition of dolomite. The temperature peak occurred at higher temperatures for S14 and S9, therefore the dolomite in S14 and S9 was characterized as having higher calcium content than the S28 and S10 dolomite.

Table 8: Summary of TG Curve Information of Cement Paste Samples Made with Different Microfines.

	% over sample weight at Temperature Range (^oC)								
Sample	**400**	**400-500**	**550-700**	**750-950**	**% $Ca(OH)_2$**	**% $CaCO_3$**	**% Ca from $Ca(OH)_2$**	**% Ca from $CaCO_3$**	**Total % Ca**
S2	25.26	5.20	3.39	0.63	20.80	7.70	11.79	3.09	15.33
S10	26.90	5.60	3.03	0.66	22.39	6.89	12.69	2.76	15.93
S14	26.42	5.54	3.51	0.75	22.15	7.99	12.55	3.20	16.24
Kaolin	26.58	5.87	2.73	0.57	23.49	6.21	13.31	2.49	16.29
Control	**22.10**	**5.75**	**4.09**	**0.96**	**23.00**	**9.30**	**13.04**	**3.73**	**16.76**
S9	27.06	5.74	3.62	0.75	22.97	8.23	13.02	3.30	16.82
CaM	25.47	5.71	3.71	0.68	22.84	8.44	12.94	3.38	16.83
S28	27.23	5.83	3.44	0.74	23.31	7.81	13.21	3.13	16.84
NaM	26.58	5.97	3.29	0.77	23.90	7.48	13.54	3.00	17.05

5.2.2.2: Group B: Microfines from Igneous Aggregates.

Thermogravimetric analysis showed that these microfines contained Fe/Al hydroxides and 1:1 and 2:1 clay minerals. The S18 microfine sample had a greater percentage of mass of 1:1 and 2:1 phyllosilicates than S2 and S19. Samples S18 and S2 showed small mass losses at temperatures associated with the decarbonation of dolomite.

5.3: Effect on Fresh Concrete Properties

Slump, unit weight, and air content were measured for each concrete mix (Table 9). The concrete batches were divided into two groups according to the mineralogy of the aggregate and microfines used in the mix. Microfines in group A were rich in dolomite-like minerals and those in group B were predominantly aluminosilicates. The results clearly show that the early properties of concrete are significantly affected by the type and quantity of microfines present in both the coarse and fine aggregates.

Table 9: Physical Properties of Fresh Concrete Prepared with Microfine Samples

Batch ID	Coating Group	AEA (oz/100lbs cement)	Slump, inches	Unit Weight, lb/ft^3	Fresh Air Content (%)
CS28	A	56	3 ½	41.80	7.0
S9		48	2 ¼	42.34	5.2
S10		37	2 ¼	41.68	6.1
S14		37	½	42.58	5.0
S28		56	5 ½	41.90	7.0
CS2	B	52	¼	41.50	5.0
S2		64	0	39.80	3.2
S18		45	¼	41.34	4.0
S19		37	2 ¼	41.56	6.7

5.3.1: Group A: Concrete Batches Containing Microfines from Dolomitic Limestone Aggregates.

Batch CS28 was made with washed aggregate as a control. Batches CS28 and S28 required 56oz/100lbs cement of air entraining agent (AEA) to reach an air content of 7 percent. Batches S10 and S14 required only 37oz/100lbs cement of AEA to achieve an air content of 6.1 percent and 5.0 percent, respectively. Batch S9 is a clear example on the influence of microfines on air content. Concrete made with this aggregate source required 48oz/100lbs cement of AEA to reach a level of 5.2 percent air. This was due to the significant quantity of 2:1 phyllosilicates present in this source. S14 was the only concrete batch from this group to display poor workability, with a slump value of 1/2 inch. The washed CS28 batch had a slump value of 3 ½ inches, while the slump value for the S28 batch was of 5 ½ inches.

5.3.2: Group B: Concrete Batches Containing Microfines from Igneous Aggregates.

Concrete batches containing S2 and S18 microfines displayed very poor workability and poor AEA efficiency. These are typical symptoms of mixes contaminated with clay minerals (Muñoz et al. 2007). The S2 mixture showed high stiffness and achieving the

target air content was impossible without introducing more water. The addition of 64oz/100lbs cement of AEA only rendered an air content of 3.2 percent. S18, with a lower M/C ratio (0.060), displayed similar but less acute symptoms. Batch S18 had a slump of 6.3 mm (0.25 inches) and an air content of 4.0 percent, with less AEA volume. Both microfines showed peaks in the XRD diffractograms associated with 2:1 phyllosilicates. Batch CS2 was made with washed aggregates from source S2. The lack of improvements on the early properties of concrete after washing was due to both the difficulty of washing fine aggregates and the tendency for the 2:1 phyllosilicate clays to adhere to the large aggregate fraction. The washing process only eliminated microfines with weak adhesion to the surface of the aggregate, leaving behind 2:1 phyllosilicates which will impair the early mechanical properties of the concrete. Batches S18 and S19 had similar microfine to cement ratios but S19 had superior early properties. S2 and the washed aggregate batch CS2 had significantly different unit weights due to the poor workability of the batch with S2 microfines.

5.4: Effect on Compressive Strength

The compressive strength of each batch was measured after curing for 7 and 28 days. Numerical values and values for calculated parameters are given in Section 10 (Table 10.2.1). As expected, all of the specimens subjected to a dry curing (DC) process exhibited lower values of compressive strength than those cured at high relative humidity (WC).

5.4.1: Group A: Concrete Batches Containing Microfines from Dolomitic Limestone Aggregates.

Wet cured concrete showed two different behaviors with respect to compressive strength (Figure 4). S28 and S9 had same strength as the washed batch CS28, while S10 and S14 showed significant improvements in strength. The magnitude of the improvements correlated with the amount of microfines in the cement. S10 and S14 microfines had less carbonate and more quartz than S28 and S9. Batches S28 and S9 slightly decreased in strength relative to the control. The increase in compression strength due to the presence of microfines slightly diminished at longer curing times.

The DC batches demonstrated the negative effect of some microfines. There was little or no gain in strength for specimens from S14 and S10 between 7 and 28 days. At 28 days the presence of microfines magnified the deleterious effects of curing under dry conditions. The control batch CS28 had a higher compressive strength than all of the batches containing microfines.

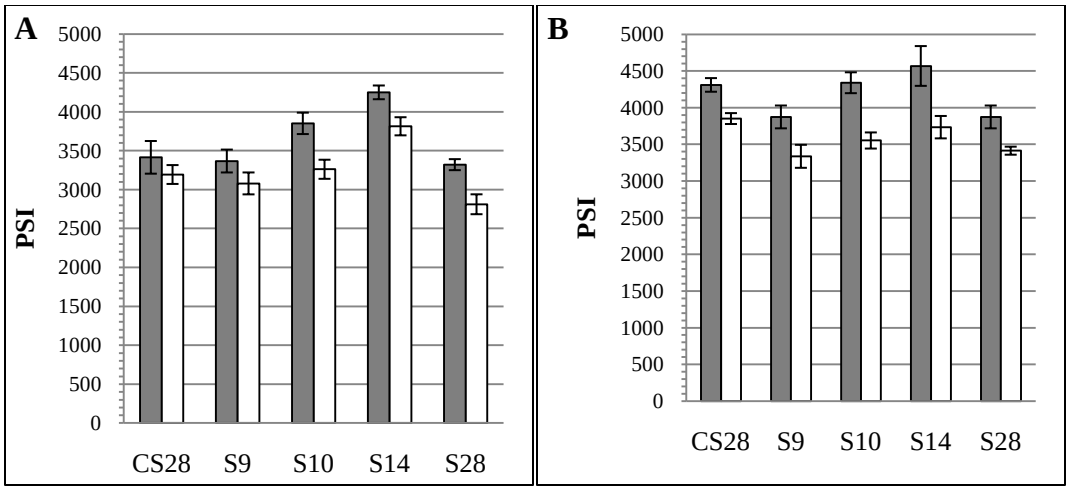

Figure 4: Values of Compressive Strength at 7 (A) and 28 (B) Days of Curing Under WC (Dark Grey Column) and DC (Light Column) for Concrete Batches of Group A

5.4.2: Group B: Concrete Batches Containing Microfines from Igneous Aggregates.

Similar trends in strength were noticed in concrete batches prepared with microfines from Group B. In those specimens with adequate curing moisture the presence of microfines did not have any obvious deleterious impact on the compressive strength at both tested curing times (see Figure 5) because water additions were not made during mixing to counteract low workability. However, clear trends are masked in this group because the control, CS2, did not display the strength gain typical of wet curing from 7 to 28 days. Batches S18 and S19, exhibited greater strength after 28 days than the washed batch, CS2, perhaps due to the potential pozzolanic reactivity of the phyllosilicates (clay) fraction in the case of S18 and decreased porosity in the case of S19.

The effect of the microfines reappeared when the batches were cured under a dry environment. The specimens containing microfines displayed lower values of compressive strength than the washed batch. The magnitude of the decrease was related to the amount of microfines in the batch except source S19. At longer curing times the differences were reduced.

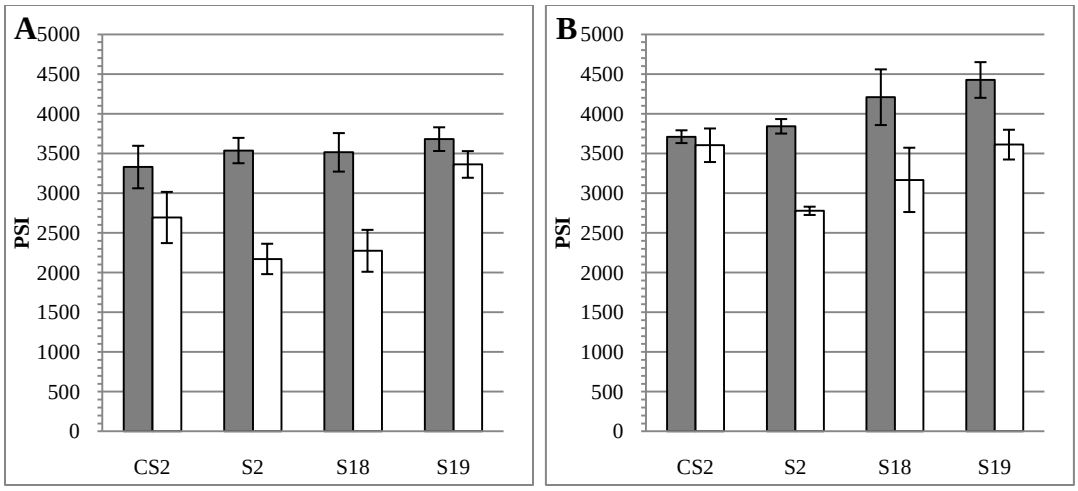

Figure 5: Values of Compressive Strength at 7 (A) and 28 (B) Days of Curing Under WC (Dark Grey Column) and DC (Light Column) for Concrete Batches of Group B

5.5: Effect on Tensile Strength

The tensile strength of each batch was measured at 7 and 28 days. The results are shown in Figures 6 and 7 and summarized in Section 10 (Table 10.2.2). No significant difference in the 7 day strength was detected between WC and DC specimens, except in batches S9 and S14. The DC samples had a lower strength at 28 days.

5.5.1: Group A: Concrete Batches Containing Microfines from Dolomitic Limestone Aggregates.

There was not a significant difference in the tensile strength values for wet cured (WC) samples after 28 days. Dry cured (DC) specimens containing microfines had lower values of tensile strength than the washed batch except S14. Sample S14 had the greatest tensile strength and the largest M/C ratio in the group. Both quantity and mineralogy of the microfines influence the tensile strength under DC conditions. Other properties such as the shape and surface area of the aggregates were not explored in this research.

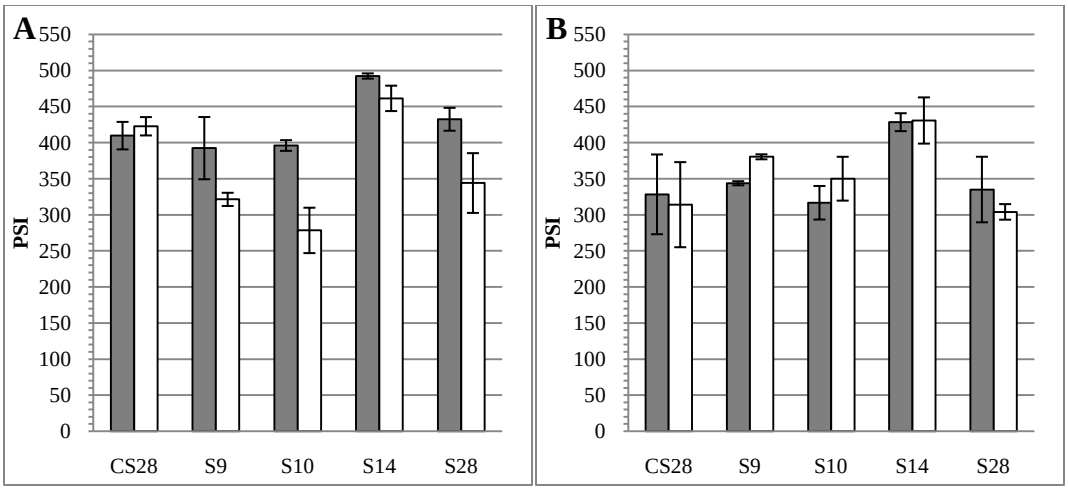

Figure 6: Values of Tensile Strength at 7 (A) and 28 (B) Days of Curing Under WC (Dark Grey Column) and DC (Light Column) for Concrete Batches of Group A

5.5.2: Group B: Concrete Batches Containing Microfines from Igneous Aggregates.

Wet cured Group B concretes had the same 28 day tensile strength as that of the washed batch, CS2. Dry cured batches increased in strength after 28 days. Beneficial pozzolanic reactions may counteract the negative effect of dry curing. The microfines of this group are characterized as having significant amounts of phyllosilicates (clays) as coatings on the aggregate surface. The combination of the pozzolanic activity of clays as aggregate coatings may improve the interfacial strength and therefore the tensile (but not compressive) strength of the material.

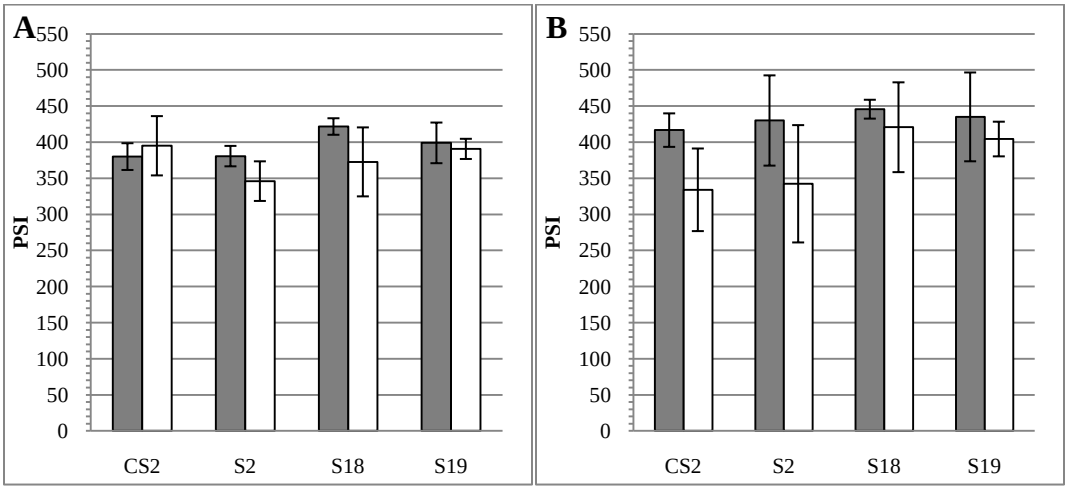

Figure 7: Values of Tensile Strength at 7 (A) and 28 (B) Days of Curing Under WC (Dark Grey Column) and DC (Light Column) for Concrete Batches of Group B

5.6: Effect on Long-term Shrinkage

Long-term shrinkage was monitored over 120 days. Table shows the shrinkage at 27, 51, and 120 days from casting for both wet curing and dry curing. Long term shrinkage (57 and 120 days) was not dramatically impacted by the presence of microfines under either curing regime, except batch S2. Sample S2 displayed significantly higher shrinkage due to the presence of 2:1 phyllosilicates and even after rewashing in the laboratory concrete containing this aggregate source had larger shrinkages. The comparison between values under different curing regimes revealed that certain microfines seem to prompt changes in shrinkage.

Table 10: Drying Shrinkage Values (%) at 27, 51, and 120 Days

	Wet Curing Process (WCP)			**Dry Curing Process (DCP)**		
Sample	27 days	51 days	120 days	27 days	51 days	120 days
CS28	0.0297	0.0400	0.0557	0.0427	0.0503	0.0660
S28	0.0303	0.0453	0.0640	0.0403	0.0530	0.0697
S9	0.0337	0.0447	0.0677	0.0397	0.0473	0.0627
S10	0.0310	0.0427	0.0577	0.0363	0.0507	0.0630
S14	0.0287	0.0417	0.0627	0.0430	0.0540	0.0673
CS2	0.0430	0.0697	0.0930	0.0573	0.0767	0.0963
S2	0.0397	0.0757	0.0953	0.0617	0.0833	0.0933
S18	0.0400	0.0557	0.0767	0.0507	0.0573	0.0767
S19	0.0267	0.0407	0.0593	0.0453	0.0523	0.0723

5.6.1: Group A: Concrete Batches Containing Microfines from Dolomitic Limestone Aggregates.

The DC concrete samples experienced slightly higher shrinkage than the WC. The difference was greater at 51 days and became lower at 120 days. Low relative humidity environments will increase the evaporation of free water and therefore will increase the amount of shrinkage (Holt and Leivo 2004).

Comparison of the different curing regimes revealed shrinkage depended more on the nature of the microfine than on its quantity. At 27 days S10 and S14 had similar shrinkage. These microfines were present in higher concentration and consisted of more crystalline quartz and less carbonates than S28 and S9. Samples S28 and S9 were made with microfines low in quartz and higher in carbonates and shrank more.

5.6.2: Group B: Concrete Batches Containing Microfines from Igneous Aggregates.

As in previous examples, dry curing conditions produced slightly higher values of shrinkage. Batches having microfines showed greater sensitivity to the curing regimen at early ages.

5.7: Effect on Capillary Water Absorption

Sorptivity was measured at 7 and 28 days following the RILEM test standard as listed in Table 3. There was correlation between sorptivity and compressive strength as shown in Figure 8 reflecting a relationship between specimen porosity and strength. The results of the capillary water test (sorptivity) are shown in Figures 9 and 10 and summarized in Section 10(Table 10.2.3).

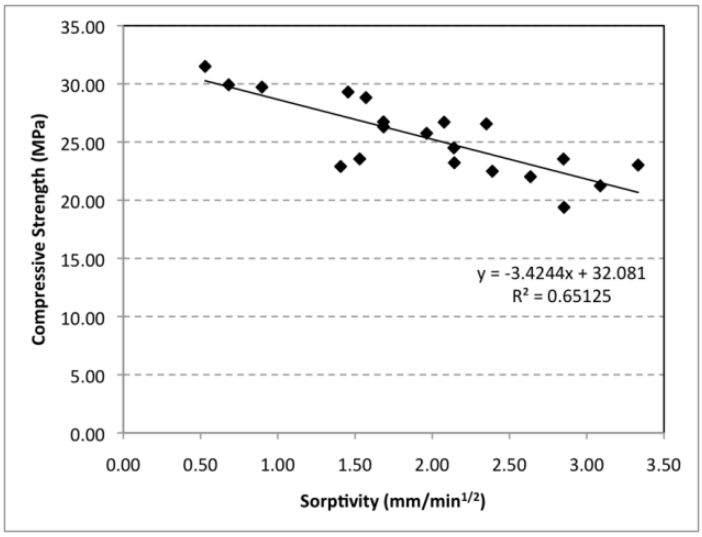

Figure 8: Correlation Between Sorptivity and Compressive Strength for the Entire Sample Population at 7 and 28 Days of Curing.

5.7.1: Group A: Concrete Batches Containing Microfines from Dolomitic Limestone Aggregates.

Sorptivity values for DC and WC batches did not correlate with the concentration of microfines in the batch. Under high relative humidity the sorptivity values decreased with longer curing times. In S10 and S14 the net decreases were greater than that of the washed batch. The magnitude of these improvements correlated with the amount of microfines in the batch. S9 and S28 did not exhibit significant differences in sorptivity between WC and DC conditions. S14 and S10 contain more quartz, primarily crystalline quartz, and significant differences result in the sorptivity over time when dry curing

conditions prevail. The transformation of dolomites under basic conditions may increase porosity and therefore sorptivity. This was not seen in the DC specimens as the low humidity quenched the hydration reactions.

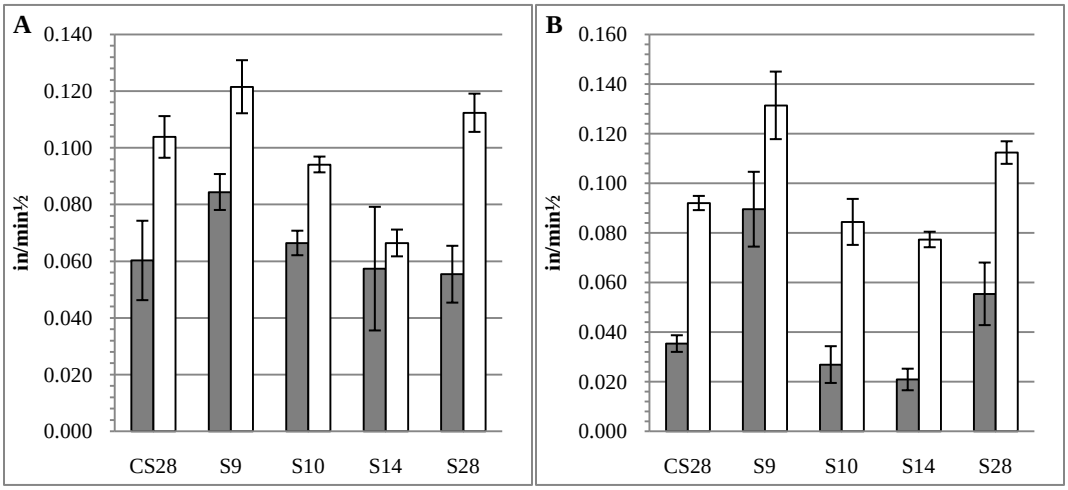

Figure 9: Sorptivity Values for WC (A) and DC (B) Concrete Specimens Made with Microfines from Group A at 7 Days (Gray Column) and 28 Days (White Column) of Curing

5.7.2: <u>Group B: Concrete Batches Containing Microfines from Igneous Aggregates</u>.

WC samples had lower sorptivity values than the DC samples, and further improvements occurred as the concrete samples aged. The DC samples showed only a small decrease or an increase in sorptivity as the samples aged (Figure 10).

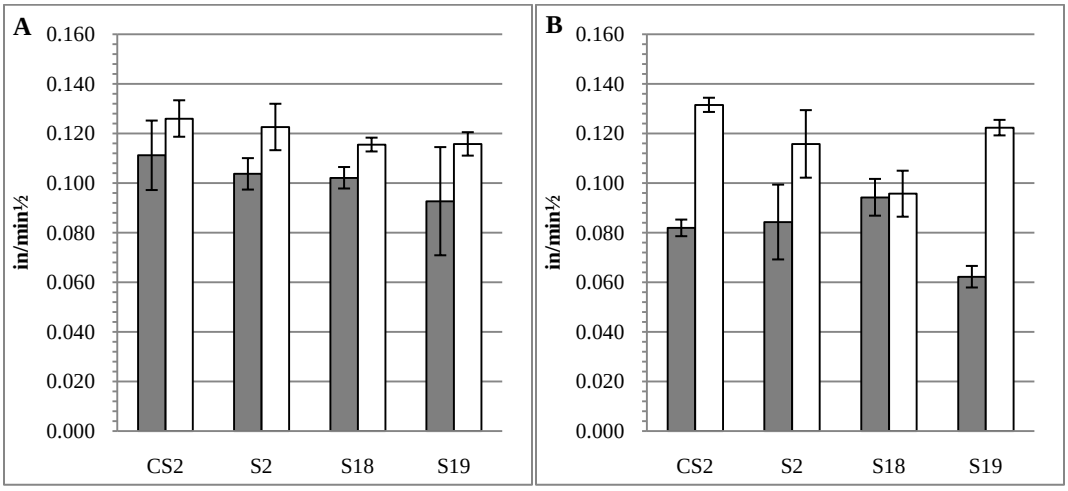

Figure 10: Sorptivity Values for WC (A) and DC (B) Concrete Specimens Made with Microfines from Group B at 7 Days (Gray Column) and 28 Days (White Column) of Curing

5.8: Effect on Rapid Chloride Penetrability

The rapid chloride penetrability (RCP) was measured in the concrete batches cured under both wet and dry conditions. The results are shown in Figure 11, and summarized in Section 10(Table 10.2.4).

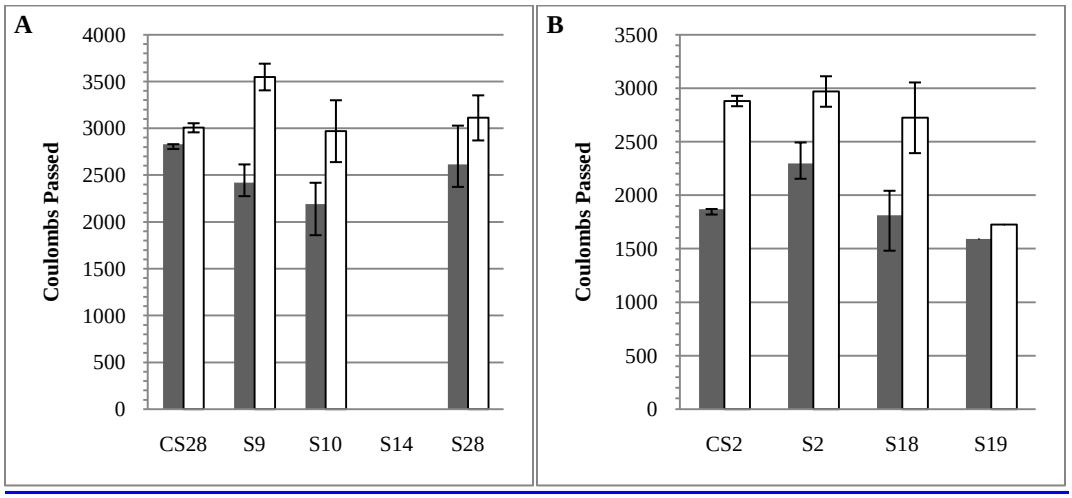

Figure 11: Rapid Chloride Penetration Test Results at 7 (A) and 28 (B) Days. Wet Cured Samples in Gray and Dry Cured Samples in White.

5.8.1: Group A: Concrete Batches Containing Microfines from Dolomitic Limestone Aggregates.

Wet cured samples exhibited decreased chloride penetration when microfines were present. Chloride penetration increased when identical concrete mixes were cured under dry conditions. Microfines, even meeting the limiting standards of ASTM C33, enhance the negative impacts of the dry curing process. These changes were not correlated with quantity or mineralogy of the samples.

5.8.2: Group B: Concrete Batches Containing Microfines from Igneous Aggregates.

Chloride penetration increases dramatically in clay-containing concrete samples that have been cured inadequately. Even the small amount of microfine material that was not removed during the washing process (C-S2) caused a marked increase in chloride penetration for DC batches. The exception was S19 that did not contain clay minerals. For S19, the value of the chloride penetrability did not change significantly due to the curing process.

5.9: Microanalysis of the Concrete Samples

5.9.1: Effect of Microfines on the Hydration Reaction and Pore Structure of Hardened Cement Paste

The microstructure of cement paste can be described as consisting of four phases: unreacted cement, aggregate interface products (C-S-H), pore products (CH), and pore space. The C-S-H phase is the major component in concrete and consists of nearly amorphous (non-crystalline) tobermorite [$Ca_5Si_6O_{16}(OH)_2$ $4H_2O$] with many imperfections. The primary particle or building block for C-S-H is still a subject of controversy. One of the leading models describes the structure of the C-S-H as a colloidal granular system (CMII Model) (Jennings et al. 2008). C-S-H is modeled as consisting of grains or globules about 4 nm across. These grains include pores with diameter between 1 and 4 nm (gel pores). This basic unit may pack differently to produce high density (HD) regions or low density (LD) regions. The pores between grains range between 4 and 100 nm in diameter.

The packing (LD or HD) and porosity in the cement can affect durability, elasticity and percolation (Jennings et al. 2008, Aono et al. 2007). Porosity and packing are influenced by water/cement ratio, microfines, curing, drying, and addition of admixtures (Jennings 2000).

5.9.1.1: X-ray Analysis

X-ray analysis was used to determine the effects of microfines on the kinetics of cement hydration in Section 10(Figures 10.3.1 - 10.3.4).

C3S was absent from the diffractograms of pastes containing dolomitic and siliceous microfines aged for 14 days. In cement paste samples with microfines rich in clay minerals, C3S was detectable after 14 days. In cement paste containing montmorillonite C3S was not detectable in samples aged for 7 days. $Ca(OH)_2$, the principal hydration product, was visible after 1 day of curing in all the cement paste samples. Quartz was detected in the diffractograms of all dry cement samples containing siliceous microfines (S2, S18 and S19) and in one with dolomitic microfines (S14). The quartz was reacted in S19 after 1 day for the rest of the pastes after 7 days. Dolomite was detected in all the dry cement mixtures with microfines associated with dolomitic aggregate sources except S28. The dolomite had reacted after 1 day in S9 and S10 and after 7 days in S14. Quartz and dolomite are shown to be reactive microfines consumed as hydration progresses.

C3S hydrates faster in cement pastes with dolomitic microfines that are quartz rich (S14 and S10), than in S9 and S28, which are rich in dolomite. Only quartz affected the hydration kinetics of cement. In pastes with siliceous microfines, only S2, which has the highest percentage clay, accelerated the disappearance of C3S peak. Montmorillonite clays increase hydration kinetics more than Kaolin clays.

5.9.1.2: Thermal Analysis

Thermogravimetric and Thermal-Differential Analysis provide quantitative information regarding the mineralogy of the sample. Cement pastes with microfines display three major mass losses. There are small differences in the content of $Ca(OH)_2$ and $CaCO_3$. These differences are statistically significant and correlate to the composition of the microfines (Table 11). Pastes with S2, S10, S14, and Kaolin have less $Ca(OH)_2$ and $CaCO_3$ than pastes with S28, S9, or montmorillonite. The microfines in the first group are siliceous while those in the second group are dolomitic. The microfines of the first group are pozzolanic and react with $Ca(OH)_2$ to form more C-S-H.

Table 11: Summary of TG Curve Information of Cement Paste Samples Made with Different Microfines

	% of Sample Lost at Temperature Range (°C)								
Sample	**400**	**400-500**	**550-700**	**750-950**	**% $Ca(OH)_2$**	**% $CaCO_3$**	**% Ca from $Ca(OH)_2$**	**% Ca from $CaCO_3$**	**Total % Ca**
S2	25.26	5.20	3.39	0.63	20.80	7.70	11.79	3.09	15.33
S10	26.90	5.60	3.03	0.66	22.39	6.89	12.69	2.76	15.93
S14	26.42	5.54	3.51	0.75	22.15	7.99	12.55	3.20	16.24
Kaolin	26.58	5.87	2.73	0.57	23.49	6.21	13.31	2.49	16.29
Control	**22.10**	**5.75**	**4.09**	**0.96**	**23.00**	**9.30**	**13.04**	**3.73**	**16.76**
S9	27.06	5.74	3.62	0.75	22.97	8.23	13.02	3.30	16.82
CaM	25.47	5.71	3.71	0.68	22.84	8.44	12.94	3.38	16.83
S28	27.23	5.83	3.44	0.74	23.31	7.81	13.21	3.13	16.84
NaM	26.58	5.97	3.29	0.77	23.90	7.48	13.54	3.00	17.05

5.9.1.3: Capillary Porosity

The porosity and pore size distribution for the hardened cement was measured by adsorption of N_2 at 77 K. Section 10(Figure 10.3.6) shows an adsorption /desorption isotherm for the control paste. The shape of this isotherm, Type IV, is typical of the isotherms for cement pastes containing microfines. The shape of the hysteresis loop (Type B) is typical of a material having slit-shaped mesopores (Gregg 1982). The measured values are presented in Table 12. BET area was not sensitive to the presence of microfines in the cement paste.

Table 12: Summary of Capillary Information of Cement Paste Samples After 14 Days of Hydration

Sample	**Pore Volume Below 100 nm diameter (cm^3/g)**	**BET Surface Area (m^2/g)**
S14	0.0255	20.2
S18	0.0282	19.0
S2	0.0338	20.9
S10	0.0496	20.9
CaM	0.0533	19.6
S19	0.0583	20.5
S9	0.0597	20.5
Control-B	0.0599	19.1
S28	0.0613	21.1
Control-A	0.0631	

Figure 12 shows the pore size distribution for 10 of the studied cement pastes. Microfines from S2, S18, S14 and S10 affect the volume and pore size distribution of capillary pores in the C-S-H matrix even at concentrations as low as 3 percent. The other microfines do not affect the porosity or pore size distribution. The potential of the microfines to change the pore structure in the cement paste correlates with mineralogy. Siliceous microfines (quartz rich) decrease the pore volume while dolomitic microfines did not. The decrease in pore volume, especially in the range of 30-80 nm, is due to the pozzolanic character of siliceous microfines.

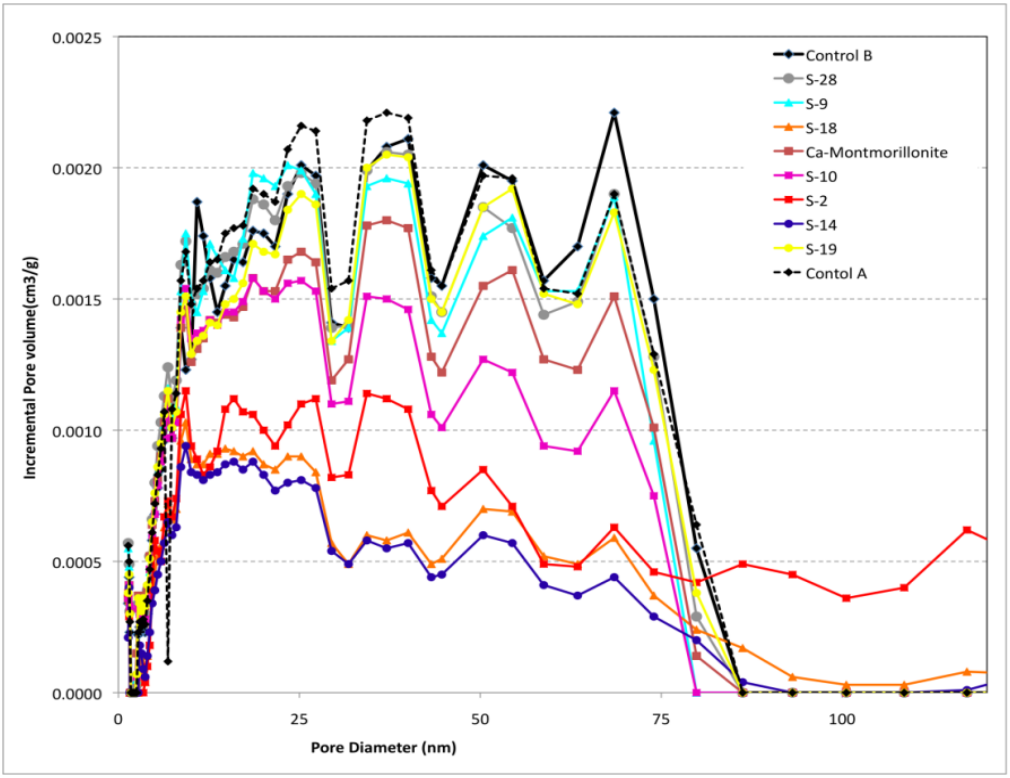

Figure 12: Pores Size Distribution of Different Cement Paste with Microfines.

5.9.1.4: Identification of the Chemical and Mineralogical Phases

Electron microscopy and EDS analysis was used to identify the principal mineral phases in the C-S-H phase of the cement paste. The changes in the chemical composition and microstructure of cement pastes induced by microfines were measured in four different concretes; siliceous (S2 and S19) and dolomitic limestone (S14 and S28). The microstructure of cement paste can be described as a mixture of unhydrated cement particles, newly formed hydration products, air, and microfines. Examples of the different mineralogical phases identified are shown in Section 10(Figures 10.4.1 - 10.4.9).

Four major phases, tricalcium silicate (C_3S), dicalcium silicate (C_2S), tricalcium aluminate (C_3A), and tetracalcium alumino ferrite (C_4AFe) were identified in all samples. The C_3S phase, (60 percent of the dry cement) was found as isolated particles between 5 and 30 μm or agglomerated with other unhydrated phases. C_2S, the second most abundant phase in the dry cement (12.3 percent), was primarily found with other cement phases as part of larger unhydrated cement particles. Particles of two calcium aluminates, C_4AFe and C_3A also occurred in unhydrated particles.

The largest portion of the volume of the cement paste was C-S-H. C-S-H showed calcium and silica as major elemental components with Ca/Si ratios ranging from 0.5 to 3.0. C-S-H particles were found in the cement paste and also the reaction rims of unhydrated cement particles. These rims are known to contain high density (HD) C-S-H (Jennings et al. 2008), which has small pore volume and small pore size. Calcium hydroxide was identified as part of the cement paste and inside pores. Several types of minerals present as microfines were identified in the cement paste of the concrete specimens.

5.9.1.5: Spatial Distribution of the Microfines in ITZ and Bulk Cement Paste and Their Influence on the Microstructure

Much of the strength of cement is due to adhesion between the cement paste and the aggregate material. Microfines with a significant content of clay will bond tightly to the aggregate and affect the interface. The ITZ of concrete S2, which contains large amounts of 2:1 phyllosilicates, should be richer in microfine particles than the ITZ of S19 that contains feldspars. Concrete made with washed aggregates (CS2) was selected as the reference for an ITZ free from microfines. An extra concrete sample contained sodium montmorillonite clay (at 2:1 phyllosilicate) as the only microfine added (labeled NaM). This concrete had a very irregular distribution of the microfines near the surface of the aggregate due to an accumulation of smectites. A representative micrograph shown in Section 10(Figure 10.5.2) displays the ITZ for these samples. The paste adjacent to the surface of the aggregate out to approximately10 μm has a different morphology than the rest of the cement paste. This segment possesses a granular texture very different from the gel-like appearance of the rest of the paste. EDS analysis in this area showed higher ratios of Si/Al.

With the exception of NaM, the microfines primarily occur in a strip 30 μm wide near the surface of the aggregate. The maximum microfine concentration was located 10 to 30 μm from the interface. The mixing procedure was to add water to the aggregate prior to adding the OPC. This caused detachment of some microfines from the aggregate surface and subsequent dispersal into the water phase. This mixing procedure caused larger

particles of the microfine coating to detach leaving behind smaller particles of silica and silicates. The small particles remaining in the 10 μm region bordering the surface react quickly with could be examined with the SEM.

The microfine concentration drops dramatically beyond 30 μm from the surface of the aggregate for all samples. All microfines tend to accumulate in a strip of cement paste, 30 μm wide, adjacent to the aggregate surface regardless of mineralogy. The microfine concentration reached a minimum between 30 and 40 μm from the aggregate surface then increased slightly in the bulk cement paste.

The microfines were concentrated in a strip confined between 10 and 30 μm from the aggregate surface. Within this band of approximately 20μm, the distribution of microfines shows different patterns based on mineralogy. The high adhesion characteristics of clay microfines caused a non-normal distribution of particles. An illustrative example is the case of the samples containing sodium montmorillonite. The maximum population of microfines was located in a 10 μm wide band adjacent to the aggregate surface. This is due strong adhesion of the montmorillonite to the aggregate surface. However, in the next 10 μm strip, the microfine density becomes minimum and then rises again to a new maximum in the next section.

5.9.1.6: Porosity in the ITZ

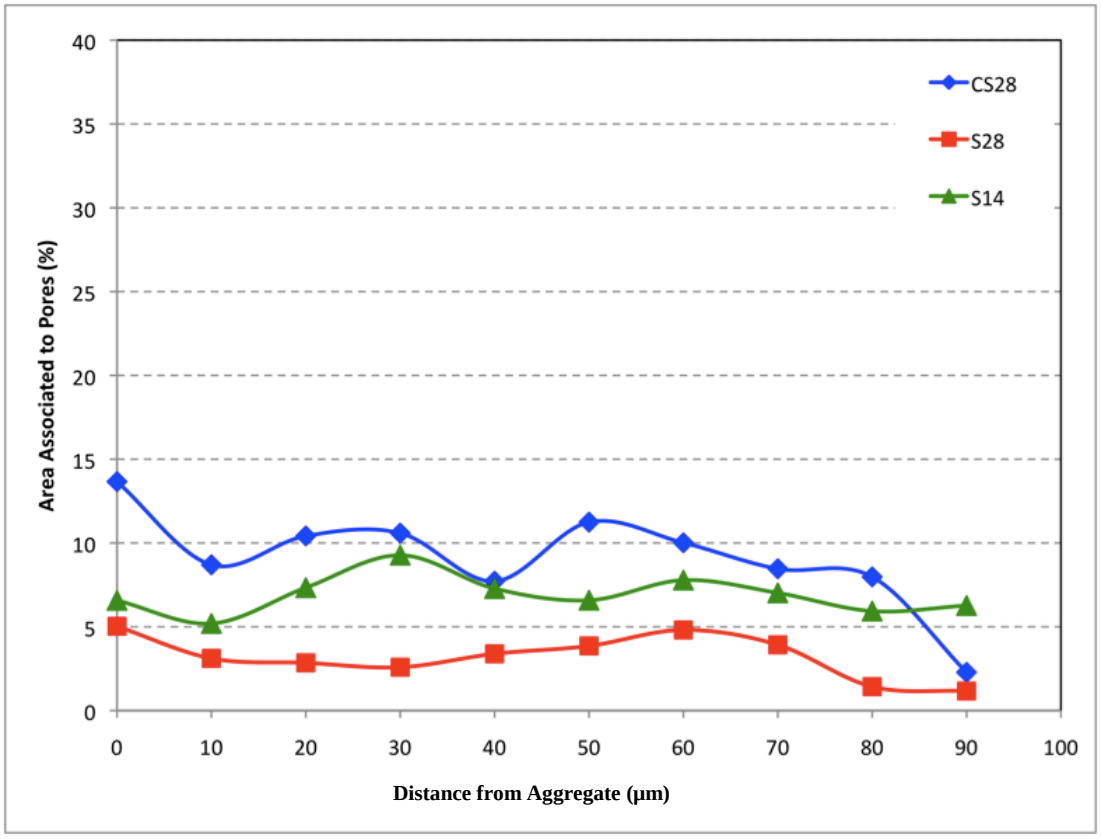

Figure 13: Average Distribution of Porosity in the Interfacial Transition Zone of Concrete Samples Made with Microfines From Dolomitic Limestone Aggregates.

BSE micrographs at 2500x magnification were taken at the interface of several coarse aggregates and used to calculate porosity. Micrographs were taken far from the edges of the SEM specimen to reduce the influence of humidity during curing. The evolution of porosity across the ITZ is shown in Figures 13 and 14. Samples S28 and S14 (containing dolomitic microfines), there was no evidence of a higher porosity in the region adjacent to the aggregate surface than more remote locations across a strip 90 µm wide around the aggregate surface. Only the samples prepared with washed aggregates showed greater porosity in the first 10 µm from the aggregate surface. This densification is due to either the pozzolanic reactivity or the filling effect of the microfine particles. The same effect can be seen when supplementary cementitious materials are added to concrete (Caliskan 2003; Kjellsen et al. 1998; Ollivier et al. 1995).

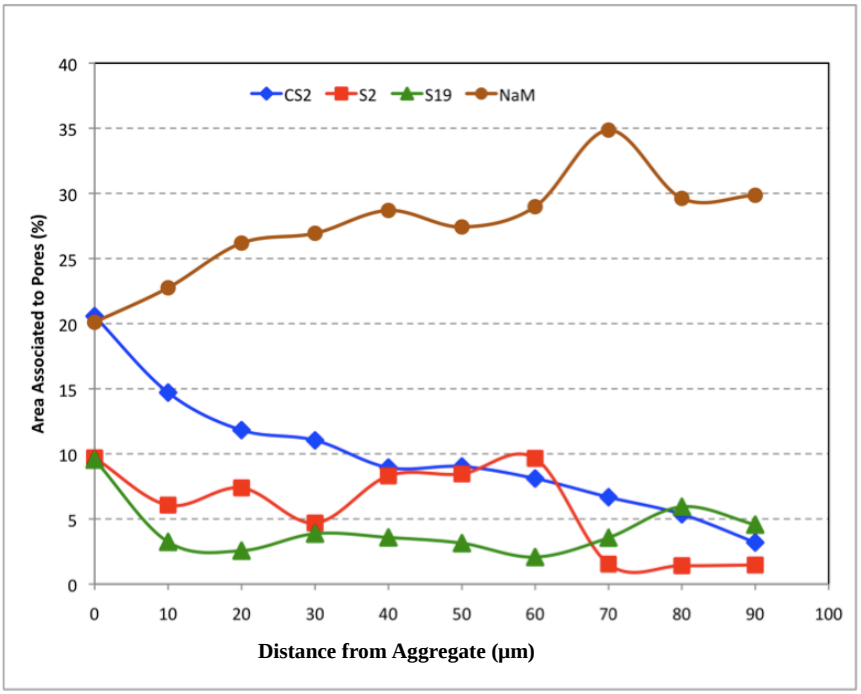

Figure 14: Average Distribution of Porosity in the Interfacial Transition Zone of Concrete Samples Made with Microfines From Siliceous Aggregates.

Samples containing siliceous natural microfines, S2 and S19 showed similar porosities across the ITZ as those containing dolomite (see Figure 14). As was observed for the concrete samples made with washed dolomitic limestone aggregates, the concrete sample prepared with washed S2 aggregates also showed a higher porosity in the 10 µm strip bordering the surface of the aggregate. This value decreases very steadily when moving away from the surface of the aggregate, reaching values below 5 percent in regions located at 70 µm from the surface. The porosity in the ITZ of the NaM concrete is very different from the rest of the cement specimens. The porosity is much higher and oscillates between 20 and 35 percent all across a 90 µm strip. It has been reported that phyllosilicates, in particular 2:1 phyllosilicates, normally generate a higher porosity in the cement paste (Abou-Zeid and Fakhry 2003; Bonavetti and Irassar 1994; Fam and Santamarina 1996; Goldbeck 1933). This phenomenon is likely related to the capacity of certain clay minerals, in particular smectites and vermiculites, to absorb and expand water. Water is lost later in the curing process and the clays then shrink to leave voids.

5.9.1.7: Porosity Profiles in the Concrete Sample

The microstructure of samples cured under wet and dry regimens was analyzed to detect differences that could explain the poor performance of concrete samples cured in a dry environment. A curing regime low in relative humidity creates gradients in the pore space that leads to a development of stress (Burlion et al. 2003; Yurtdas et al. 2004; Yurtdas et al. 2006). This stress can result in the development of structural flaws that decrease the strength and durability of concrete.

A porosity profile was obtained by measuring the porosity at different distances from the external surface. All of the concrete samples exhibited similar porosity distribution. The region located near the external surface had higher porosity than the regions located deep within the sample. The porosity decreased progressively with increasing depth into the concrete. The value of the relative humidity used for curing significantly affected the initial value of porosity and the length of its profile. This influence was notably stronger in the concrete samples containing microfines from dolomitic limestone aggregates (Figure 15). The porosity values for the most external regions of this group of samples cured in a dry regime varied between 15 to 35 percent, while under a wet environment this porosity decreased to values between 5 and 25 percent. The depth of the profiles was dramatically decreased from more than 1400 μm for DC samples to 400 μm wet cured (WC). Under a dry environment the amount of microfines controlled the initial value of porosity and the length of the profile. The samples with a higher content of microfines from dolomitic limestone aggregates had a higher porosity just below the external surface. The presence of microfines also provoked deeper profiles of porosity. The normal values of bulk porosity, 5 percent, were achieved at 300, 900, and 1000 μm, respectively.

The porosity profiles (Figure 16) from samples with siliceous aggregates did not follow the same pattern described above. They exhibited less sensitivity to humidity during the curing processes. For both curing regimes the initial porosity varied from 10 to 30 percent and the depth of the profile was below 800 μm. The amount of microfines did not affect porosity or the depth of the porosity profile. The sample CS2, made with washed aggregates, and S19, with microfines free from phyllosilicates, had greater initial porosities near the surface and deeper porosity profiles. The presence of phyllosilicates played an important role in the initial porosity and length of the profile. Their presence appeared to decrease shallow porosity and the length of the porosity profile.

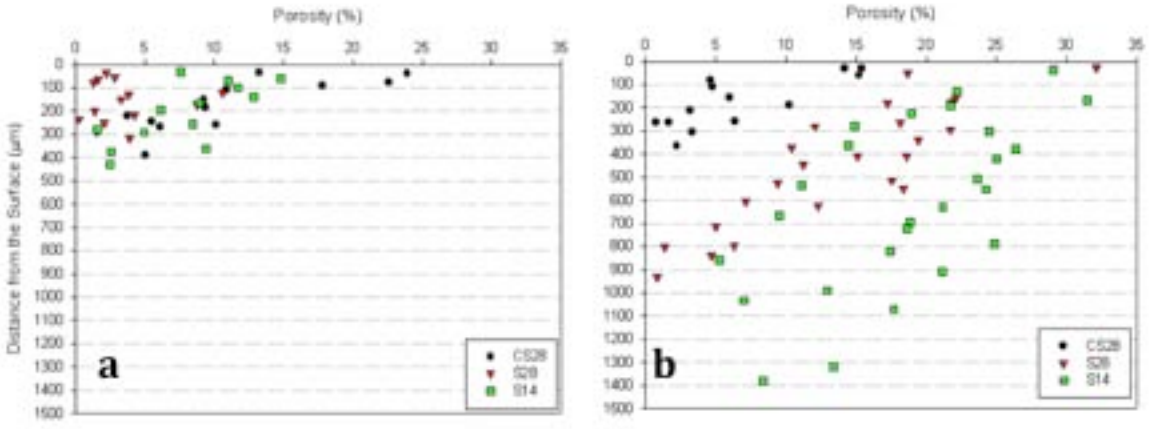

Figure 15: Porosity Profiles of Samples Made with Microfines From Dolomitic Limestone Aggregates Under Wet Curing Process (a) and Dry Curing Process (b).

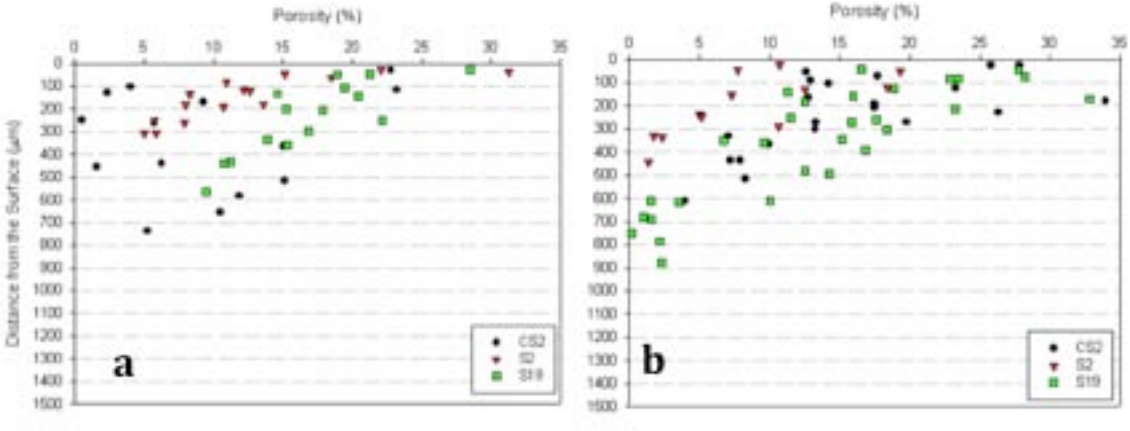

Figure 16: Porosity Profiles of Samples made with Microfines From Siliceous Aggregates Under Wet Curing Process (a) and Dry Curing Process (b).

5.10: Conductivity Test for Estimating the Potential for the Effect of Microfines on Concrete Performance

5.10.1: Cation/Electrolyte Selection

This sensitivity of the conductivity method was tested for solutions containing different molar fractions of Ca-Na nitrates, Ca-K nitrates, Ca-Mg nitrates, K-Mg nitrates, and Ca-Na-K nitrates. Nitrates were selected as the anion because of its low equivalent single ion conducivity and lack of complex ion formation or formation of insoluble salts. The mentioned cations were selected because they are the most common exchangeable

cations in clays. Other cation combinations are possible if the clay is first fully exchanged prior to analysis.

Figures 17 and 18 show the experimental and calculated conductivities of select cation pairs. From Figure 17, it can be seen that, in the case of Ca and Na, the test lacks sensitivity due to the fact that these two ions have similar equivalent single ion conductivities. On the other hand, the highest sensitivity is reached for cation pairs Ca and K or Mg and K. In all of the systems tested, the predicted conductivity values are very close to those experimentally measured, especially for molar fractions of calcium below 0.35.

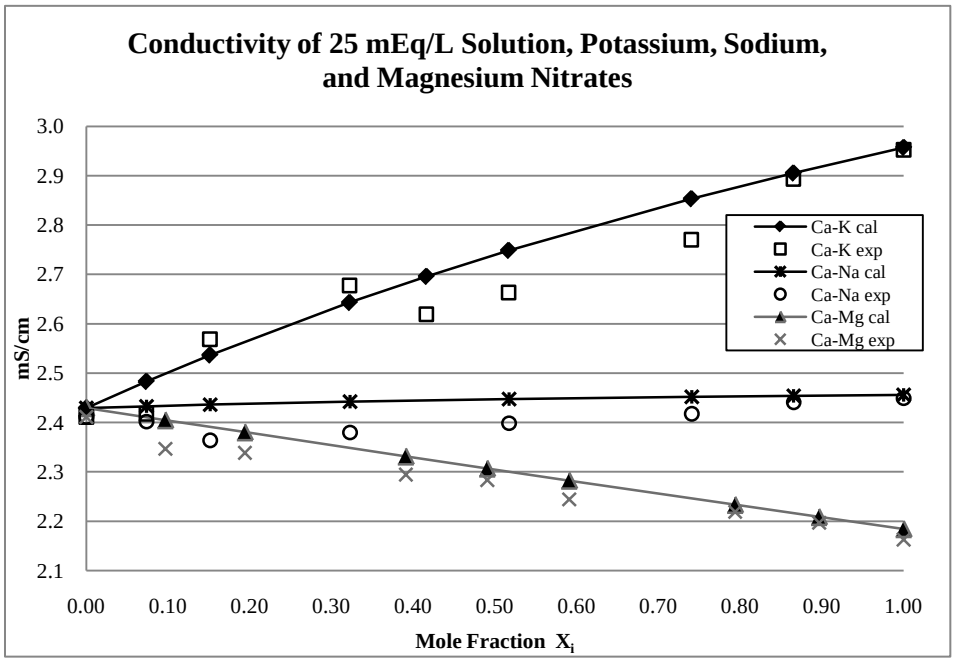

Figure 17: Comparison Between Calculated (full markers) and Measured Conductivity (empty markers) for Binary Electrolytes Solutions. Note: the Molar Fraction of Calcium is 1 at the Origin

Since the equivalent single ion conductivity values for Ca^{++} and Na^{+} is identical, the Ca-Na-K solution is equivalent to a Ca-K solution. Therefore, in a ternary solution, the sum of the equivalent fractions of Ca and Na will correspond with the molar fraction of Ca in the binary solution. As shown in Figure 18 the K-Mg system shows a marked and linear change in conductivity as a function of the mole-fraction of magnesium in the solution. This suggests that the K/Mg nitrate binary pair is ideal for use in the proposed testing method, especially at low fractions of K (below 0.4) that would likely be encountered in Mg exchanges on K saturated exchanging clays.

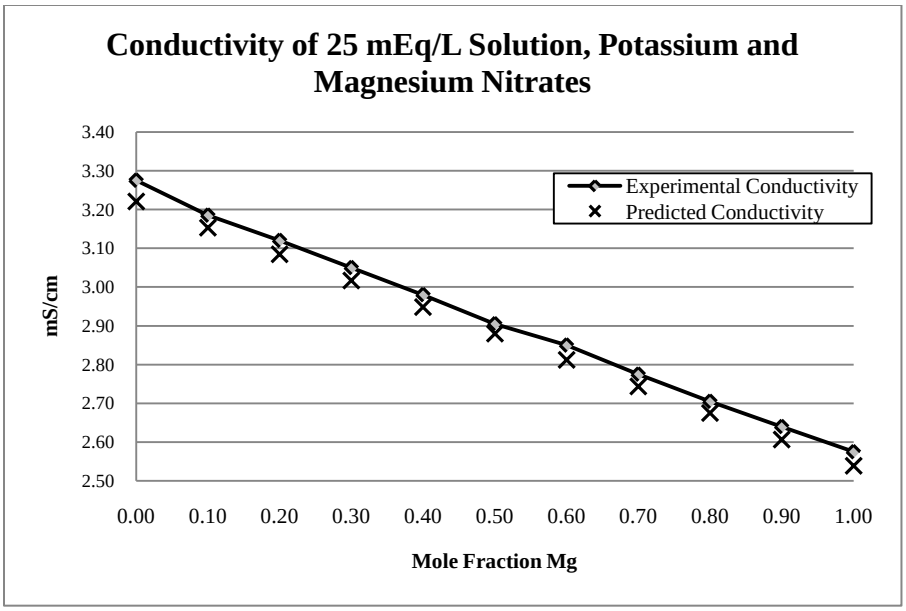

Figure 18: Comparison Between Calculated (full markers) and Measured Conductivity (empty markers) for a K-Mg Binary Electrolyte Solution

5.10.2: The Effect of Suspended Clay Particles on Conductivity

Table 13 shows that the conductivity in the filtrate was significantly higher than in the suspensions in the case of lithium and potassium nitrate. In $Mg(NO_3)_2$ solutions, the conductivity for the suspension and filtrate was the same. Under these experimental conditions of solid volume fraction and concentration of electrolyte, separation of the microfines from aggregates and further filtration is necessary when microfines are exchanged with Li and K nitrate solutions and unnecessary when magnesium nitrate solutions are employed.

Table 13: Comparison of Conductivity of Suspensions Ca-Montmorillonite in Either LiNO3, KNO3 or Mg(NO3)2 25 mEq/L Solutions with the Conductivity of the Corresponding Filtrates

	σ_{Exp}(mS/cm)		$\Delta\sigma$ (mS/cm)	
Salt	**ID Sample**	**Clay Suspension**	**Filtrate**	
$LiNO_3$	1E4	2.138	2.217	0.079
	1E5	2.138	2.217	0.079
	1E6	2.138	2.217	0.079
KNO_3	1E1	2.836	2.880	0.044
	1E2	2.853	2.871	0.018
	1E3	2.844	2.871	0.027
$Mg(NO_3)_2$	2E1	2.297	2.306	0.009
	2E2	2.297	2.297	0.000
	2E3	2.297	2.288	-0.009

5.10.3: Effect of Solid and Electrolyte Concentration on Sensitivity and Accuracy of the Method

Larger concentrations of microfines should increase the sensitivity of the method as the fraction of exchanged cation in the solution increases. This will also increase the effect of the charged particles in the conductivity of the suspensions and introduce higher concentrations of background electrolyte (from leaching) that will add to the conductivity of the filtrate. Higher concentrations of electrolyte will help to achieve a more complete cation exchange with the clay, decrease the effect of the particles on the conductivity of the suspension, but unfortunately, also decrease sensitivity as a smaller fraction of cations will be exchanged.

Shown in Table14 are results from two sets of experiments in which a concentration of calcium montmorillonite of 0.5 ± 0.1 g /100 ml was used to further test the validity of the conductivity test. In this case, a prewashed clay was exchanged in a solution of $Mg(NO_3)_2$ of nominal concentrations of 15 and 10 mEq/L (50ml) .

Table 14: Comparison of Calculated and Experimental Molar Fraction and CEC of Ca-Montmorillonite Exchanged with and Mg(NO3)2 of 15 and 10 mEq/L Nominal Concentrations

	Data from Conductivity Test					Data from ICP			
ID Sample	Mass (g)	Initial Conc (mEq/L)	σ_{Exp} (mS/cm)	X_{Ca}	CEC	Conc	X_{Ca}	σ_{Cal}	CEC (mEq/100g)
2E4	0.519	15.44	1.484	0.98	151.3	16.04	0.17	1.446	52.0
2E5	0.459	15.44	1.502	1.14	82.4	16.62	0.19	1.498	69.6
2E6	0.491	15.44	1.484	0.98	104.9	16.29	0.17	1.467	56.7
3E1	0.497	11.18	1.041	0.31	69.8	11.35	0.28	1.053	62.8
3E2	0.511	11.18	1.032	0.19	42.0	11.26	0.25	1.043	54.4
3E3	0.482	11.18	1.048	0.39	90.9	11.41	0.28	1.059	66.2

The experimental conductivity was very close to the calculated for both concentrations of electrolyte. The CEC values from conductivity are closer to the Inductively Coupled Plasma analysis (ICP) values when more dilute electrolytes are used. The sum of the concentrations of Ca and Mg determined by ICP after the exchange in the filtrate was consistently higher that the total concentration of magnesium ions initially in solution, although by a very small amount (0.2 to 0.07 percent). At present, we believe that the higher value for the sum of [Ca]+[Mg] in the filtrate than initial [Mg] in the electrolyte is associated with leaching of Mg from the clay due to some dissolution (montmorillonite has Mg ions in the octahedral layer). This effect is higher for the experiments in higher concentrations of electrolyte, as would be expected when ionic strength is higher.

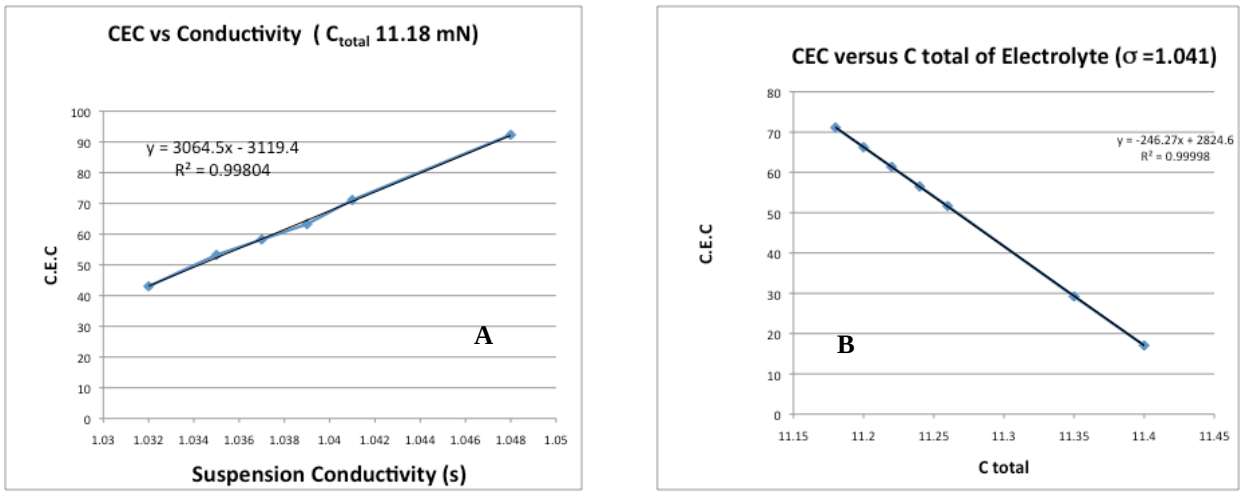

Figure 19: Sensitivity of the CEC Values to Changes in Either Conductivity or Initial Concentration of Electrolyte

As Figure 19 shows, very small variations in either suspension conductivity or C_{total} of electrolyte in the filtrate cause large changes in CEC values for the clay. This can be remedied by washing the aggregate before testing.

5.10.4: Influence of the Pre-Washing Process of the Clay

The results from experiments to determine the effect of clay washing are presented in Table15. The calculated conductivity of the filtrate from ICP data was very close to that of the suspension. The experimental conductivity in the filtered solution was slightly higher. As in the case of the experiments performed in Mg nitrate, the sum of the equivalent concentration of K and Ca in the filtrate is larger than that initially in the electrolyte. Due to this leaching of ions, the initial concentration of electrolyte cannot be used as C_{total} in the calculation of the molar fraction of Ca. The use of the initial concentration of ions in this calculation leads to very small negative values for the molar fraction of Ca. When using the sum of [K] and [Ca] to calculate the molar fraction Ca the resulting values are very close to those obtained by ICP.

Table 15: Comparison of Calculated and Experimental Molar Fraction and CEC of Pre-washed Ca-Montmorillonite Exchanged with and KNO3 at Approximately 10 mEq/L

	Data from Conductivity Test					Data from ICP			
ID Sample	**Mass (g)**	**Initial Conc (mEq/L)**	**σ_{Exp} (mS/cm)**	**X_{Ca}**	**CEC (mEq/100g)**	**Conc (mEq/L)**	**X_{Ca}**	**σ_{Cal} (mS/cm)**	**CEC (mEq/100g)**
5W1	0.478	9.33	1.239	-0.03	-5.633	9.65	0.13	1.229	26.860
5W2	0.463	9.33	1.240	-0.03	-6.239	9.64	0.12	1.231	25.112
5W3	0.516	9.33	1.241	-0.03	-6.139	9.93	0.13	1.262	25.962
5E1	0.760	9.33	1.237	-0.02	-2.357	9.78	0.16	1.236	20.413
5E2	0.767	9.33	1.238	-0.02	-2.693	9.76	0.16	1.234	20.305
5E3	0.756	9.33	1.237	-0.02	-2.370	9.80	0.16	1.240	20.272

The poor results in Table 15 are due to three issues. Under these experimental conditions the sensitivity of the method is very small. This small sensitivity results in very large interferences associated with the leaching of small quantities of calcium, potassium, or magnesium from the clay. The concentration of leached ions is larger than the concentration of the exchanged Ca resulting in negative numbers of their molar fraction (see column X_{Ca}). A second problem is that the conductivity of the suspension is lower than that of the filtrate; therefore filtration of the clay suspension is required. A third problem is that using KNO_3 as the exchanging ion yielded a CEC of only half that obtained using $Mg(NO_3)_2$, thus the Ca in the original clay is only partially exchanged by K at these concentrations.

New exchange experiments were performed with a solution of $Mg(NO_3)_2$ using a pre-washed clay (Table 16). In these systems the sum of equivalent concentration of Mg and Ca was similar to that of the initial concentration, thus, there is not a detectable leaching of these ions. The values for the CEC from conductivity are similar to those obtained from ICP. The CEC average for all the experiments is about 20 percent higher when measured using the conductivity method.

Table 16: Comparison of Calculated and Experimental CEC of Pre-washed Ca-Montmorillonite Exchanged with Mg(NO3)2 at Approximately 10 and 25 mEq/L

	Data from Conductivity Test					Data from ICP			
ID Sample	**Mass (g)**	**Initial Conc (meq/L)**	**σ_{Exp} (ms/cm)**	**X_{Ca}**	**CEC (mEq/100g)**	**Conc (meq/L)**	**X_{Ca}**	**σ_{Cal} (mS/cm)**	**CEC (mEq/100g)**
4E1	0.239	10.78	0.986	0.06	13.104	10.70	0.14	0.987	44.185
4E2	0.241	10.78	1.000	0.23	52.283	10.82	0.20	1.001	46.568
4E3	0.241	10.78	1.003	0.27	60.232	10.83	0.21	1.003	34.245
6E1	0.269	26.11	2.286	0.27	64.795	25.84	0.19	2.251	44.904
6E2	0.249	26.11	2.277	0.22	57.000	25.61	0.19	2.232	47.794
6E3	0.253	26.11	2.314	0.42	107.285	25.57	0.34	2.256	85.272

5.10.5: Testing the Method With K-montmorillonite

A set of experiments was performed using montmorillonite that had been initially exchanged with potassium to improve the sensitivity of the method. The clay was initially exchanged with 1N KCl solution for 24 hours, followed by four rinses and centrifugations. This clay was exchanged in 25 and 50 mEq/L solutions of $Mg(NO_3)_2$ for 24 hours, after which the conductivity of the suspension was measured. The suspension was then centrifuged at ~8500 gravities for 30 minutes and the conductivity of the supernatant measured. The conductivity of the K-Mg system changes linearly with changes in equivalent fraction, so determination of the concentration of K to determine CEC for a sample is simplified. The supernatant was then analyzed via ICP to determine the true CEC for comparison. Results are reported in Table 17.

Table 17: CEC Values for Clays Exchanged With Potassium

0.500g Samples K Montmorillonite Exchanged With Solutions of Mg(NO3)2 (30Ml)									
		Calculated Eq Fraction Mg		pH	Calculated CEC meq/100g		CEC from ICP	Relative Error	
Sample	Nominal Conc.	Susp.	Filtrate	Filtrate	Susp.	Filtrate		Susp.	Filtrate
M-25-1	2.43E-02	0.82	0.80	3.4	86	96	84	2%	14%
M-25-2	2.43E-02	0.80	0.78	3.3	96	106	99	-3%	7%
M-25-3	2.43E-02	0.80	0.80	3.4	96	96	87	10%	10%
Average	2.43E-02	0.81	0.80	3.4	**92**	**99**	**90**		
		Standard Deviation			5.8	5.8	7.7		
M-50-1	5.20E-02	0.92	0.91	3.5	85	96	111	-24%	-14%
M-50-2	5.20E-02	0.93	0.89	3.4	76	118	105	-28%	12%
M-50-3	5.20E-02	0.95	0.90	3.4	52	107	120		-11%
Average	5.20E-02	0.93	0.90	3.4	**71**	**107**	**112**		
		Standard Deviation			17.0	11.0	7.4		

The cation exchange values measured using this method are within 15 percent of the ICP values when the solution is centrifuged and the conductivity measurement made in the supernatant. The low pH of the exchanged solution shows that some fraction of the Mg in the electrolyte exchanged with protonated exchange sites on the montmorillonite. This will increase the conductivity of the solution/ suspension and be the cause of the higher numbers for CEC rendered by the conductivity method (7-14 percent) with respect to the measured ICP values.

6: Comparison of Wisconsin Microfines with those in Other States – Concurrent Study

As part of a concurrent national study (IPRF Project 01-G-002-06-5), aggregates associated with source S14 were evaluated in concrete as part of a comparison with concrete made with microfines gathered in four other states (California, Utah, Wyoming and Colorado). The S14 aggregate was chosen because preliminary data suggested it would largely be innocuous while the other sources of aggregates displayed various levels of reactivity including alkali-silica reactivity.

This concurrent study provided additional information on the impact of microfines in concrete. The emphasis was on understanding the role of 1:1 and 2:1 phyllosilicates.

Microfines can be highly reactive with the potential to cause undesirable impacts in the presence of other chemicals and materials. For example, Figure 20 shows the additions of a typical air entraining agent and the resulting air content. With this particular microfine, the air entraining agent was rendered ineffective regardless of admixture amount.

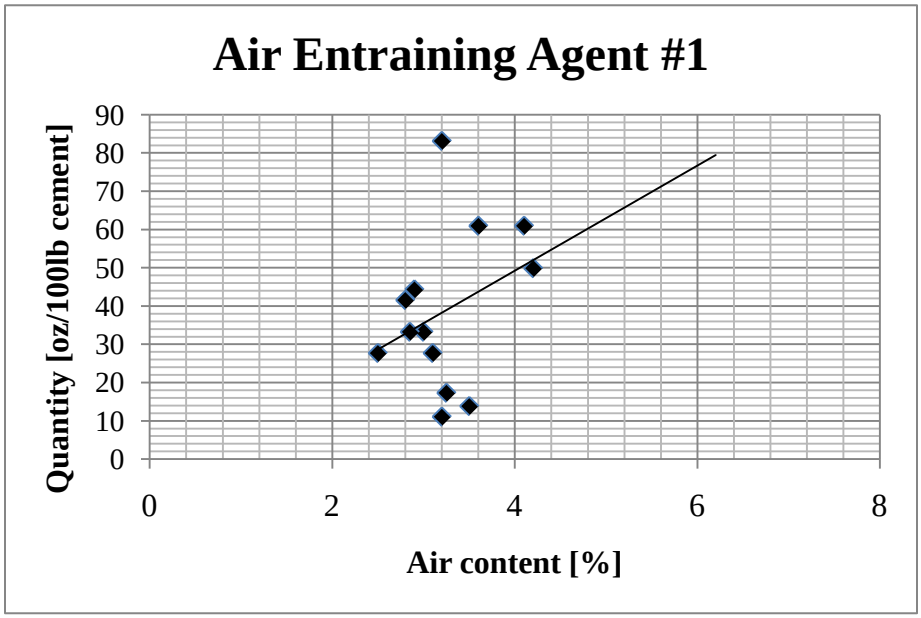

Figure 20: Effectiveness of An Air Entraining Agent (AEA) in a Concrete Mixture Containing 5 Percent Microfines by Coarse Aggregate Weight (Aggregates from Wisconsin and Microfines from Wyoming). The Recommended AEA dosage was 1 to 3 fl. oz. per 100 lbs of Cement.

In the presence of certain anti-icing and deicing chemicals, laboratory tests show that some microfines prompt large chemically-driven expansions and poor freeze-thaw durability. These observations are based on concrete specimens containing 5 percent microfines based on coarse aggregate weight. There is clear evidence from this study that total coarse and fine aggregate microfines in the range of 5 to 6 percent of the weight of the coarse aggregates cause deleterious concrete performance under certain non-ideal conditions. These non-ideal conditions include the presence of chemical anti-icing agents, uncontrolled water additions to offset loss of workability resulting from microfines and potentially other intentional or unintentional chemical additions from admixtures or pozzolanic materials. From this study we know that some microfines that occur in various locations across the continental United States can be disruptive and harmful to concrete performance at these additions rates. These harmful effects have even been observed

when the microfines have been added to otherwise high quality aggregates from Wisconsin.

In examining Table 6, the microfines determined to be largely innocuous in this study tended to occur in the largest quantities (that approached or exceeded WisDOT limits). Those naturally occurring microfines that held the potential to be most deleterious tended to occur in the range of 1 to 2 percent of the parent aggregate by weight and well below the WisDOT limits. Eleven of the original 28 samples (40 percent) had a definite presence of clay particles and an additional 29 percent had some indication of clay particles. We know from the national study that clays do cause significant deleterious impacts under certain conditions but in this study they occurred in relatively small quantities. One must conclude from these observations that the types of clays in Wisconsin do not occur in sufficient quantities and with sufficient deleterious impacts (those associated with 2:1 phyllosilicates) or that the detailed evaluation of the seven microfine sources did not include a more deleterious clay condition that may be present in the larger population of possible Wisconsin concrete aggregates.

7: Summary and Conclusions

7.1: Microfine Characterization

Analysis of the microfines showed that 69 percent of the aggregate samples provided by the WisDOT contained clay minerals. The CEC values of the microfines suggested a mix of different clay minerals (1:1 phyllosilicates with low or medium CEC and 2:1 phyllosilicates with higher CEC). The mix of clay minerals as well as the variable quantity did not result in a definitive impact from the microfines in all situations.

The X-ray diffraction and thermo gravimetric revealed the following:

- Amorphous materials that change form and react in deleterious ways were not present in large quantities in any of the seven samples studied in detail.
- Microfines could be divided into two groups: dolomitic (S9, S10, S14, and S28) and igneous (S2, S18, and S19).
- Dolomitic microfines contained quartz, dolomite, proto-dolomite, and calcite as major constituents.
- Igneous microfines contain significant amounts of feldspar along with quartz. Microcline, anorthite, and albite were detected in S2, S18, and S19 microfines, respectively. S2 and S18 also contained clay minerals (1:1 and 2:1 phyllosilicates).

In the spectrum of possible microfines that exist on a national scale, the samples collected in Wisconsin for detailed analysis contained relatively small quantities of clays considered to be most deleterious. While it appears that this could be a general characterization of the microfines associated with Wisconsin aggregates, we cannot rule out that the small number of samples (7), subject to the more detailed microfine analysis, simply missed more deleterious sources that may exist in the state.

7.2: Effects on Concrete Properties

The group of microfines from igneous sources containing clay minerals clearly impaired the workability and the ability of the AEA to achieve the desired air contents, even though the quantities of microfines containing significant levels of clay particles were relatively low and well below the WisDOT limits.

Concrete specimens containing microfines cured under standard laboratory conditions (100% RH) had similar or, in some cases, better performance than specimens made with well-washed aggregates. However, matched specimens with microfines cured under drier conditions (45% $\pm$ 15 RH) performed worse than specimens without microfines. The exception was drying shrinkage, where the presence of microfines did not have a significant impact.

7.2.1: Group A: Concrete Batches Containing Microfines From Dolomitic Limestone Aggregates.

- Compression strength: Under wet curing conditions and concentrations below the thresholds required under WisDOT specifications, the presence of microfines did not degrade the 28-day compressive strength. Microfines with few carbonate minerals and significant amounts of quartz enhanced the compressive strength up to 24 percent with wet curing. The magnitude of the improvement correlated with the amount of microfines in the mix and diminished at longer curing times. Under dry curing conditions the microfines negatively impacted the final compressive strength, especially at longer curing times.

- Tensile strength: Under wet curing conditions tensile strength was not influenced by the presence of microfines. In samples cured under dry conditions, the presence of microfines decreased tensile strength up to 34 percent. These results did not show a correlation with respect to the mineralogy or the quantity of the microfines.

- Drying shrinkage: Microfines rich in quartz showed little difference between drying shrinkage values for specimens cured under both environments.

- Capillary water absorption: Microfines that were rich in quartz improved sorptivity at longer curing times than those specimens made without microfines. Carbonate rich microfines did not show any improvements during the same curing period. The sorptivity did not change with longer curing times in dry cured samples.

- Rapid Chloride Penetrability: The presence of microfines resulted in concrete specimens being more susceptible to chloride penetration when, the specimens were poorly cured.

7.2.2: Group B: Concrete Batches Containing Microfines From Igneous Aggregates.

- Compression Strength: The compressive strength was not influenced by the presence of this group of microfines in samples cured under wet conditions. Specimens containing clay and dry cured had significantly lower compressive strengths, as compared to matched concrete specimens that were prepared with washed aggregate.

- Tensile Strength: Group B microfine content had little effect on the tensile strength of the concrete.

- Drying Shrinkage: Aggregate sources associated with clay minerals significantly increased the drying shrinkage of concrete.

- Capillary water absorption: Microfines containing phyllosilicates decreased the porosity of the cement. The pozzolanic activity of these clay minerals filled pores in the concrete.

- Rapid Chloride Penetrability: Microfines containing phyllosilicates decreased the susceptibility of the concrete to chloride penetration.

WisDOT P200 thresholds appeared reliable in preventing significant deleterious concrete performance, when specimens were cured under wet curing conditions. Low

humidity during the curing process will disproportionately damage the quality of the concrete containing microfines. These effects strongly depend on the mineralogy of the microfines.

7.3: Microanalysis of Concrete Samples

The study of the effect of carbonate and siliceous microfines in the microstructure of hardened cement paste has revealed the following:

- Addition of siliceous microfines and carbonate microfines rich in quartz results in cement pastes having much lower pore volume in the capillary pore size region (1-100 nm). This effect is especially notable with pore diameters larger than 40 nm.

- Microfines with clays have a pozzolanic reactivity detectable in cement paste even at concentrations as low as 3 percent of total weight of aggregate.

- Microfine particles are still visible in the concrete after 28 days of curing and affect the interfacial transition zone. These particles are mainly located in a strip of cement paste 30 μm wide, adjacent to the surface of coarse aggregates.

- Dolomitic microfines leach Mg ions that subsequently produce either brucite or magnesium silicates. The impact of Mg ion movement warrants further study.

- Microfines containing sodium montmorillonite form a very granular ITZ, that can prevent the adhesion of C-S-H to the aggregate surface.

- Siliceous and dolomitic microfines decrease the porosity of ITZ. Sodium montmorillonite promotes an increase in this region's porosity.

- Concrete typically has a higher porosity in the paste near the surface than in the bulk. The decrease in porosity is progressive with depth. The presence of microfines, either dolomitic or siliceous, did not affect the porosity profile in wet cured concrete but for dry cured concretes, the porosity beneath the surface increased.

7.4: Conductivity Test for Cation Exchange Capacity

It has been shown that a conductivity-based approach can be used to measure cation exchange capacity (CEC) in microfine samples. The primary advantage of measuring cation exchange capacity is that it allows for direct determination of the presence of 2:1 phyllosilicates. While the methylene blue test (MBT) also is a measure of the CEC, the CEC tests pursued in this test provided a direct and less subjective measure of CEC. In addition, the CEC test methods pursued in this research were aimed at identifying the exchangeable cation which would allow precise identification of the mineralogy of the clay mineral. While CEC can be directly measured with sophisticated laboratory equipment (ICP), such equipment typically does not exist in DOT laboratories. The objective here was to reduce the complexity of the test, by using a simple laboratory conductivity meter and measuring changes in conductivity from direct emersion of aggregate samples including microfines in solutions. This approach did not display sufficient sensitivity to be a viable field technique.

This method provided the best results when the clay microfines were first isolated and then were first exchanged with a K salt, followed by a careful rinsing to remove soluble species, previous to the exchange with a Mg salt of known concentration. This method yielded results that were similar to the values obtained via ICP analysis. This method could be a useful replacement for the MBT as it does not depend on subjective observations by the operator. Measurements of conductivity are very fast and simple, however this approach requires more effort than previously envisioned. The isolation of microfines from the aggregate source and the pre-processing involve significantly more technician time and effort. None-the-less, this method if fully developed could provide a superior diagnostic tool than currently available with the MBT or California Cleanness tests.

8: Recommendations

The results of this research suggest the current threshold in content for naturally occurring microfines associated with coarse and fine aggregates in the WisDOT Standard Specification results in acceptable concrete performance when conditions are optimal and meet typical ASTM laboratory test requirements. This research outcome is consistent with that of the earlier study on the role of microfines in WHRP study #0092-00-07. When microfines are present in aggregates, if air entrainment, uncontrolled water additions, certain intentional or unintentional chemical additions, and curing are not carefully monitored and controlled, then microfines in Wisconsin concrete aggregates can and do cause deleterious impacts. It is clear, that microfines in small quantities from other parts of the United States are deleterious, even under more ideal conditions. Wisconsin microfines appear less deleterious but the level of research to adequately assess microfines in the state remains a work in progress. Only seven sources were analyzed and assessed in detail in this study and to provide reasonable control conditions, some of the seven were believed to be innocuous even before evaluation.

ASTM-type concrete conditions are rarely met in the field and clearly one or more of the factors that can prompt deleterious influence of microfines, can and often do occur in the field production of concrete. Given the mismatch between laboratory and field curing and the increasing introduction of chemical complexity into concrete mix design, research that addresses concrete performance under controlled conditions that simulate factors in field production and placement is strongly needed. The ability to enhance the state's investment in highway pavements and to prevent premature distress that has been experienced over the past decade requires a knowledge base built on this type of research. Only with this type of research can the full significance of concrete microfines be established and strategies developed to control or avoid their introduction in situations where their impact is deleterious.

9: Bibliography

Abou-Zeid, M. N., and Fakhry, M. M. (2003). "Short-term impact of high-aggregate fines content on concrete incorporating water-reducing admixtures." *ACI Materials Journal*, 100(4), 280-285.

Aono, Y., Matsushita, F., Shibata, S., and Hama, Y. (2007). "Nano-structural changes of C-S-H in hardened cement paste during drying at 50 degrees C." *Journal of Advanced Concrete Technology*, 5(3), 313-323.

Atis, C. D., and Bilim, C. (2007). "Wet and dry cured compressive strength of concrete containing ground granulated blast-furnace slag." *Building and Environment*, 42(8), 3060-3065.

Beltzung, F., and Wittmann, F. H. (2005). "Role of disjoining pressure in cement based materials." *Cement and Concrete Research*, 35(12), 2364-2370.

Bentz, D. P. (2007). "Internal curing of high-performance blended cement mortars." *ACI Materials Journal*, 104(4), 408-414.

Bentz, D. P., and Jensen, O. M. (2004). "Mitigation strategies for autogenous shrinkage cracking." *Cement & Concrete Composites*, 26(6), 677-685.

Bonavetti, V. L., and Irassar, E. F. (1994). "The Effect of Stone Dust Content in Sand." *Cement and Concrete Research*, 24(3), 580-590.

Burlion, N., Skoczylas, F., and Dubois, T. (2003). "Induced anisotropic permeability due to drying of concrete." *Cement and Concrete Research*, 33(5), 679-687.

Caliskan, S. (2003). "Aggregate/mortar interface: influence of silica fume at the micro- and macro-level." *Cement & Concrete Composites*, 25(4-5), 557-564.

Chan, S. Y. N., and Ji, X. H. (1998). "Water sorptivity and chloride diffusivity of oil shale ash concrete." *Construction and Building Materials*, 12(4), Cover3-+.

Diamond, S., and Huang, J. D. (2001). "The ITZ in concrete - a different view based on image analysis and SEM observations." *Cement & Concrete Composites*, 23(2-3), 179-188.

Diamond, S., White, J. L., and Dolch, W. L. (1966). "Effects of Isomorphous Substitution in Hydrothermally-Synthesized Tobermorite." *American Mineralogist*, 51(3-4), 388-&.

Dontsova KM, Norton LD, Johnston CT, Bigham JM, "Influence of exchangeable cations on water adsorption by soil clays," Soil Science Society of America Journal, V. 68, No. 4, Jul-Aug. 2004, pp. 1218-27.

Fam, M. A., and Santamarina, J. C. (1996). "Study of clay-cement slurries with mechanical and electromagnetic waves." *Journal of Geotechnical Engineering-Asce*, 122(5), 365-373.

Goldbeck, A. T. (1933). "Nature and effect of surface coatings on coarse aggregates." *American Highways*, 12(3), 9-13.

Gregg, S. J. (1982). *Adsorption, surface area, and porosity*, Academic Press.

Gullerud, K., and Cramer, S. (2002). "Effects of Aggregate Coatings and Films on Concrete Performance." *0092-00-07*, Wisconsin Department of Transportation, Madison.

Guneyisi, E., Gesoglu, M., and Mermerdas, K. (2008). "Improving strength, drying shrinkage, and pore structure of concrete using metakaolin." *Materials and Structures*, 41(5), 937-949.

Guneyisi, E., and Mermerdas, K. (2007). "Comparative study on strength sorptivity and chloride ingress characteristics of air-cured and water-cured concrete modified with metakaolin." *Materials and Structures*, 2007(40), 1161-1171.

He, C. L., Osbaeck, B., and Makovicky, E. (1995). "Pozzolanic Reactions of 6 Principal Clay-Minerals - Activation, Reactivity Assessments and Technological Effects." *Cement and Concrete Research*, 25(8), 1691-1702.

Holt, E., and Leivo, M. (2004). "Cracking risks associated with early age shrinkage." *Cement & Concrete Composites*, 26(5), 521-530.

Hosking, J. R., and Pike, D. C. (1985). "The Methylene-Blue Dye Adsorption Test in Relation to Aggregate Drying Shrinkage." *Journal of Chemical Technology and Biotechnology A-Chemical Technology*, 35(4), 185-194.

Igarashi, S., Watanabe, A., and Kawamura, M. (2005). "Evaluation of capillary pore size characteristics in high-strength concrete at early ages." *Cement and Concrete Research*, 35(3), 513-519.

Jaynes, W. F., and Bigham, J. M. (1986). "Multiple Cation-Exchange Capacity Measurements on Standard Clays Using a Commercial Mechanical Extractor." *Clays and Clay Minerals*, 34(1), 93-98.

Jennings, H. M. (2000). "A model for the microstructure of calcium silicate hydrate in cement paste." *Cement and Concrete Research*, 30(1), 101-116.

Jennings, H. M., Bullard, J. W., Thomas, J. J., Andrade, J. E., Chen, J. J., and Scherer, G. W. (2008). "Characterization and modeling of pores and surfaces in cement paste: Correlations to processing and properties." *Journal of Advanced Concrete Technology*, 6(1), 5-29.

Kanna, V., Olson, R. A., and Jennings, H. M. (1998). "Effect of shrinkage and moisture content on the physical characteristics of blended cement mortars." *Cement and Concrete Research*, 28(10), 1467-1477.

Kjellsen, K. O., Wallevik, O. H., and Fjallberg, L. (1998). "Microstructure and microchemistry of the paste-aggregate interfacial transition zone of high-performance concrete." *Advances in Cement Research*, 10(1), 33-40.

Korb, J. P., Monteilhet, L., McDonald, P. J., and Mitchell, J. (2007). "Microstructure and texture of hydrated cement-based materials: A proton field cycling relaxometry approach." *Cement and Concrete Research*, 37(3), 295-302.

Lange, D. A., Jennings, H. M., and Shah, S. P. (1994). "Image-Analysis Techniques for Characterization of Pore Structure of Cement-Based Materials." *Cement and Concrete Research*, 24(5), 841-853.

Lee, S. T. (2008). "Effects of curing procedures on the strength and permeability of cementitious composites incorporating GGBFS." *Journal of Ceramic Processing Research*, 9(4), 358-361.

Malathy, R., and Subramanian, K. (2007). "Drying shrinkage of cementitious composites with mineral admixtures." *Indian Journal of Engineering and Materials Sciences*, 14(2), 146-150.

Malhotra, V. M., and Mehta, P. K. (1996). *Pozzolanic and cementitious materials*, Gordon and Breach, Australia.

Menendez, G., Bonavetti, V., and Irassar, E. (2007). "Ternary blend cements concrete. Part II: Transport mechanism." *Materiales De Construccion*, 57(285), 31-43.

Munoz, J. F., Gullerud, K. J., Cramer, S. M., Tejedor, M. I., and Anderson, M. A. (2010). "Effects of Coarse Aggregate Coatings on Concrete Performance." *Journal of Materials in Civil Engineering*, 22(1), 96-103.

Muñoz, J. F., Sanfilippo, J. M., Cramer, S. M., Tejedor, I., and Anderson, M. A. "The Role of Aggregate Microfines in the Alkali Silica Reaction: Enemy or Ally?" *ICAR's 17th Annual Symposium Aggregates: Asphalt Concrete, Portland Cement Concrete, Bases, and Fines*, Austin, Tx, 18.

Muñoz, J. F., Tejedor, M. I., Anderson, M. A., and Cramer, S. M. (2007). "Expanded study on the effects of aggregate coating and films on concrete performance." *0092-04-12*, Wisconsin Department of Transportation, Madison, Wi.

Neville, A. M. (1996). *Properties of concrete*, J. Wiley, New York.

Nonat, A. (2004). "The structure and stoichiometry of C-S-H." *Cement and Concrete Research*, 34(9), 1521-1528.

Ollivier, J. P., Maso, J. C., and Bourdette, B. (1995). "Interfacial Transition Zone in Concrete." *Advanced Cement Based Materials*, 2(1), 30-38.

Ozer, B., and Ozkul, M. H. (2004). "The influence of initial water curing on the strength development of ordinary portland and pozzolanic cement concretes." *Cement and Concrete Research*, 34(1), 13-18.

Popovics, S. (1998). *Strength and Related Properties of Concrete: a Quantitative Approach*, Wiley, New York.

Quiroga, P. N., Ahn, N., and Fowler, D. W. (2006). "Concrete mixtures with high microfines." *ACI Materials Journal*, 103(4), 258-264.

Ramezanianpour, A. A., and Malholtra, V. M. (1995). "Effect of Curing on the Compressive Strength, Resistance to Chloride-Ion Penetration and Porosity of Concretes Incorporating Slag, Fly Ash or Silica Fume." *Cement & Concrete Composites*, 17, 125-133.

Richardson, I. G. (1999). "The nature of C-S-H in hardened cements." *Cement and Concrete Research*, 29(8), 1131-1147.

Safiuddin, M., Raman, S. N., and Zain, M. F. M. (2007). "Effect of Different Curing Methods on the Properties of Microsilica Concrete." *Australian Journal of Basic and Applied Sciences*, 1(2), 87-95.

Samtani, M., Dollimore, D., and Alexander, K. (2001). "Thermal decomposition of dolomite in an atmosphere of carbon dioxide. The effect of procedural variables in thermal analysis." *Journal of Thermal Analysis and Calorimetry*, 65(1), 93-101.

Scrivener, K. L., and Nemati, K. M. (1996). "The percolation of pore space in the cement paste aggregate interfacial zone of concrete." *Cement and Concrete Research*, 26(1), 35-40.

Skoczylas, F., Burlion, N., and Yurtdas, I. (2007). "About drying effects and poro-mechanical behaviour of mortars." *Cement & Concrete Composites*, 29(5), 383-390.

Tourenq, C., and Tran, N. L. (1997). "Assessment of clays in aggregates. A track for further research." *Bulletin of the International Association of Engineering Geology*(56), 97-102.

Yurtdas, I., Burlion, N., and Skoczylas, F. (2004). "Triaxial mechanical behaviour of mortar: Effects of drying." *Cement and Concrete Research*, 34(7), 1131-1143.

Yurtdas, I., Peng, H., Burlion, N., and Skoczylas, F. (2006). "Influences of water by cement ratio on mechanical properties of mortars submitted to drying." *Cement and Concrete Research*, 36(7), 1286-1293.

Zhu, W. Z., and Bartos, P. J. M. (2003). "Permeation properties of self-compacting concrete." *Cement and Concrete Research*, 33(6), 921-926.

10: Appendix

10.1: Selection of the Aggregates

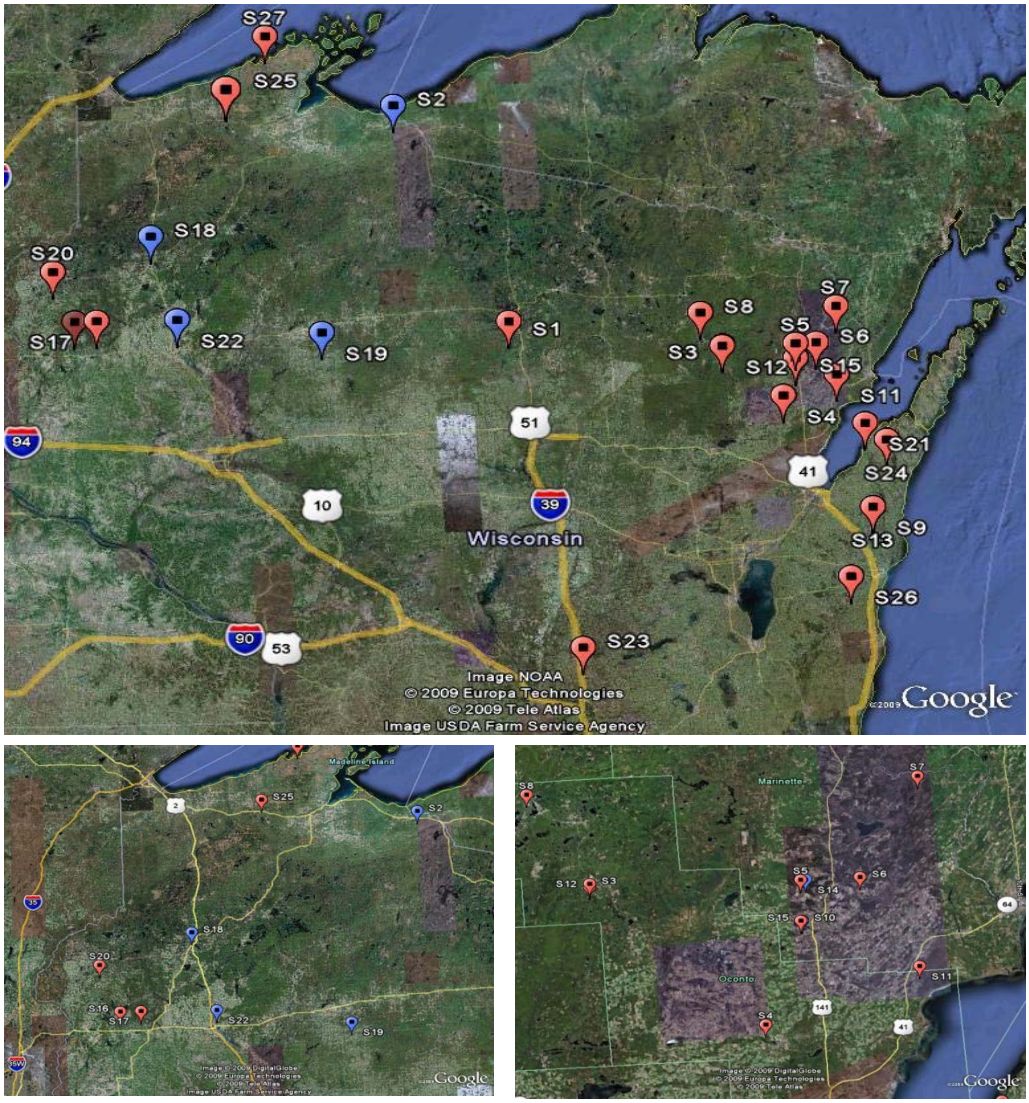

Figure 10.1.1: Geographic Locations of Pre-selected Samples (Red Mark) and Finally Selected Samples for Study (Blue Mark).

Table 10.1.1: Database of Preselected Samples by the WisDOT

ID	Location by Wisconsin County
S1	Lincoln Co.
S2	Iron Co.
S3	Oconto Co.
S4	Oconto Co.
S5	Marinette Co.
S6	Marinette Co.
S7	Marinette Co.
S8	Oconto Co.
S9	Manitowoc Co.
S10	Marinette Co.
S11	Oconto Co.
S12	Oconto Co.
S13	Manitowoc Co.
S14	Marinette Co.
S15	Marinette Co.
S16	Polk Co.
S17	Polk Co.
S18	Washburn Co.
S19	Taylor Co.
S20	Polk Co.
S21	Door Co.
S22	Barrow Co.
S23	Waushara Co.
S24	Kewaunee Co.
S25	Bayfield Co.
S26	Manitowoc Co.
S27	Bayfield Co.
S28	Manitowoc Co.

10.2: Physical Properties

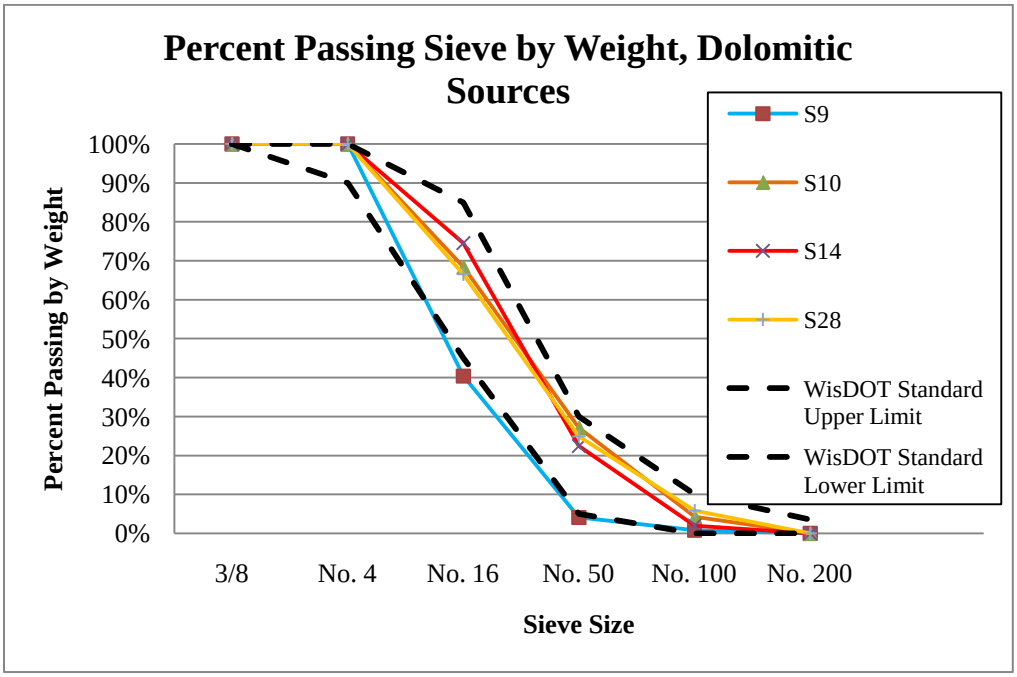

Figure 10.2.1: Sieve Analysis Results for Fine Aggregates From Dolomitic Sources

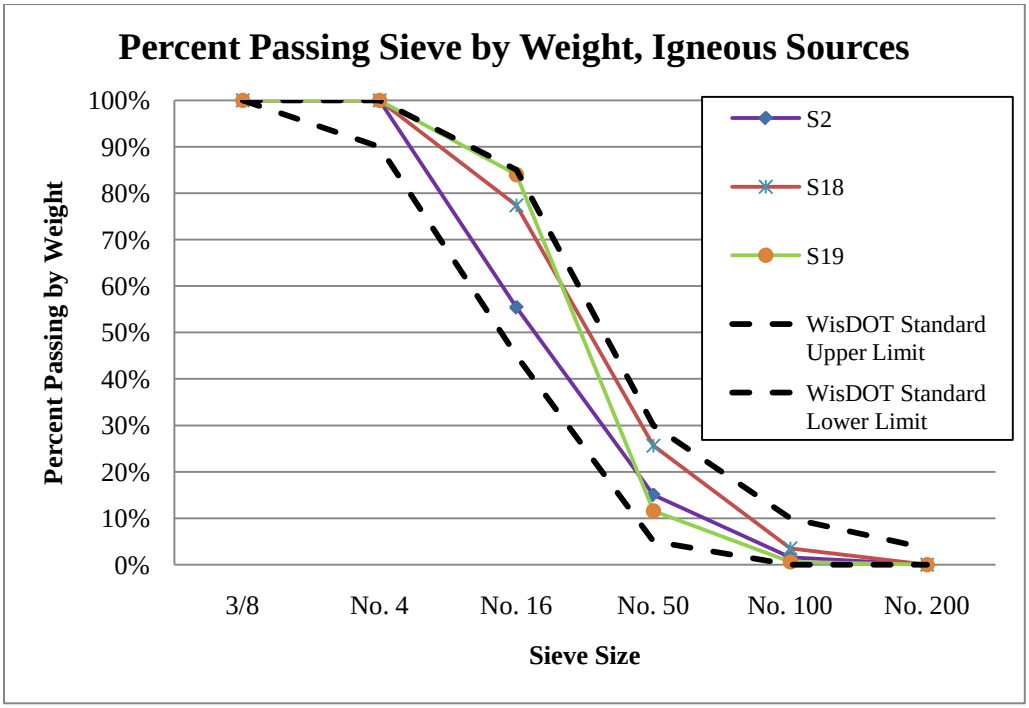

Figure 10.2.2: Sieve Analysis Results for Fine Aggregates From Igneous Sources

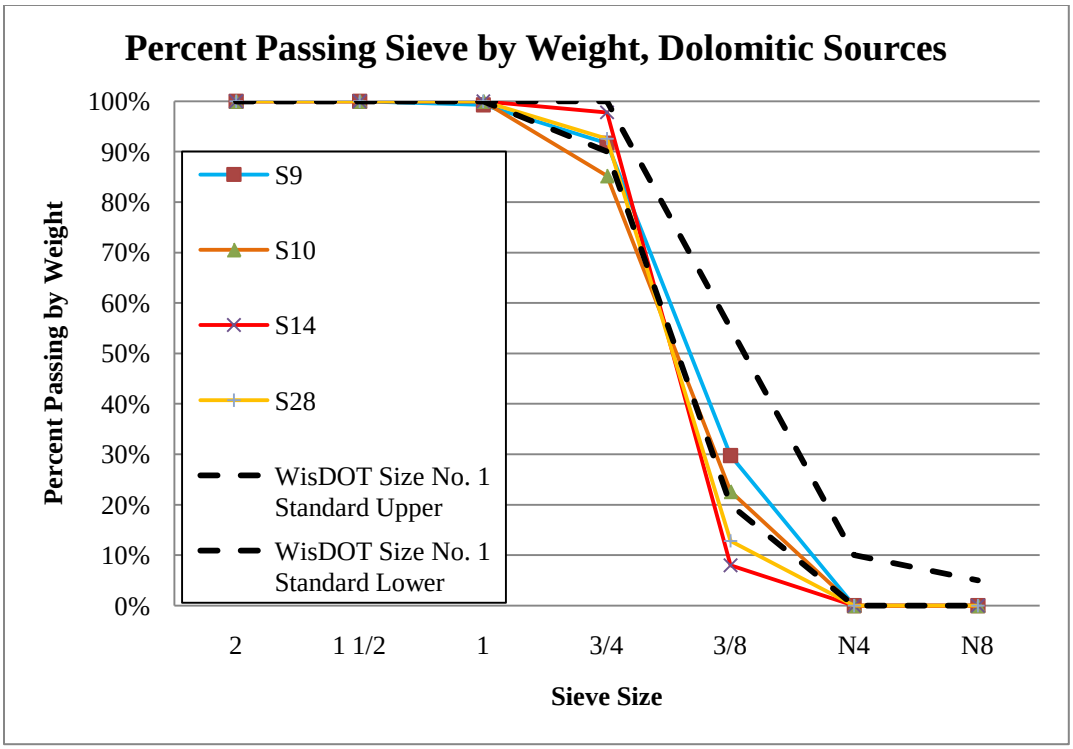

Figure 10.2.3: Sieve Analysis Results for Coarse Aggregates From Dolomitic Sources

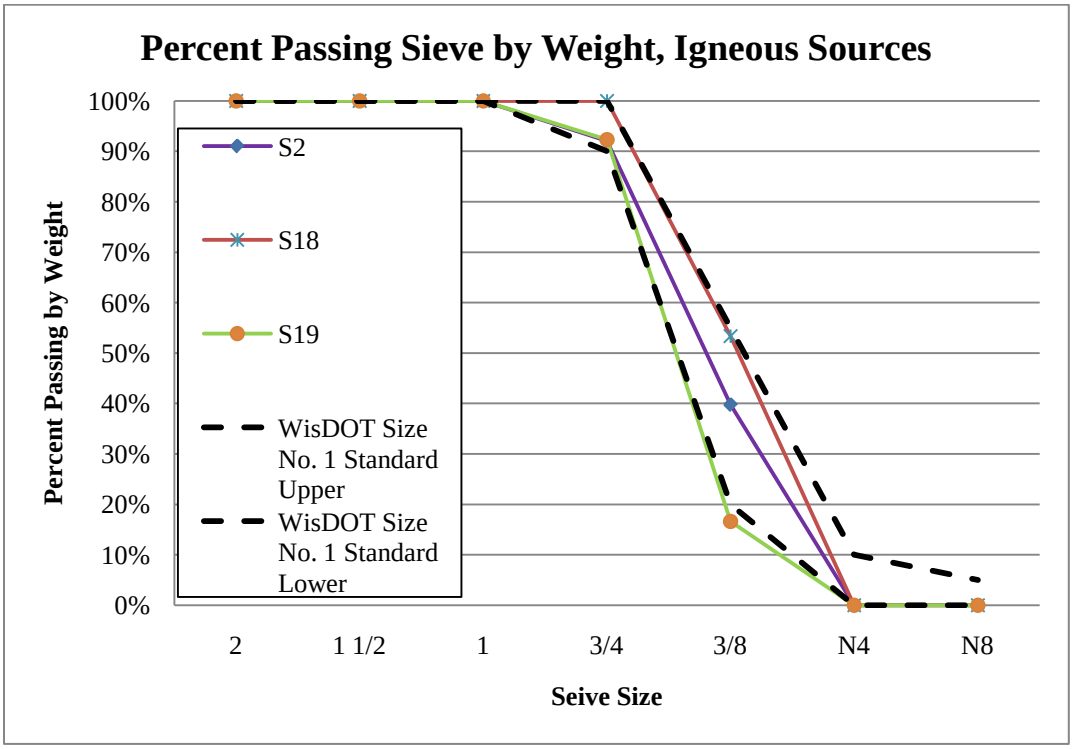

Figure 10.2.4: Sieve Analysis Results for Coarse Aggregates From Igneous Sources

Table 10.2.1: Summary of Compression Strength Results and Estimated Secant Young's Modulus

		7 Days			28 Days		
Curing Process	**Batch**	**Strength, MPa (PSI)**	**± MPa (PSI)**	**E_S, GPa (10^6 PSI)**	**Strength, MPa (PSI)**	**± MPa (PSI)**	**E_S, GPa (10^6 PSI)**
Wet (WCP)	C-S28	23.55 (3415.14)	1.28 (185.18)	7.21 (1.046)	29.72 (4310.65)	0.57 (82.24)	10.05 (1.457)
	S28	22.90 (3321.16)	0.43 (62.28)	7.25 (1.051)	28.82 (4179.47)	1.21 (176.33)	9.45 (1.371)
	S9	23.22 (3367.76)	0.90 (129.41)	7.96 (1.155)	26.71 (3874.14)	0.95 (137.40)	9.30 (1.349)
	S10	26.73 (3877.20)	1.11 (160.46)	8.87 (1.286)	29.92 (4339.99)	0.87 (125.70)	8.56 (0.820)
	S14	29.30 (4249.61)	0.54 (78.07)	9.91 (1.437)	31.5 (4569.04)	1.65 (239.48)	9.95 (1.443)
	C-S2	22.95 (3328.95)	1.63 (236.28)	7.36 (1.067)	25.59 (3711.09)	0.49 (70.83)	8.46 (1.227)
	S2	24.38 (3536.66)	0.97 (141.34)	8.31 (1.205)	26.49 (3841.97)	0.55 (80.63)	9.20 (1.334)
	S18	24.23 (3513.69)	1.48 (214.42)	9.78 (1.418)	29.01 (4208.15)	2.14 (310.08)	10.30 (1.494)
	S19	25.37 (3680.46)	0.91 (131.97)	7.33 (1.063)	30.51 (24425.24)	1.37 (198.82)	11.58 (1.680)
Dry (DCP)	C-S28	22.02 (3194.00)	0.74 (107.43)	7.74 (1.122)	26.56 (3852.18)	0.45 (65.73)	8.95 (1.298)
	S28	19.39 (2812.23)	0.78 (112.82)	6.45 (0.936)	23.54 (3414.09)	0.33 (48.46)	7.99 (1.159)
	S9	21.24 (3080.20)	0.86 (124.65)	7.85 (1.138)	23.02 (3337.63)	0.95 (138.57)	8.74 (1.267)
	S10	22.49 (3261.84)	0.75 (108.58)	8.35 (1.211)	24.50 (3553.21)	0.67 (96.74)	8.11 (1.177)
	S14	26.30 (3814.21)	0.71 (102.74)	10.08 (1.462)	25.75 (3734.54)	0.93 (134.98)	9.36 (1.358)
	C-S2	18.57 (2693.82)	1.96 (285.09)	6.55 (0.950)	24.84 (3603.44)	1.29 (186.73)	6.49 (0.941)
	S2	14.97 (2171.833)	1.16 (168.99)	4.58 (0.664)	19.14 (2776.37)	0.45 (65.05)	6.37 (0.924)
	S18	15.68 (2274.41)	1.61 (233.10)	8.02 (1.164)	21.84 (3167.36)	2.47 (358.05)	7.40 (1.073)
	S19	23.18 (3361.91)	1.02 (148.23)	8.65 (1.255)	24.9 (3611.58)	1.44 (165.38)	8.71 (1.263)

Table 10.2.2: Summary of Tensile Strength Results.

		7 Days		28 Days	
Curing Process	**Batch**	**Strength, MPa (PSI)**	**± MPa (PSI)**	**Strength, MPa (PSI)**	**± MPa (PSI)**
Wet (WCP)	C-S28	2.26 (328.29)	0.33 (48.63)	2.82 (409.70)	0.12 (16.70)
	S28	2.31 (335.14)	0.28 (40.41)	2.98 (432.39)	0.10 (14.35)
	S9	2.37 (343.64)	0.02 (3.35)	2.70 (392.27)	0.26 (38.24)
	S10	2.19 (317.21)	0.20 (29.01)	2.75 (398.72)	0.04 (5.79)
	S14	2.95 (428.39)	0.08 (11.06)	(3.40 493.36)	0.03 (3.75)
	C-S2	2.62 (380.26)	0.11 (16.60)	2.87 (416.56)	0.14 (20.35)
	S2	2.62 (380.32)	0.09 (12.65)	2.96 (429.95)	0.38 (55.24)
	S18	2.91 (421.74)	0.07 (10.12)	3.07 (445.69)	0.08 (11.68)
	S19	2.75 (398.83)	0.17 (25.09)	3.00 (435.15)	0.38 (54.60)
Dry (DCP)	C-S28	2.16 (314.14)	0.36 (52.19)	2.92 (423.65)	0.11 (15.75)
	S28	2.10 (304.14)	0.07 (9.73)	2.51 (364.91)	0.04 (5.95)
	S9	2.62 (380.05)	0.03 (4.77)	2.22 (322.00)	0.08 (11.59)
	S10	2.41 (349.91)	0.18 (26.56)	1.92 (278.37)	0.19 (27.95)
	S14	2.98 (430.42)	0.19 (28.38)	3.18 (460.94)	0.11 (15.50)
	C-S2	2.72 (395.12)	0.25 (36.53)	2.30 (333.63)	0.35 (50.50)
	S2	2.37 (343.80)	0.23 (33.99)	2.36 (342.31)	0.49 (71.82)
	S18	2.40 (348.49)	0.06 (8.35)	2.90 (420.31)	0.38 (54.98)
	S19	2.69 (390.78)	0.08 (12.09)	2.79 (404.28)	0.15 (21.30)

Table 10.2.3: Summary of Capillary Water Absorption Results.

	Curing Time	7 days		28 days	
Curing Process	**Batch**	**Sorptivity ($mm/min^{1/2}$)**	**± S.D.**	**Sorptivity ($mm/min^{1/2}$)**	**± S.D.**
Wet (WCP)	C-S28	1.53	0.32	0.90	0.07
	S28	1.41	0.23	1.57	0.05
	S9	2.14	0.14	2.08	0.07
	S10	1.68	0.10	0.68	0.17
	S14	1.45	0.49	0.53	0.10
Dry (DCP)	C-S28	2.64	0.16	2.35	0.08
	S28	2.85	0.16	2.85	0.10
	S9	3.09	0.21	3.33	0.31
	S10	2.39	0.06	2.14	0.21
	S14	1.69	0.10	1.96	0.07

Table 10.2.4: Summary of Rapid Chloride Penetrability Results.

Curing Process	Wet (WCP)		Dry (DCP)	
Batch	**Total Charge Passed (Coulombs)**	**± S.D.**	**Total Charge Passed (Coulombs)**	**± S.D.**
C-S28	2828.32	2.75	3006.49	43.00
S28	2616.12	365.46	3112.20	212.84
S9	2502.00	136.77	3548.90	125.91
S10	2080.13	103.99	2970.30	291.91
C-S2	1868.68	261.29	2881.03	208.85
S2	2255.07	305.37	2969.85	278.44
S18	1795.45	190.66	2728.40	159.21
S19	1577.14	170.35	1722.51	55.810

10.3: Cement Paste Characterization Data

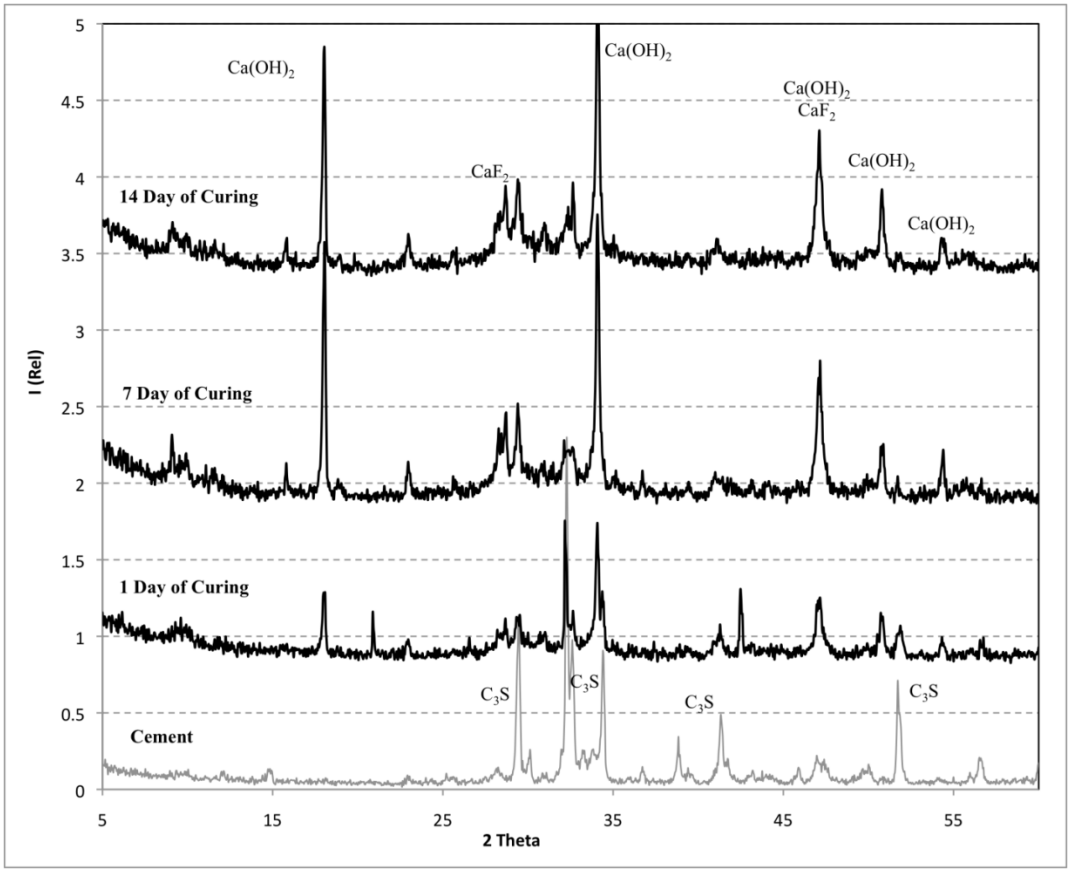

Figure 10.3.1: X-ray Diffraction Patterns for the Cement Paste Control at Different Aging Times.

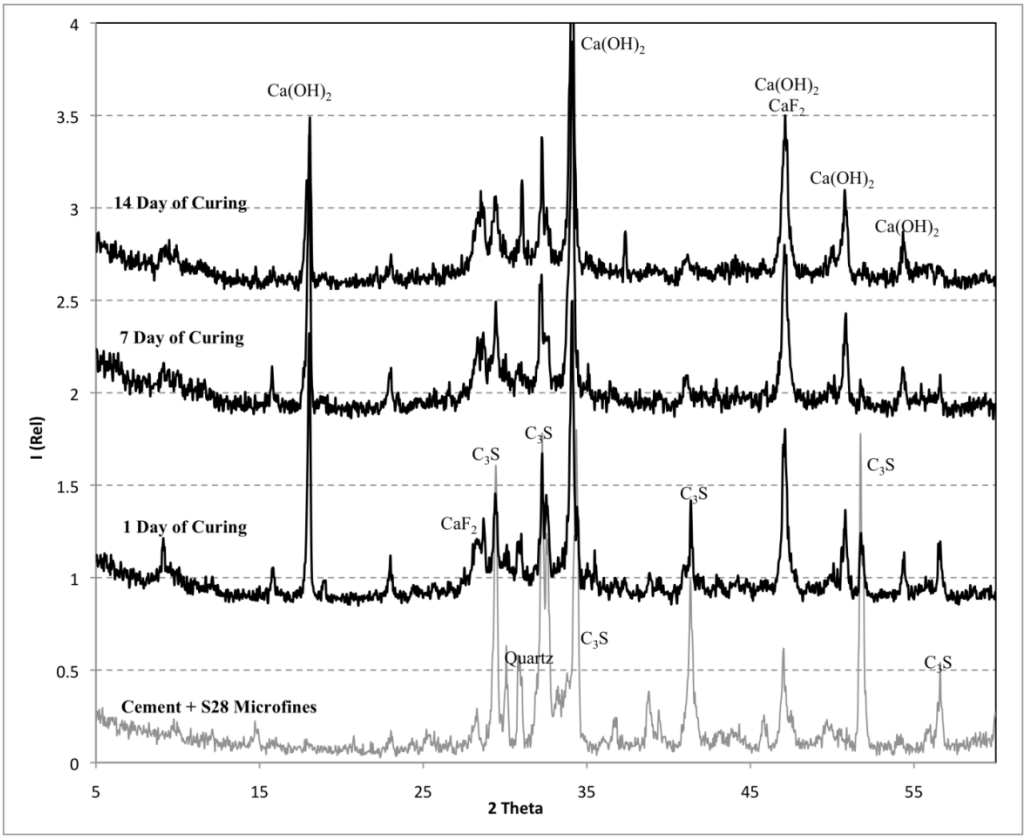

Figure 10.3.2: X-ray Diffraction Patterns of Cement Paste Containing a Carbonate Microfine (S28) at Different Aging Times.

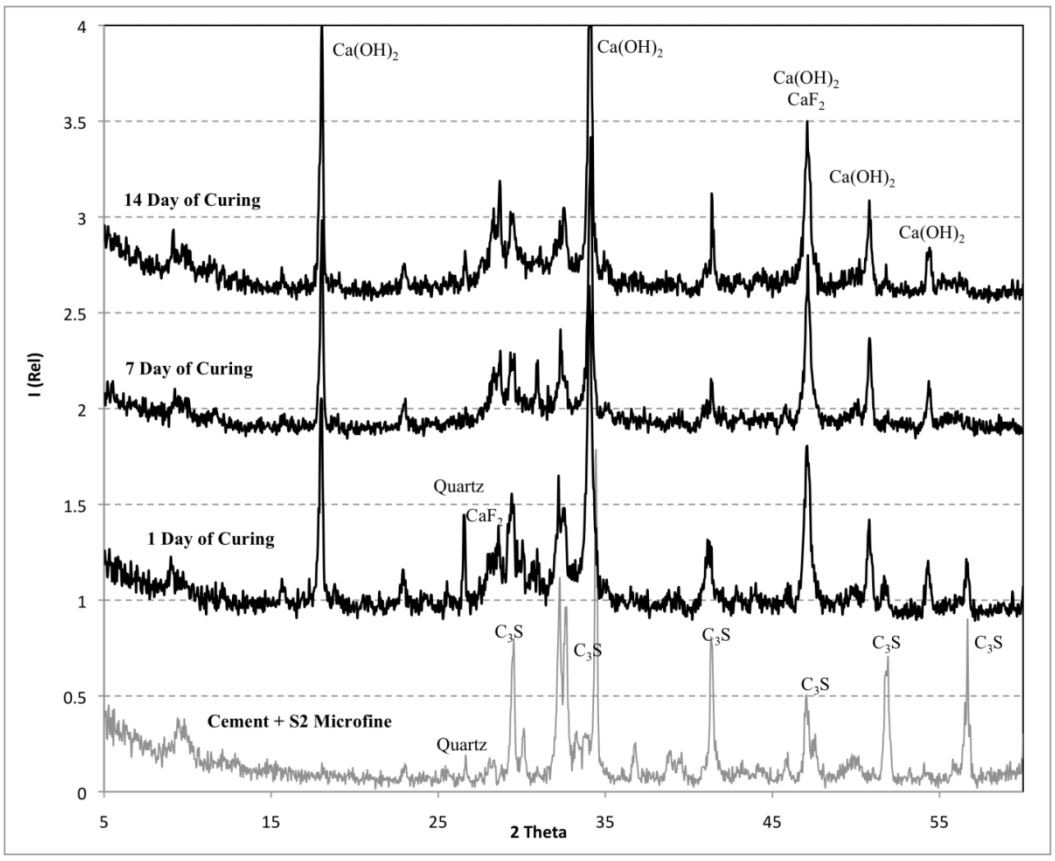

Figure 10.3.3: X-ray Diffraction Patterns of Cement Paste Containing a Siliceous Microfine (S2) at Different Aging Times

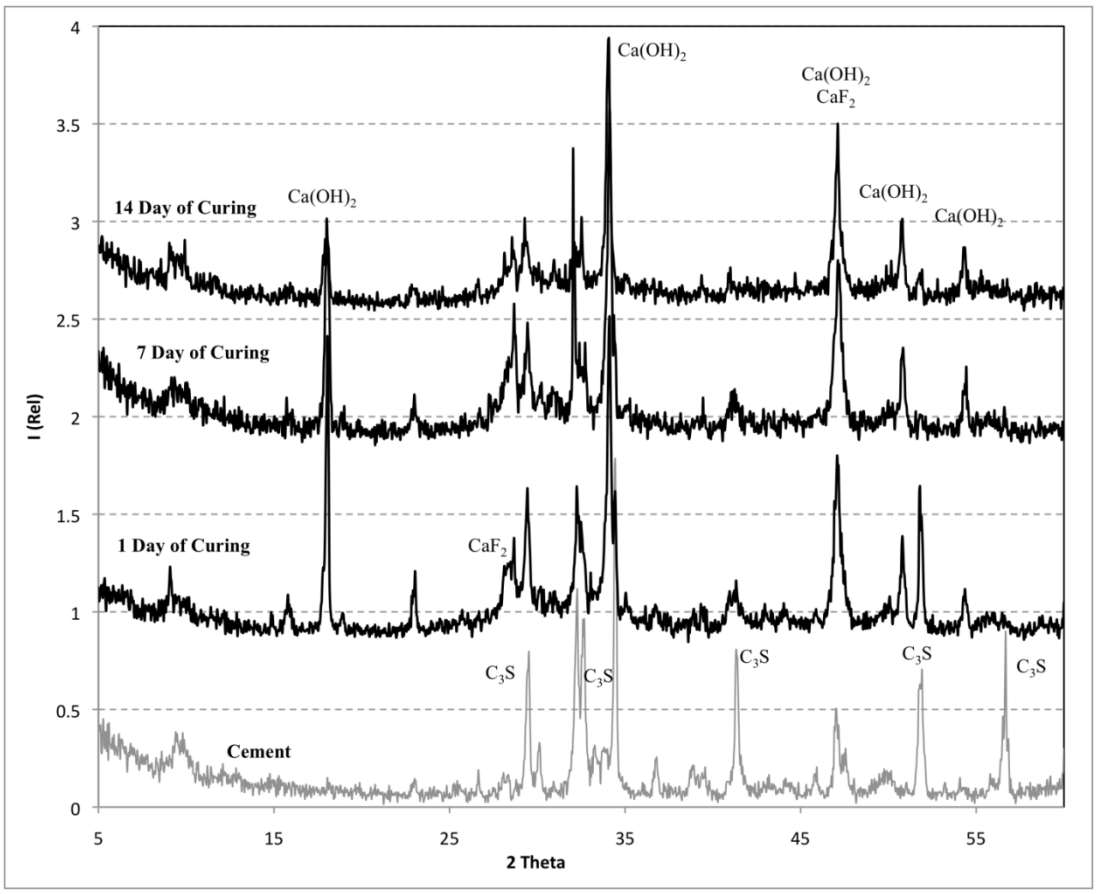

Figure 10.3.4: X-ray Diffraction Patterns for the Cement Paste Containing Microfines of CaM at Different Aging Times.

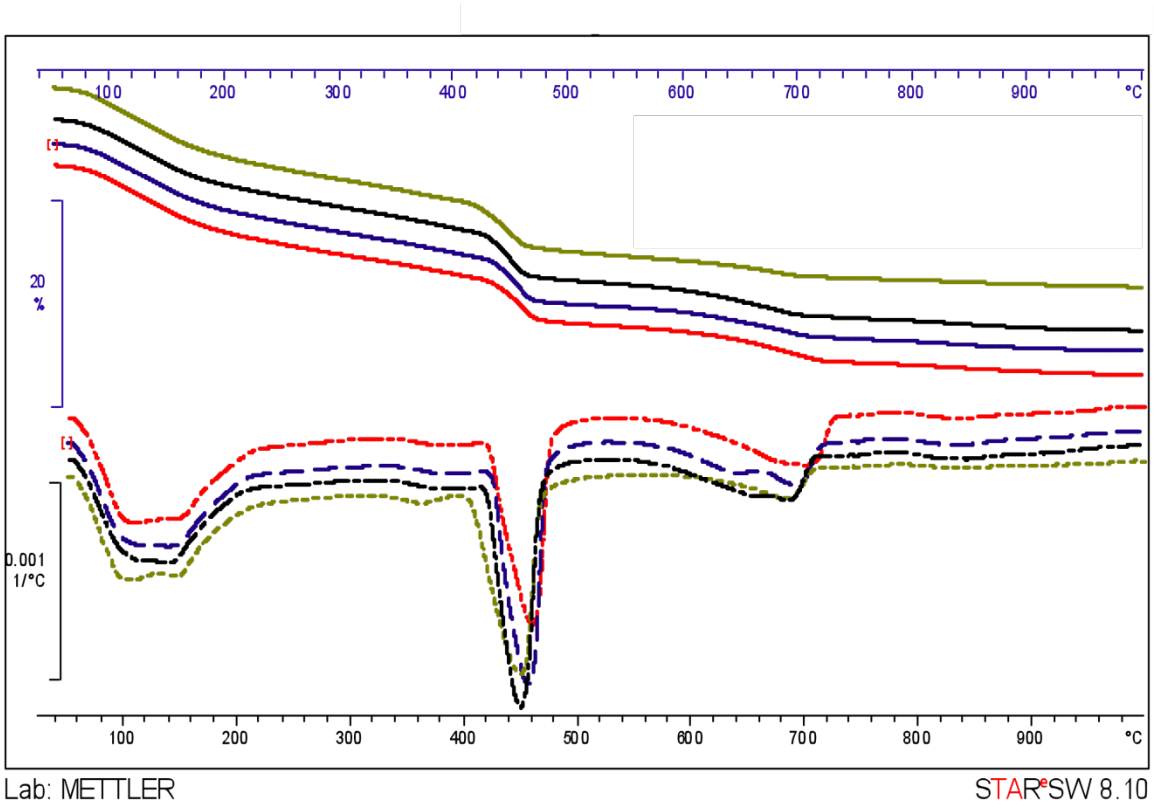

Figure 10.3.5: TG (Top) and DTA (Bottom) Curves for Cement Paste Samples Containing Kaolin (Green), S14 Miccrofines (Dark Blue), S2 Microfines (Red), and the Control (black).

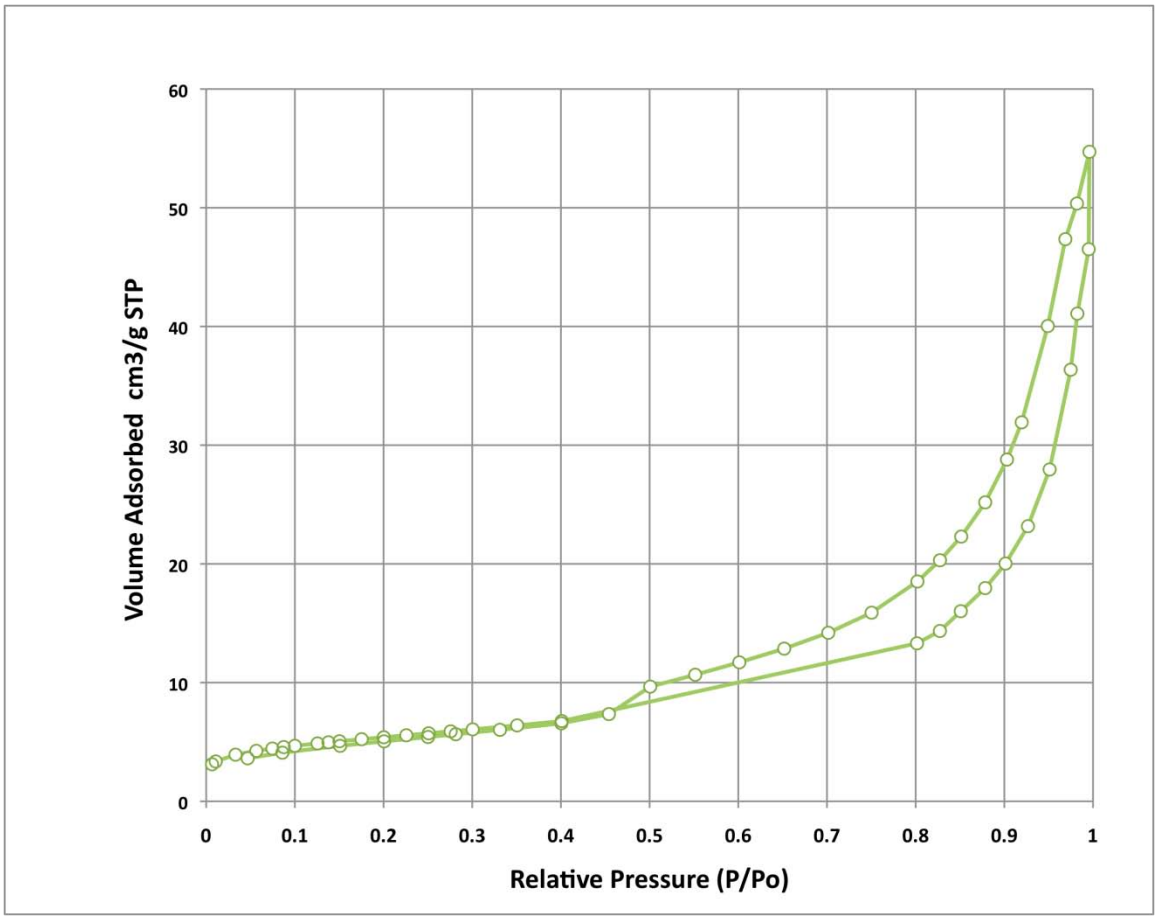

Figure 10.3.6: Adsorption / Desorption Isotherm for the Cement Paste Control.

10.4: Principal Mineral Phase in Concrete Samples

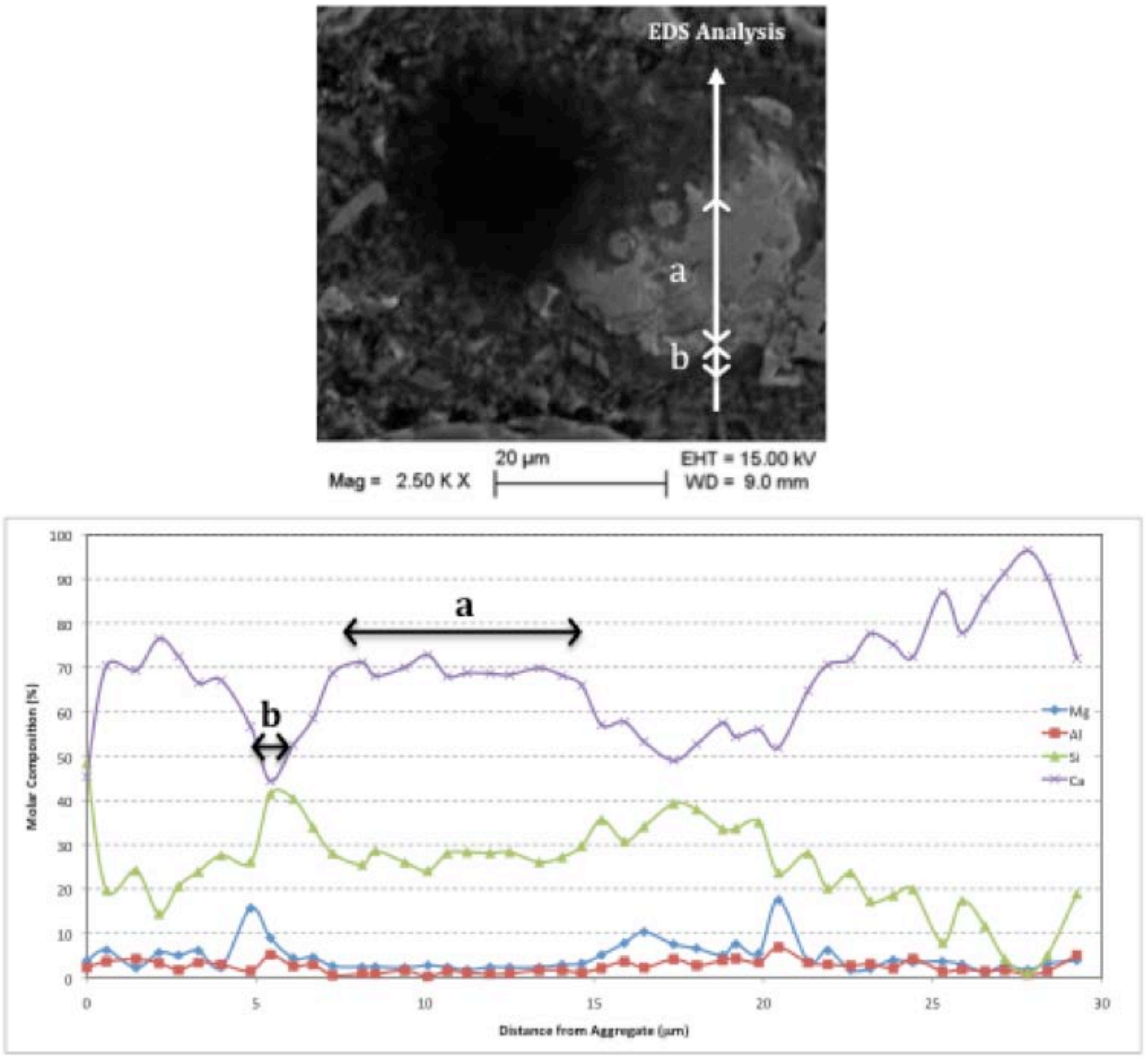

Figure 10.4.1: BSE Image and EDS Analysis of C3S (a) and C-S-H (b).

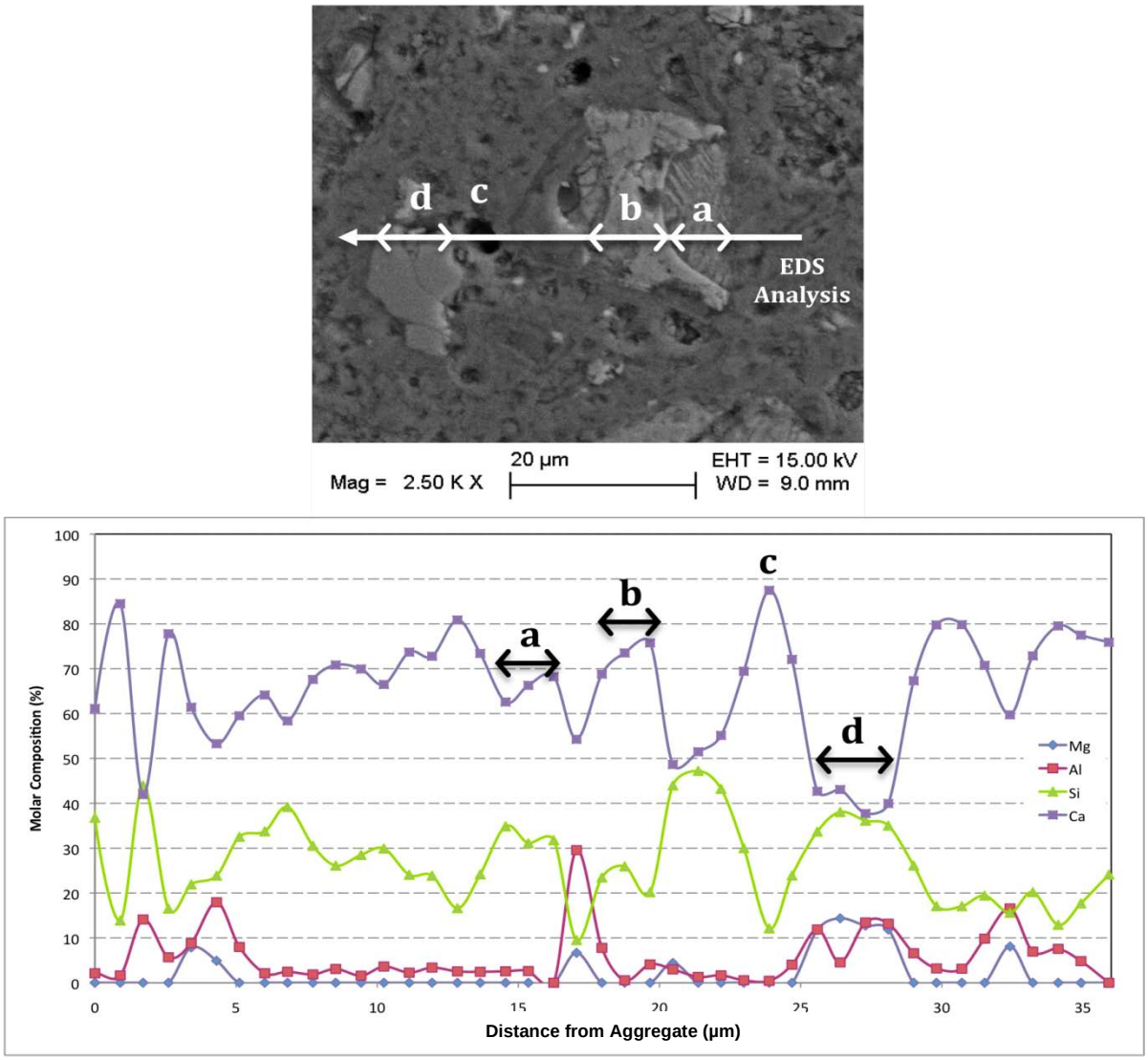

Figure 10.4.2: BSE Image and EDS Analysis of C2S (a), C3S (b), Pore Rich in Ca(OH)2 (c), and Dolomite (d).

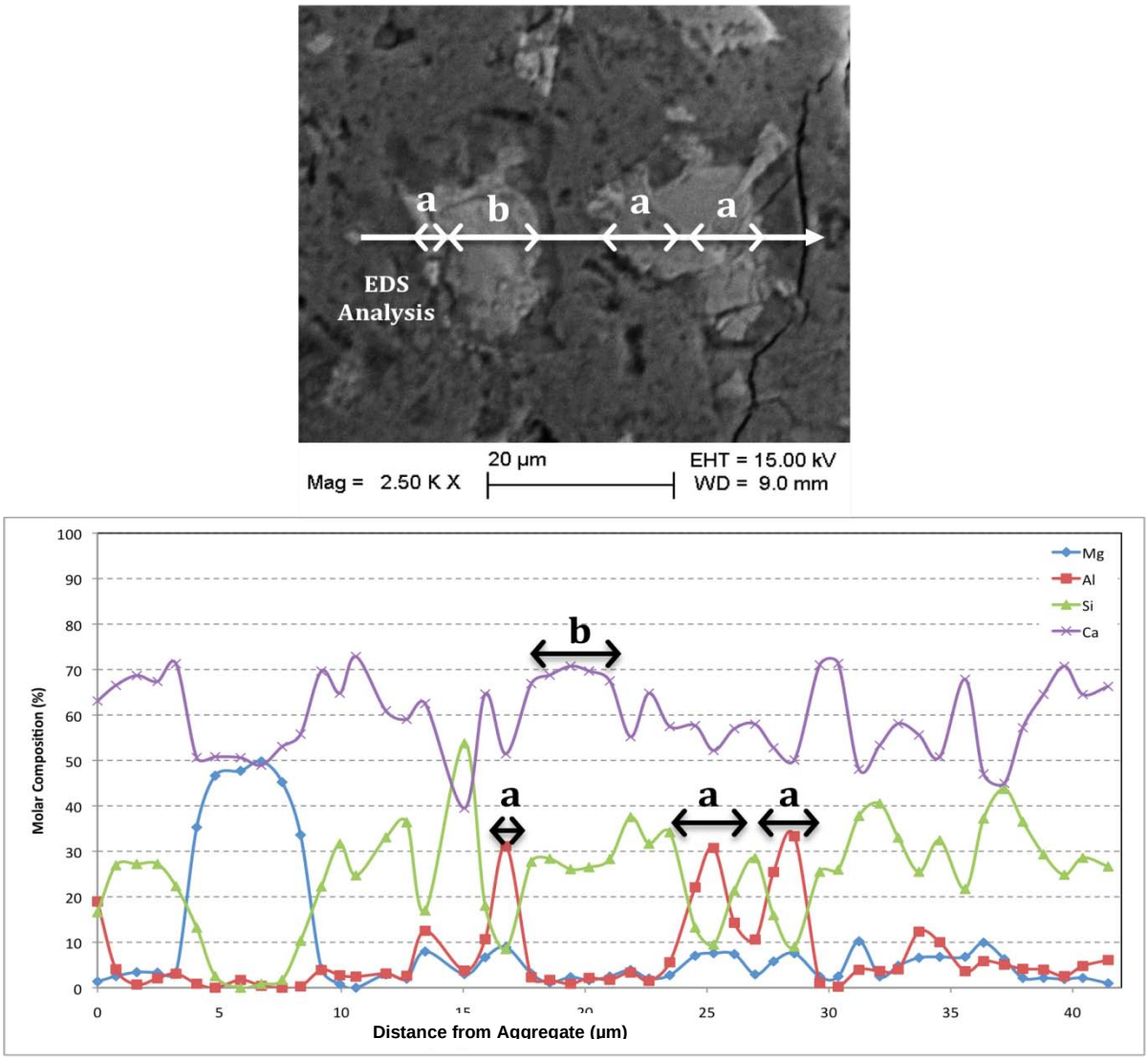

Figure 10.4.3: BSE Image and EDS Analysis of C3A (a) and C3S (b).

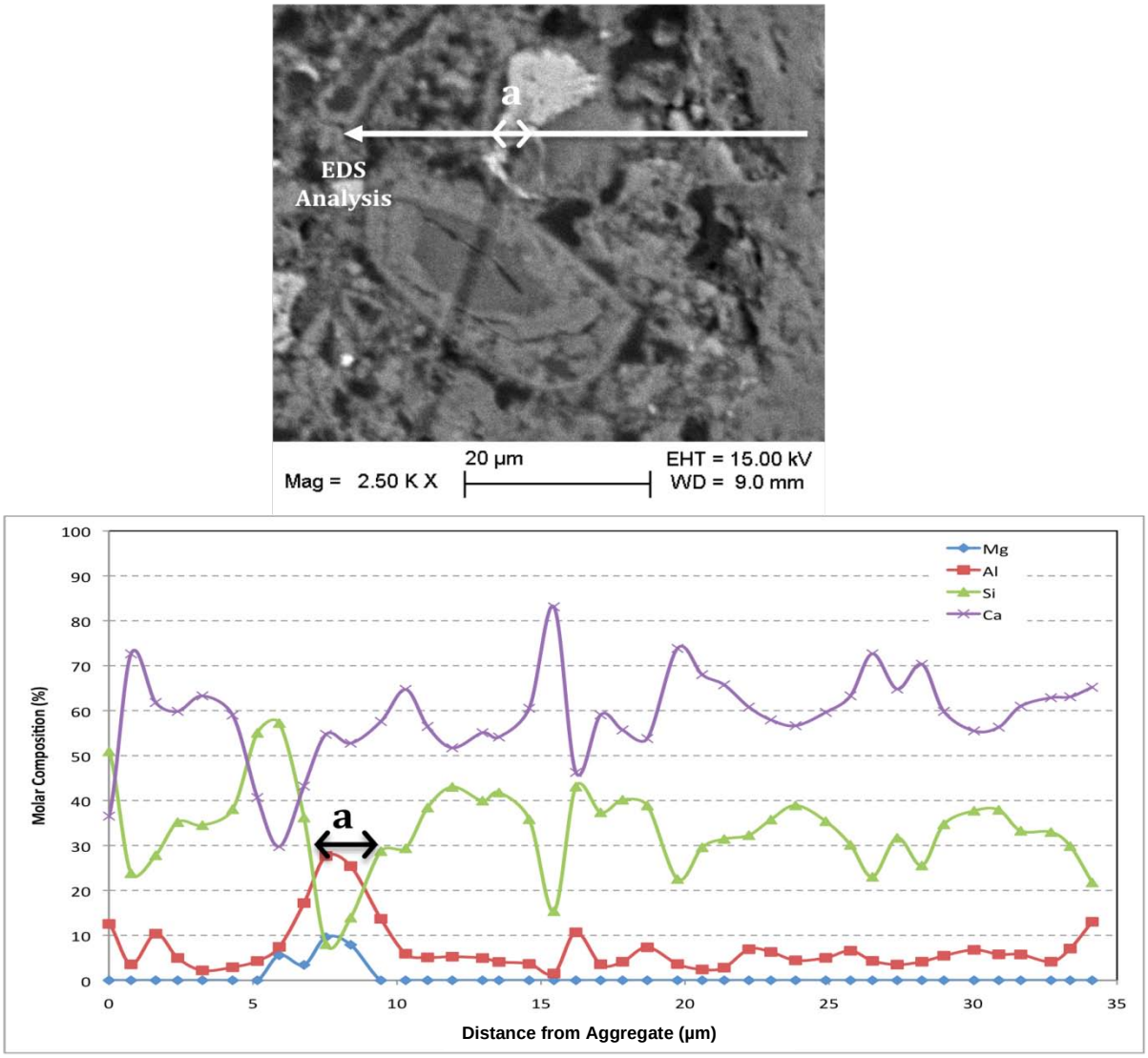

Figure 10.4.4: BSE Image and EDS Analysis of C4AFe (a).

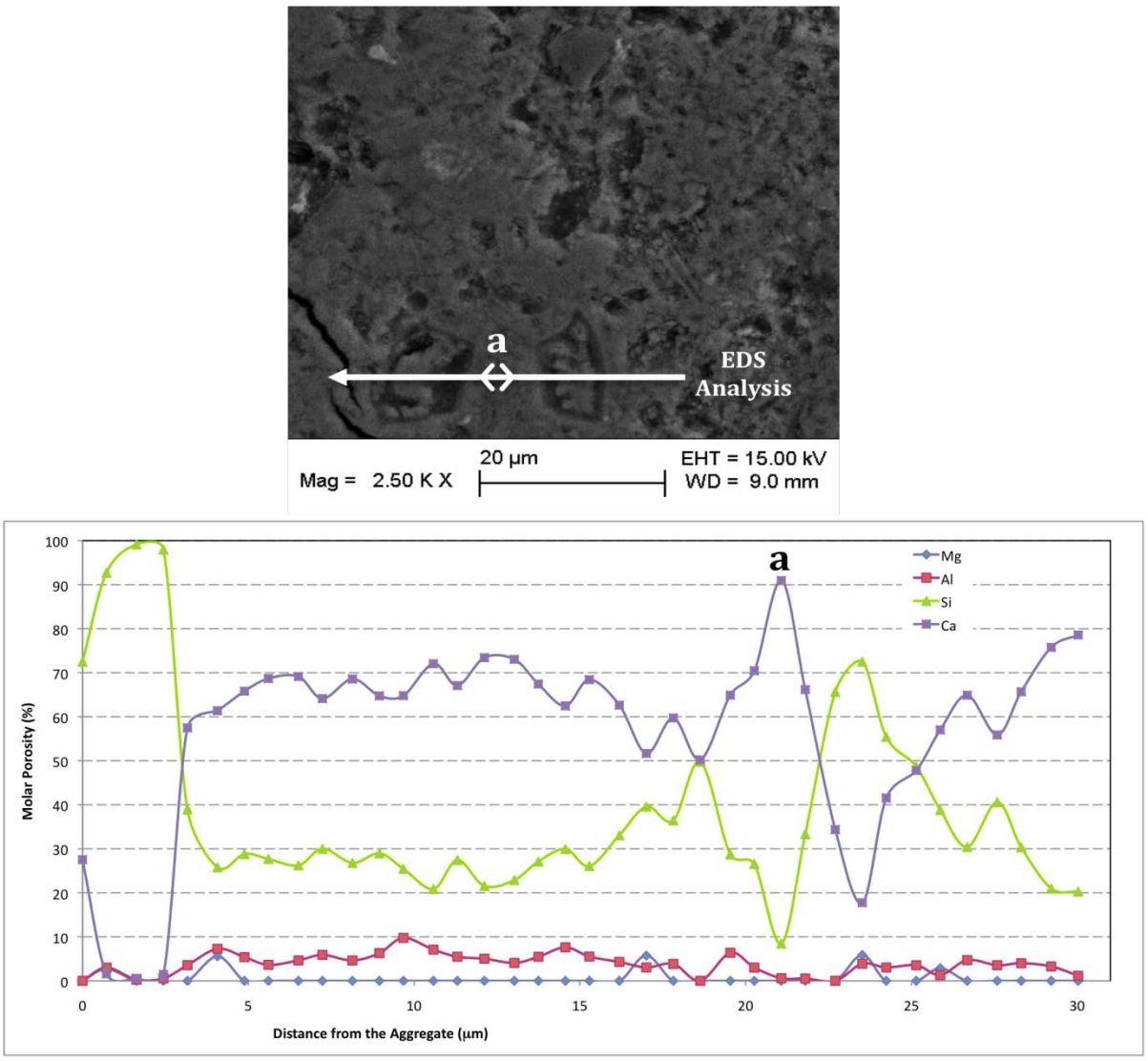

Figure 10.4.5: BSE Image and EDS Analysis of Ca(OH)2 (a).

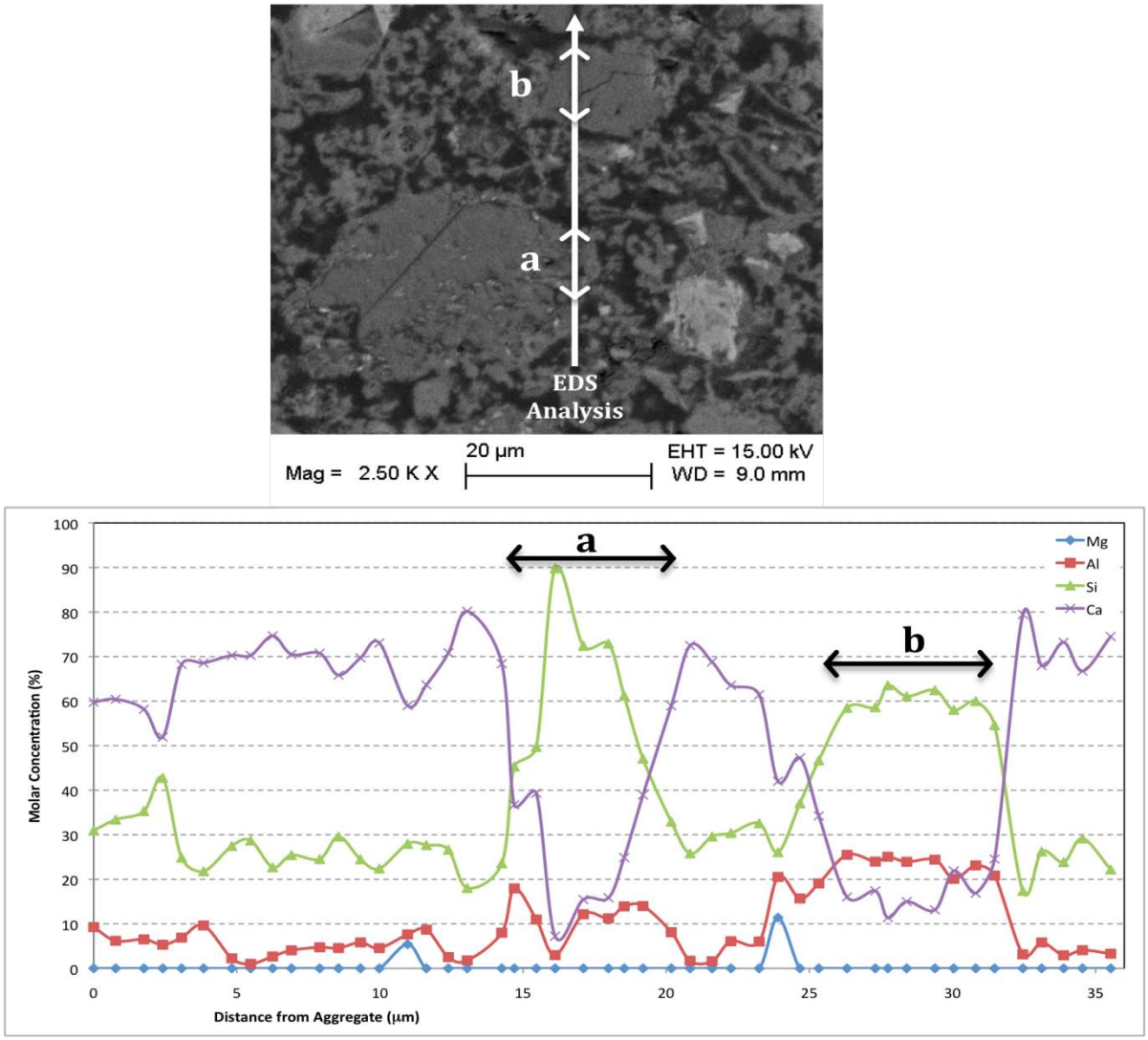

Figure 10.4.6: BSE Image and EDS Analysis of Quartz (a) and Feldspar (b).

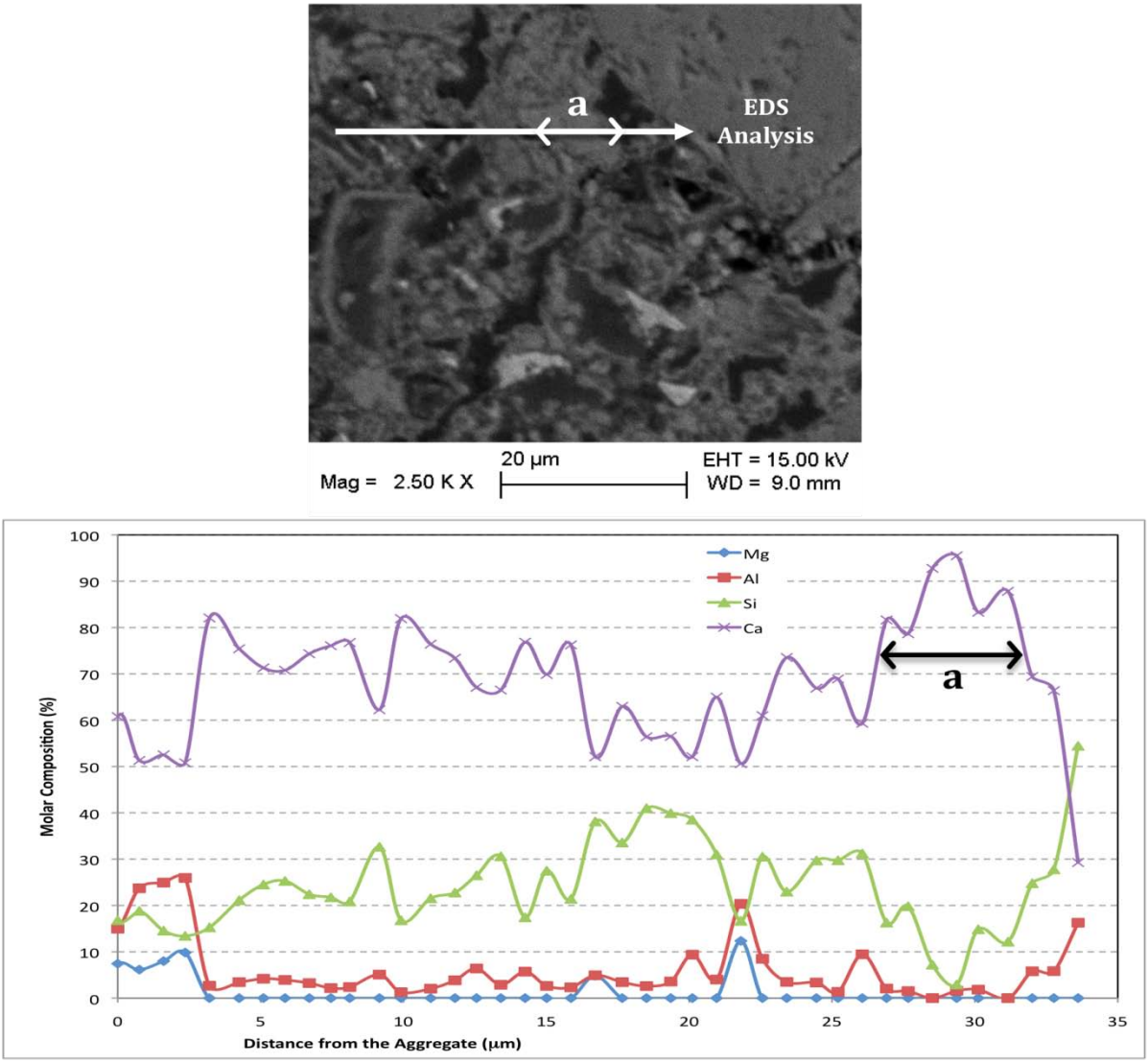

Figure 10.4.7: BSE Image and EDS Analysis of Calcite (a).

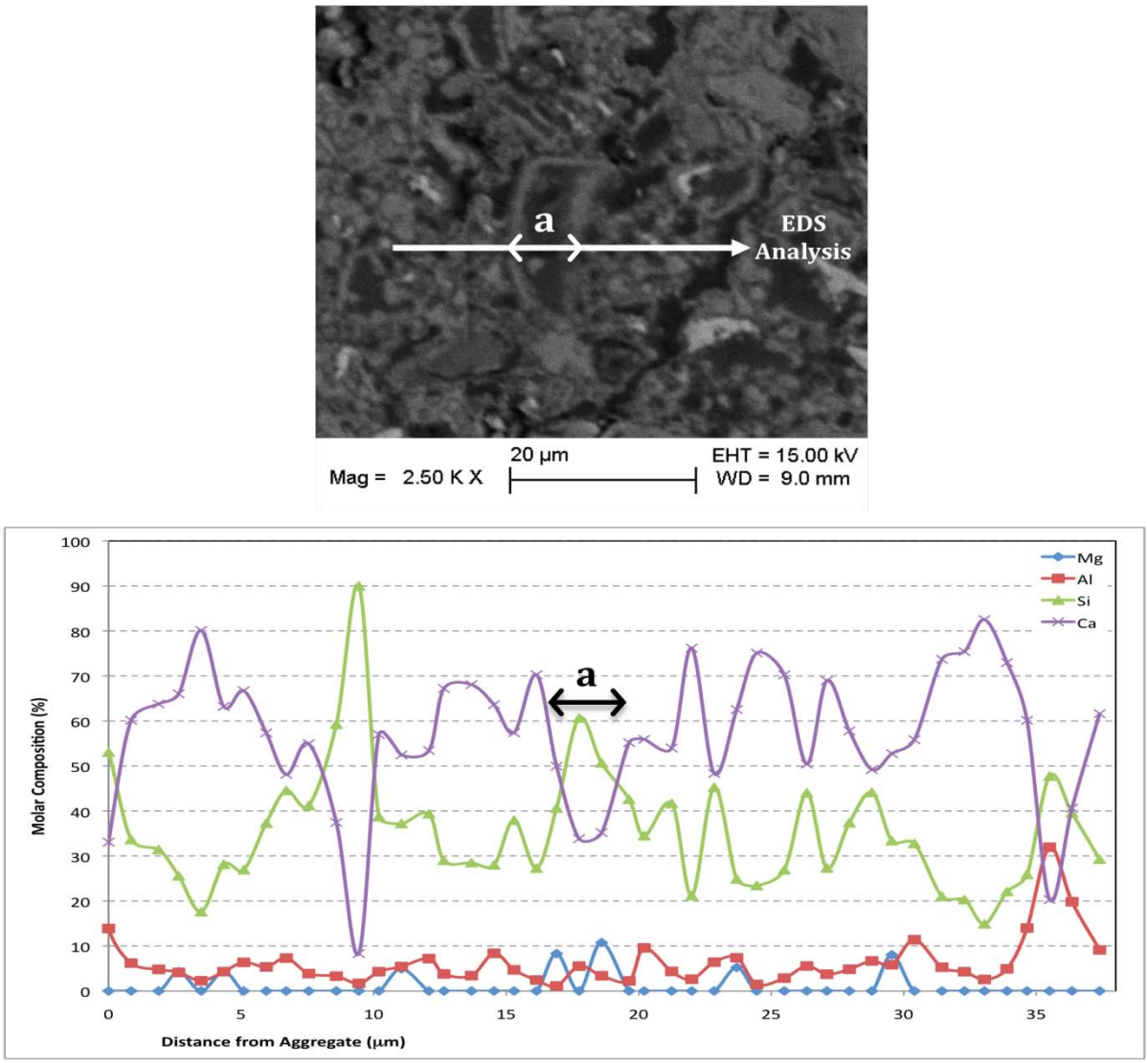

Figure 10.4.8: BSE Image and EDS Analysis of Calcium Silicate (a).

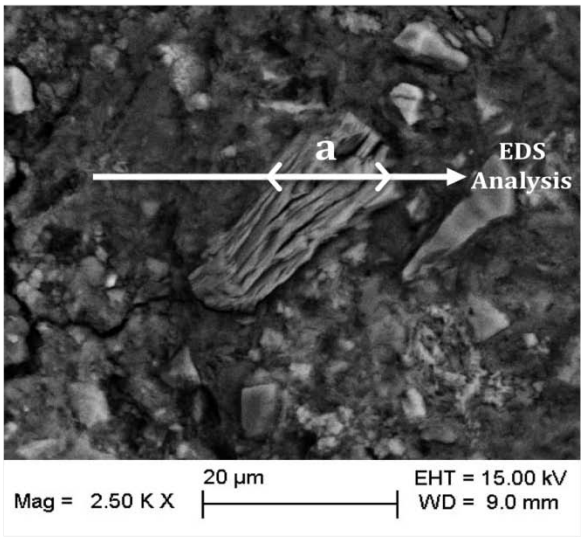

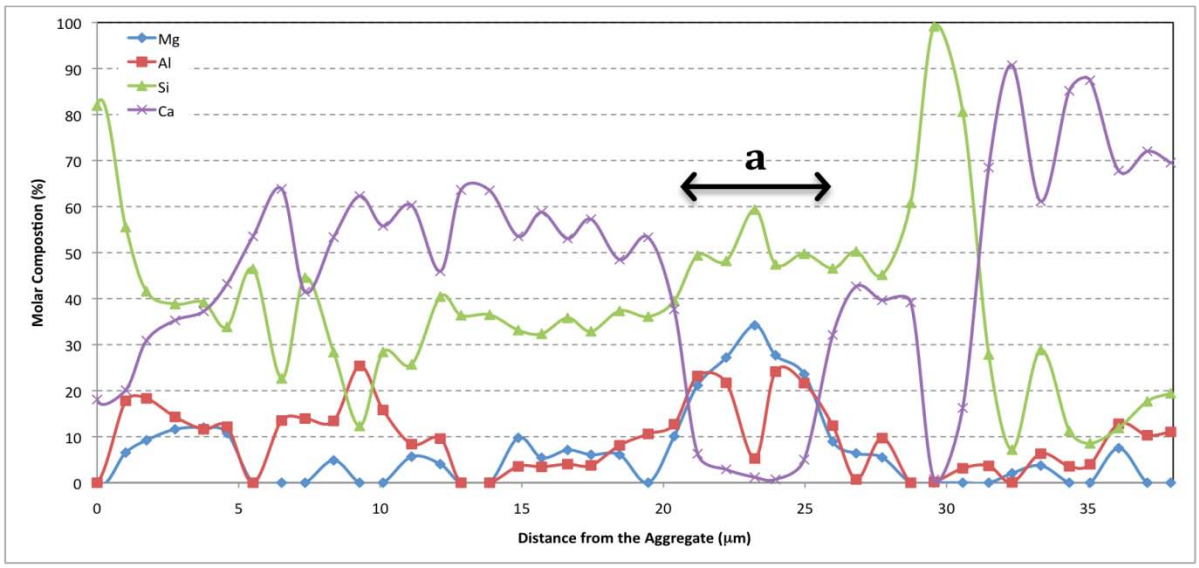

Figure 10.4.9: BSE Image and EDS Analysis of Sodium Montmorillonite (a).

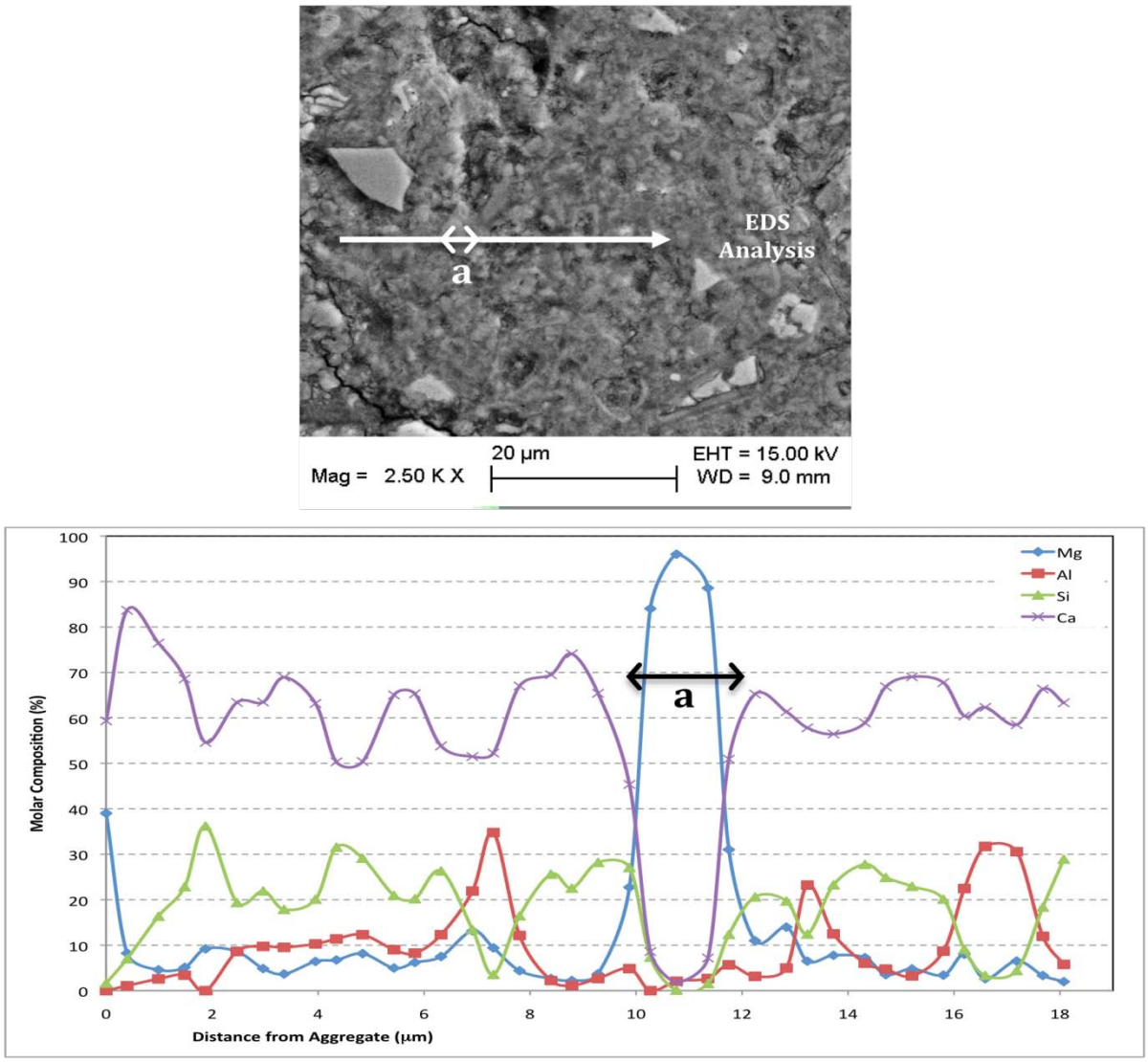

Figure 10.4.10: BSE Image and EDS Analysis of Brucite (a).

10.5: SEM Characterization of Concrete Containing Sodium Montmorillonite Coarse Aggregate Coatings

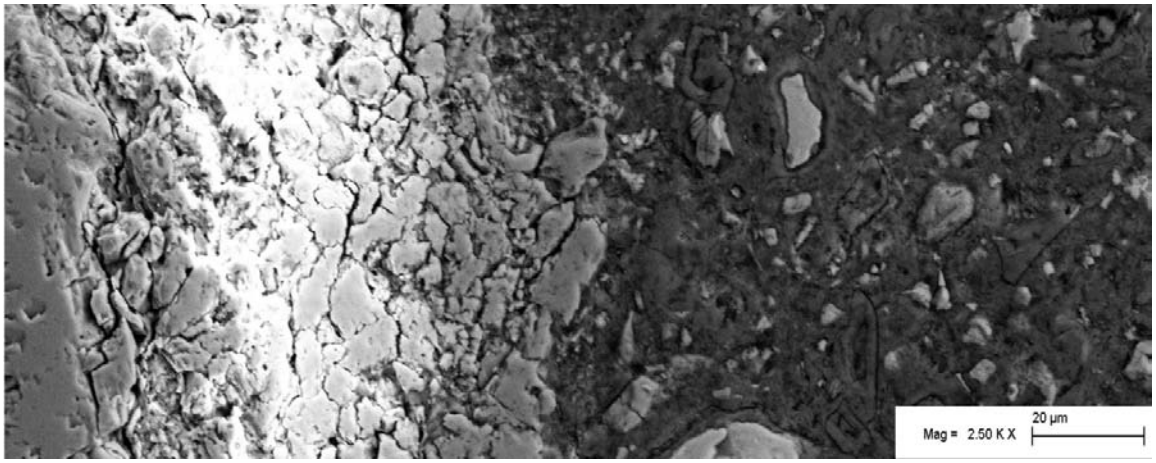

Figure 10.5.1: BSE Image of a Sodium Montmorillonite Coating Over a Coarse Aggregate.

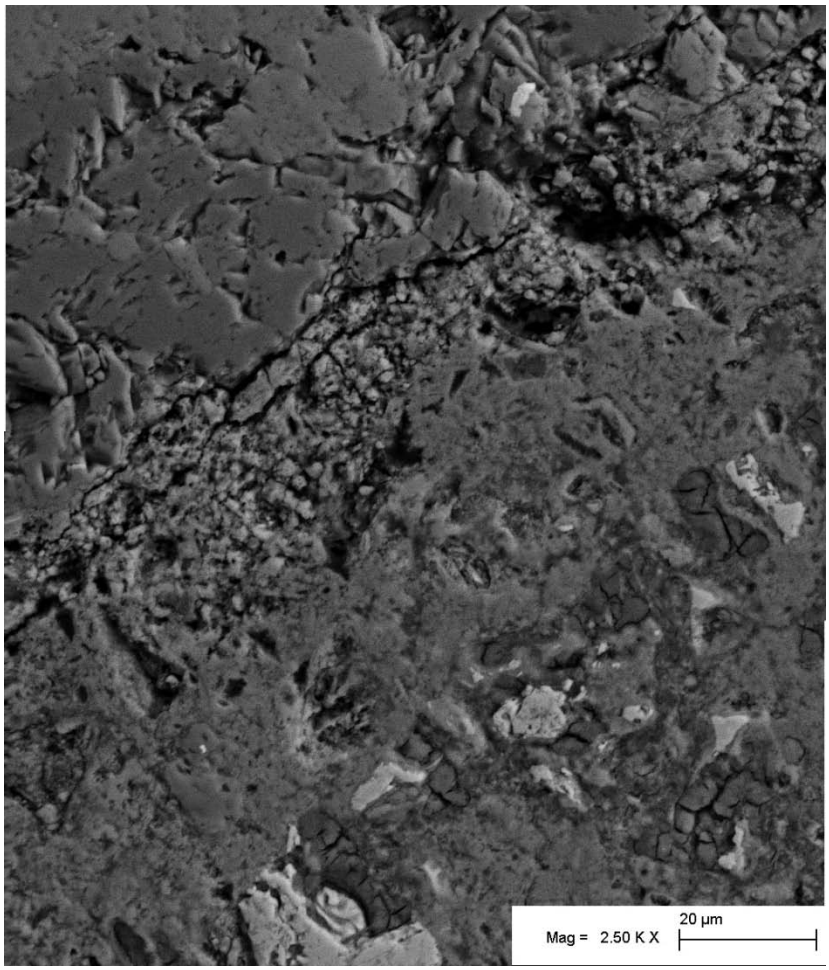

Figure 10.5.2 BSE Image of a Reacted Sodium Montmorillonite Coating Under a Coarse Aggregate.

Wisconsin Highway Research Program
University of Wisconsin-Madison
1415 Engineering Drive
Madison, WI 53706
608/262-2013
www.whrp.org